Title
A CCMPUTATIONAL MODEL FOR CRITICAL FLOW THROUGH INTERGRANULAR STRESS CORROSION CRACKS

Author
Schrock, V.E.

Publication Date
1986-08-01

Lawrence Berkeley Laboratory

UNIVERSITY OF CALIFORNIA

Engineering Division

A COMPUTATIONAL MODEL FOR CRITICAL FLOW THROUGH INTERGRANULAR STRESS CORROSION CRACKS

V.E. Schrock. S.T. Revankar, S.Y. Lee, and C.-H. Wang

August 1986

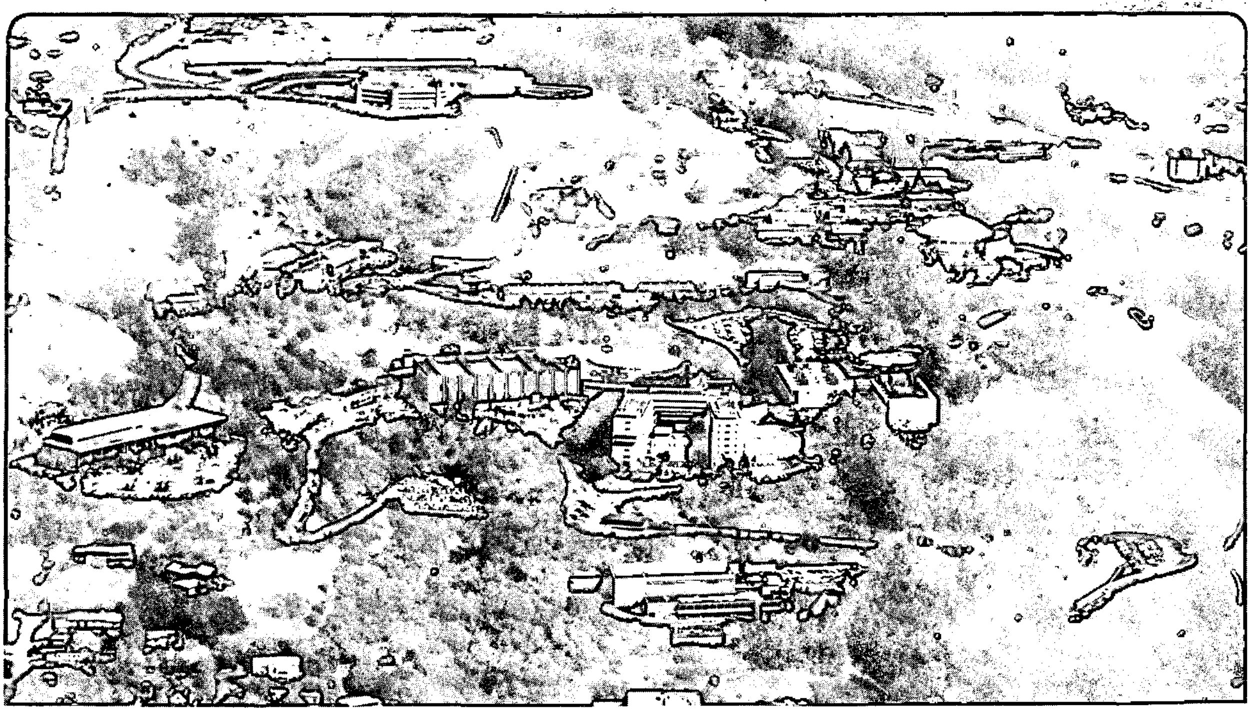

Prepared for the U.S. Department of Energy under Contract DE-AC03-76SF00098

DISCLAIMER

A Computational Model for Critical Flow Through Intergranular Stress Corrosion Cracks

by

V. E. Schrock, S. T. Revankar, S. Y. Lee & C-H Wang

Report submitted to the
Office of Nuclear Regulatory Research
U.S. Nuclear Regulatory Commission
Washington, D.C. 20555

University of California
Lawrence Berkeley Laboratory
Engineering Division
Berkeley, California 94720

This work was supported by the Nuclear Regulatory Commission through U.S. Department of Energy Contract No. DE-AC03-76SF00098.

CONTENTS

ABSTRACT

The presence of intergranular stress corrosion cracks (IGSCC) in thermal stressed zones in stainless steel piping and associated components is of much concern in reactor safety. The prediction of leak rates through the cracks is important in assessing the plant reliability. An analytical model has been developed to predict flow rates of initially subcooled or saturated water through these cracks. The model assumes the flow in the crack to be homogeneous and in thermal equilibrium. The crack geometry was idealized as a convergent straight slit of constant gap thickness. The fluid is assumed to enter the crack without separation. The one dimensional model accounts for the changing cross sectional area in the flow direction. The effects of wall friction, expansions/contractions and tortuosity of the actual flow path are lumped into an equivalent friction. The numerical scheme developed for the model solution has been programed into a Fortran computer code called SOURCE. A companion subroutine STEAM provides the saturated fluid properties. Inputs to SOURCE are the upstream stagnation pressure and temperature, the crack geometry specification, and the equivalent friction factor.

SOURCE has been assessed against the experimental data obtained in the Battelle Columbus Laboratories (BCL) study using actual crack specimens. From a parametric study of the BCL data using SOURCE, a subcooling correction factor was developed to modify source predictions. A general methodology was developed for predicting a lumped friction factor (includes effects of bends, contractions and expansions) for use in SOURCE. Corrected SOURCE predictions using the general friction factor methodology agree well with BCL data. This method is recommended for estimating leak rates and assessing the leak-before-break criterion.

ILLUSTRATIONS

NOMENCLATURE

Symbol	Description	Dimension
A	Cross-sectional area of crack	L^2
a	Half of entrance crack width	L
C	Subcooling Correction Factor	-
c	Half of exit crack width	L
D	Equivalent hydraulic diameter	L
E	Modulus of elasticity	$ML^{-3}t^{-2}$
f	Friction factor	-
g_c	Gravitational conversion factor	Lt^{-2}
G	Mass flux	$ML^{-2}t^{-1}$
h	Specific enthapy	Lt^{-2}
K	Pressure loss coefficients	
L	Depth of crack	L
ℓ	Surface crack length	L
M	Mach number	
$\dot{m}$	Mass flow rate	Mt^{-1}
P	Pressure	$ML^{-3}t^{-2}$
P_m	Wetted perimeter	L
T	Temperature	T
t	Equivalent slit thickness	L
v	Specific volume	L^3M^{-1}
V	Fluid velocity	Lt^{-1}
w	Local width of crack	L
x	Thermodynamic quality	
z	Length variable along crack channel	L

Greek Letters

δ	Average crack thickness (Figure 3.2)	L
Δ	Difference	
ε	Surface roughness of crack wall	L
θ	Percentage tolerance	
ρ	Density	$L^{-3}M$
Σ	Summation	-
σ	Tangential stress	$ML^{-3}t^{-2}$
σ_y	Yield stress	$ML^{-3}t^{-2}$
τ_w	Wall shear stress	$ML^{-3}t^{-2}$

Subscripts

o	Stagnation
1	Entrance
a	Sound speed
c	Choking condition
e	Crack exit
f	Saturated liquid
fg	Saturated liquid-vapor difference
fl	Evaluated at flashing plane
g	Saturated vapor
i	Grid point
ℓ	Liquid or flashing point
s	Evaluated at constant entropy
T	Total
sat	Evaluated at saturation condition corresponding at the local pressure
sub	Subcooling

Superscripts

-	Average

1. INTRODUCTION

The presence of intergranular stress corrosion cracks (IGSCC) in the weld heat affected zones of types 304 and 316 stainless steel piping and associated components of commercial boiling water reactors (BWR) and steam generator tubes in pressurized water reactors (PWR) has attracted considerable attention over the past several years. [1,2]. Because of economic and safety considerations, it is highly desirable to determine if the failure of the piping system will occur in a 'leak-before-break' mode. Leak-before-break is demonstrated by establishing that postulated cracks in a pipe will be detected by leak detection methods before such cracks reach a critical size to cause unstable fracture. The ability to predict the leak rates through the cracks in piping and generator tubes before the crack size becomes critical is vital to demonstrate leak-before-break.

Most reports on the critical two-phase flow are related to flow in pipes, nozzles and orifices and there is little direct literature available on a flow rate of two-phase flow through tight cracks (crack width of less than 1 mm). Agostinelli et al.[3] studied flows of flashing water and steam through smooth annular passages of hydraulic diameters with constant area in the range of 0.15 mm to 0.43 mm. Test data were obtained with stagnation conditions of pressure ranging from 3.50 to 20.51 MPa and fluid subcoolings from 9.3^{o}C to 67^{o}C. Hendricks et al.[4] made a qualitative study of radially inward flow through 0.076 mm annular clearance between two glass plates using liquid nitrogen. In their experiments for inlet conditions with 10 K or larger subcoolings, flashing was seen to occur near the end of the 0.72 cm flow passage. Simoneau [5] carried out an experimental study of two-phase nitrogen flow through a rectangular slit. The test section used was 2.54 cm in length and width, with an opening dimension which was nominally 0.292 mm. He concluded that a uniform two phase flow pattern existed in most of the test runs and that vaporization was occurring at or near the exit plane, for the tests carried out with stagnation pressures up to 6.8 MPa and for four different subcoolings in the range $0.84 < T_R < 1.03$, $T_R = T_o/T_c$. Amos and Schrock [6] carried out experiments on constant area rectangular slits 20 mm in width and opening dimension range nominally from 0.127 to 0.318 mm. Stagnation pressure ranged between 4.1 and 16.2 MPa and water subcoolings from zero to 65^{o}C. The length-to-hydraulic diameter ratios (L/D) of slits were between 83 and 400, with flow direction dimension fixed at 6.35 cm. Their study strongly suggested that the frictional effects are predominant in two-phase critical flows with large L/D.

More recently an experimental and analytical research program to study IGSCC associated with BWR piping was carried out at Battelle Columbus Laboratories (BCL) by Collier et al. [7] under the joint sponsorship of the Electric Power Research Institute (EPRI) and the BWR Owners Group. The experiments were carried out in two phases. In the first phase, simulated cracks were used. For simulated cracks, the ratio L/D and the surface roughness could be controlled. In the second phase, actual

IGSCC in stainless steel pipes were utilized. An analytical model to predict two-phase flow through cracks was developed [8] based on the non-equilibrium model suggested by Henry [9]. The model was developed by extending the Henry model to account for wall friction, flow area change and bends in the flow path. Further modifications were made to this model by Abdollahian and Chexal [10] to improve its agreement with the data. Both versions of this model, coded into programs LEAK and LEAK 01 respectively, assumed that flashing always begins at an L/D of 12 and that the quality varies linearly with distance along the flow path. Quality was evaluated assuming an isentropic process in LEAK and an isenthalpic process in LEAK 01. The calculations were done by separately calculating channel pressure drop due to momentum and friction based upon length averaged conditions rather than solving the equations in a marching method to obtain the distribution of pressure and quality along the crack length (flow direction).

The present study, aimed at developing a computational scheme for steady state two-phase critical flow through IGSCC, takes account of more realistic assumptions in modelling the flow through cracks. From the theoretical and experimental study by Amos and Schrock [6] it was observed that the predictions of critical two-phase flow through simulated cracks of large L/D using the homogeneous equilibrium model (HEM) agreed fairly well when compared with their experimental measurements (with deviations less than 20%). As the IGSCC have large L/D ratios, in the present study the HEM (with account of wall friction, area change and tortuosity) is used with a correction factor dependent upon upstream subcooling. The computational scheme is coded into a Fortran program called SOURCE. The inputs to the program require stagnation conditions and specifications of crack geometry. A properties subroutine, STEAM, is provided to the SOURCE code to calculate the fluid thermodynamic properties. The STEAM subroutine was developed using the equations for water given by Ishimoto et al.[15]. In the following sections the development of the computational scheme and the prediction of BCL tests are presented. A method of estimating the crack equivalent friction factor is also presented along with predicted results using these friction factors. The SOURCE flow chart and listing are presented in Appendices B and C, respectively.

2. CHARACTERISTICS OF FLOW THROUGH IGSCC

The BCL tests [7] on actual IGSCC were carried out on two stainless steel pipes which contained approximately 90 percent through-the-wall circumferential cracks. The crack depths were not actually uniform and an electric potential technique was used to locate the deepest section. At this location a portion of the pipe surface was machined away to expose the tip of the IGSCC. Progressively deeper cuts were made to obtain various L/D ratios. Figure 2.1 shows a sketch of the crack used by BCL. The exit to entrance area ratio for cracks was determined by inspection of the flow surface convergence following the experiments. The measured leak rates and the test parameters are given in Table 2.1.

From the stress analysis [11] the crack cross sectional area, A, can be related to the surface crack length, ℓ, as

$$A = \frac{\sigma}{2E} \ell^2 \; F\left(\frac{\sigma}{\sigma_y}\right) \qquad (2.1)$$

Here the function F is of order unity. All the symbols are defined in the nomenclature.

For a typical stress of $\sigma = 8 \times 10^3$ psi and $E = 26 \times 10^6$ psi, the area A is given as $A \simeq 5 \times 10^{-4} \ell^2$. Hence the equivalent slit thickness t Figure 2.1 is given as

$$t = 5 \times 10^{-4} \ell \qquad (2.2)$$

Equation (2.2) gives an idea of crack width to length ratio. As indicated earlier it is important to define the margins for "leak-before-break" (LBB) i.e., the leak rate through a crack before failure of the pipe with events such as burst or break. With an assumed typical critical mass flux $G \sim 3900\ lb_m/ft^2 sec.$, the estimations [12] of the crack length that will give the observable flow rate of 5 GPM and the critical crack length before break are given in Table 2.2 for different pipe sizes.

Usually the non circular flow cross sections are modelled by defining an equivalent diameter and using the correlations developed for round tubes. The crack width in BCL experiments was between 0.02 mm and 0.2 mm, the ratio of the crack opening length to width was between 30 and 150 and the L/D varied from 50 to 475. When the pipes were destructively tested after the BCL phase II tests, the flow path was found to have a number of turns.

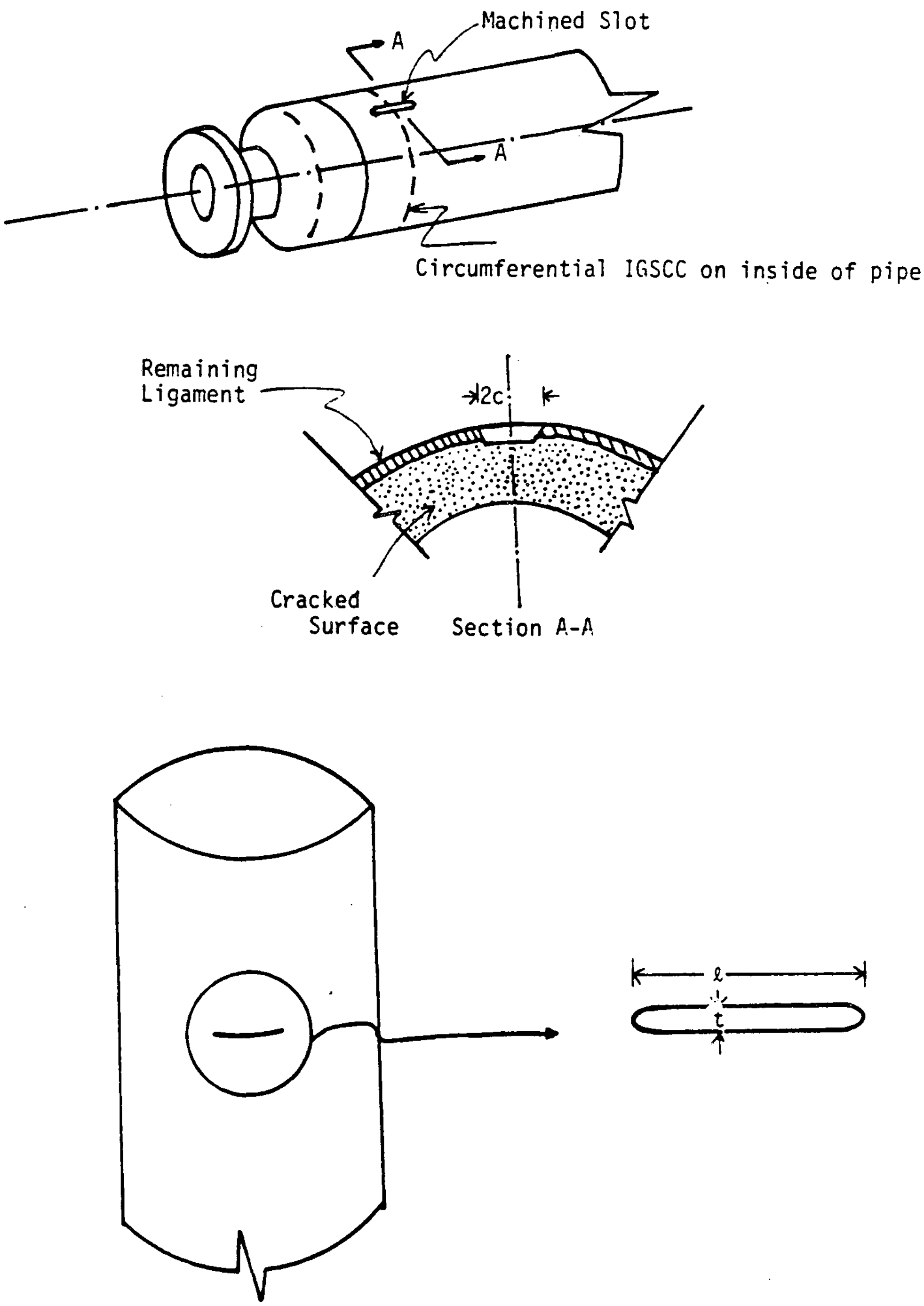

Figure 2.1 Illustration of BCL IGSCC Test Sections

Table 2.1 Test Parameters for BCL Phase II Experiments

	Stagnation Conditions			Crack Geometry					Measured
Test No.	P_o (MPa)	T_o (°C)	ΔT Subcooling (°C)	Depth L. (mm)	Width δ (mm)	Length 2c (mm)	Area Ratio AR	Opening Area A_2 (mm^2)	Leak Rate W (kg/s)
1	7.316	272.8	18.4	19.27	0.074	3.63	0.1	0.268	1.02×10^{-3}
2	7.316	272.8	18.4	"	"	"	"	"	"
3	8.667	267.2	34.2	"	"	"	"	"	1.10×10^{-3}
4	9.412	260.6	46.8	"	"	"	"	"	"
5	9.412	260.6	46.8	"	"	"	"	"	"
6	9.322	267.8	38.8	"	"	"	"	"	"
7	9.301	284.4	22.1	18.63	0.0220	0.74	0.04	0.0162	5.49×10^{-5}
8	9.446	281.7	25.9	"	0.0218	"	"	0.0161	6.66×10^{-5}
9	9.467	278.3	29.4	"	0.0216	"	"	0.0159	3.08×10^{-5}
10	5.702	273.3	.1	"	0.0208	"	"	0.0153	3.08×10^{-5}
11	5.971	262.8	13.6	"	0.0201	"	"	0.0148	1.34×10^{-5}
12	5.868	260.0	15.2	"	0.0199	"	"	0.0146	1.09×10^{-4}
13	5.854	268.3	6.7	"	0.0205	"	"	0.0151	1.51×10^{-4}
14	5.868	272.8	2.4	"	0.0208	"	"	0.0153	1.01×10^{-4}
15	3.523	251.7	-7.1	"	0.0190	"	"	0.0140	9.30×10^{-5}
16	3.379	241.1	1.1	"	0.0183	"	"	0.0135	1.05×10^{-4}
17	5.681	278.9	-5.7	"	0.0212	"	"	0.0156	1.01×10^{-4}
18	7.081	260.0	27.6	"	--	"	"	--	6.21×10^{-5}
19	7.309	273.9	15.8	19.27	0.108	9.53	0.13	1.026	3.04×10^{-2}
20	7.309	282.2	7.4	"	"	"	"	"	2.90×10^{-2}
21	9.005	280.0	24.2	"	"	"	"	"	4.85×10^{-2}
22	9.005	273.3	30.8	"	"	"	"	"	4.62×10^{-2}
23	8.964	256.7	39.3	"	"	"	"	"	4.52×10^{-2}
24	8.888	256.7	36.3	"	"	"	"	"	4.44×10^{-2}
25	7.164	256.1	32.2	"	"	"	"	"	3.67×10^{-2}
26	7.164	256.7	31.7	"	"	"	"	"	3.59×10^{-2}
27	5.571	260.6	11.4	"	"	"	"	"	2.51×10^{-2}
28	5.626	267.8	4.8	"	"	"	"	"	2.35×10^{-2}
29	5.592	241.7	30.5	"	"	"	"	"	3.01×10^{-2}
30	5.592	243.9	28.3	"	"	"	"	"	2.98×10^{-2}
31	7.219	242.8	46.1	"	"	"	"	"	3.96×10^{-2}
32	7.219	238.3	46.6	"	"	"	"	"	3.94×10^{-2}
33	8.812	241.7	60.9	"	"	"	"	"	4.51×10^{-2}
34	8.812	235.0	67.6	"	"	"	"	"	4.73×10^{-2}
35	7.129	226.1	61.9	"	"	"	"	"	3.84×10^{-2}
36	7.129	222.8	65.2	"	"	"	"	"	3.92×10^{-2}
37	5.592	220.0	52.2	"	"	"	"	"	3.84×10^{-2}
38	5.44	223.2	47.1	"	"	"	"	"	2.97×10^{-2}
39	3.937	230.6	20.3	"	"	"	"	"	2.62×10^{-2}
40	3.937	232.8	18.1	"	"	"	"	"	1.57×10^{-2}

Table 2.1 (continued)

Test No.	Stagnation Conditions P_0 (MPa)	T_0 (°C)	ΔT Subcooling (°C)	Crack Geometry Depth L (mm)	Width δ (mm)	Length 2c (mm)	Area Ratio AR	Opening Area A (mm^2)	Measured Leak Rate W (kg/s)
41	7.309	278.9	10.8	18.63	0.0535	1.59	0.09	0.0849	1.81×10^{-3}
42	8.060	277.2	19.2	"	0.0534	"	"	0.0848	1.98×10^{-3}
43	8.722	276.7	25.2	"	0.0535	"	"	0.0850	2.19×10^{-3}
44	9.377	274.4	32.6	"	0.0533	"	"	0.0847	2.37×10^{-3}
45	7.35	278.3	11.9	"	0.0534	"	"	0.0848	3.62×10^{-4}
46	8.067	275.0	21.4	"	0.0530	"	"	0.0842	5.26×10^{-4}
47	8.757	275.0	27.2	"	0.0533	"	"	0.0845	3.91×10^{-3}
48	9.432	272.2	35.3	"	0.0530	"	"	0.0841	4.37×10^{-3}
49	7.35	276.1	13.9	"	0.0530	"	"	0.0841	3.22×10^{-3}
50	8.067	274.4	20.3	"	0.0529	"	"	0.0840	3.59×10^{-3}
51	5.213	258.3	9.4	"	0.0490	"	"	0.0778	2.51×10^{-3}
52	6.923	253.9	32.1	"	0.0487	"	"	0.0773	3.54×10^{-3}
53	8.646	252.8	48.5	"	0.0491	"	"	0.0779	4.11×10^{-3}
54	5.213	256.7	11.1	"	0.0487	"	"	0.0773	2.20×10^{-3}
55	6.902	254.4	31.4	"	0.0488	"	"	0.0775	2.61×10^{-3}
56	8.646	253.3	47.9	"	0.0492	"	"	0.0781	3.17×10^{-3}
57	3.413	233.9	8.9	"	0.0438	"	"	0.0696	7.57×10^{-4}
58	5.171	232.8	34.5	"	0.0442	"	"	0.0711	9.03×10^{-4}
59	6.923	231.1	54.9	"	0.0445	"	"	0.0706	1.50×10^{-3}
60	8.646	228.9	72.4	"	0.0446	"	"	0.0708	1.85×10^{-3}
61	8.646	231.7	69.6	"	0.0451	"	"	0.0717	1.75×10^{-3}
62	7.033	228.3	58.0	"	0.0440	"	"	0.0698	1.76×10^{-3}
63	5.206	225.0	42.7	"	0.0428	"	"	0.0679	1.53×10^{-3}
64	3.448	222.8	20.6	"	0.0415	"	"	0.0663	1.33×10^{-3}
65	3.461	235.0	8.6	"	0.0441	"	"	0.0700	1.84×10^{-3}
66	5.185	232.2	35.3	"	0.0441	"	"	0.0700	2.32×10^{-3}
67	6.895	230.0	55.8	"	0.0443	"	"	0.0703	2.69×10^{-3}
68	8.646	228.3	71.8	"	0.0445	"	"	0.0707	2.69×10^{-3}
69	8.626	241.7	59.4	19.27	0.235	27.89	0.21	6.547	1.51×10^{-1}
70	6.936	236.8	49.5	"	0.227	"	"	6.338	1.39×10^{-1}
71	6.861	236.7	48.8	"	0.227	"	"	6.334	1.57×10^{-1}
72	8.536	241.1	59.3	"	0.234	"	"	6.528	1.75×10^{-1}
73	5.109	252.8	13.7	"	0.178	"	"	4.952	1.41×10^{-1}
74	6.861	253.9	31.6	"	0.243	"	"	6.787	1.69×10^{-1}
75	8.605	254.4	46.5	"	0.247	"	"	6.882	1.91×10^{-1}
76	8.598	250.6	50.3	"	0.243	"	"	6.779	2.00×10^{-1}
77	6.861	248.3	37.1	"	0.238	"	"	6.641	1.78×10^{-1}
78	5.192	246.1	21.4	"	0.173	"	"	4.828	1.51×10^{-1}
79	3.937	240.6	10.3	"	0.144	"	"	4.024	1.28×10^{-1}
80	5.089	236.1	30.2	"	0.166	"	"	4.633	1.55×10^{-1}
81	6.771	237.2	47.3	"	0.228	"	"	6.345	1.76×10^{-1}
82	8.577	234.4	66.3	"	0.228	"	"	6.355	1.99×10^{-1}

In Figure 2.2 photomicrographs of typical IGSCC in weld sensitized type 304 stainless steel are shown. These pictures reveal the tortuous and irregular nature of the channel with many expansions and contractions along the passage.

Table 2.2 Leak Before Failure Criterion

G_c = 3900 lb_m/ft^2 sec. Assumed.

Pipe ID in.	Pipe Wall Thickness, in.	ℓ_{5GPM} in.	ℓ_{crit}, in.	$\frac{\ell_{5GPM}}{\ell_{crit}}$
4	0.3	4.5	6.5	0.69
10	0.7	6.9	16	0.43
24	1.0	7.0	36	0.20

It should be noted that the BCL method of measuring the average crack thickness δ was not documented. Inconsistencies may be noted between some mass flowrate data and crack opening areas given in Table 2.1. It seems likely that this may be due in part to the difficulty in measuring δ. Another source of discrepancies may be the non-uniformity of δ and possible plugging of some cracks by small solid particles. These difficulties are real and impact the predictive capability of any model.

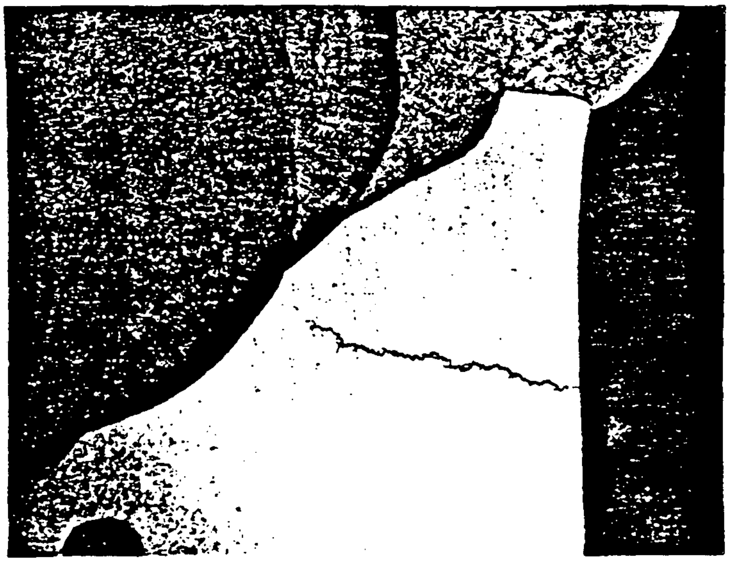

IGSCC IN WELD HEAT AFFECTED ZONE - 8X

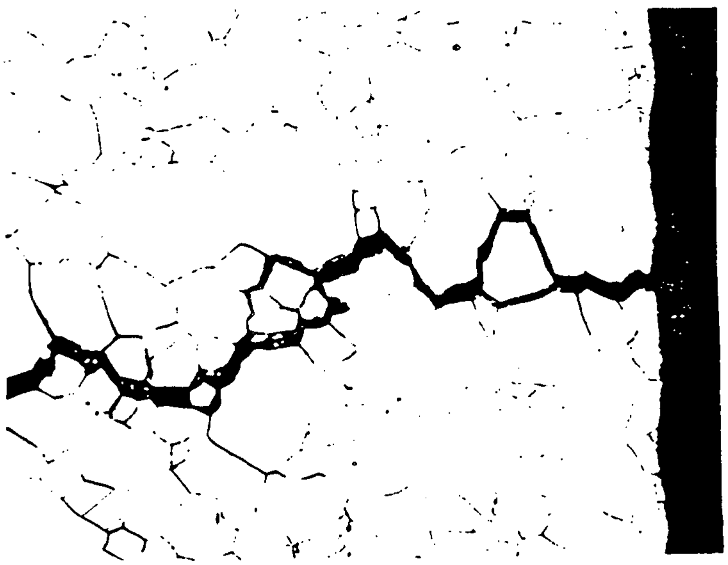

HIGHER MAGNIFICATION - 125X

Figure 2.2 Photomicrograph of Typical IGSCC in Weld Sensitized Type 304 Stainless Steel

3. MODELLING

In the models developed by Collier [7] and by Abdollahian and Chexal [10] it was assumed, similar to Henry's model [9], that the flow was homogeneous and the non-equilibrium effects were taken into account through the empirical parameter, N, which is a function of equilibrium quality and the flow path length to diameter ratio L/D. In addition to these assumptions the critical flow model developed and coded in the program LEAK included friction and acceleration pressure drops within the flow path and the pressure drop at entrance (sharp-edged entrance was assumed). In the code LEAK 00 the quality in the crack duct was assumed to vary linearly along the flow direction and was evaluated with assumption of isentropic flow. The friction pressure drop was calculated with the mass flux evaluated as the average of inlet and outlet mass flux. The surface roughness was taken as ε = 0.00178 mm and six 45 degree turns in the flow path were assumed to determine the friction pressure drop. In a subsequent code, LEAK 01, the quality was evaluated from an isenthalpic assumption, which is more nearly correct thermodynamically. The average mass flux was evaluated with the assumption of linearly varying cross-sectional area of the crack duct. For the friction pressure drop evaluation, a surface roughness of ε = 0.0051 mm and twenty 45-degree turns in the flow path were assumed.

In actual pipe IGSCCs the entrance to the crack duct does not represent sharp-edged geometry. The crack L/D ratios are large (>50) hence the homogeneous equilibrium assumption with a rounded entrance seems more appropriate. The values for L/D beyond which homogeneous equilibrium assumptions can be made have been reported in the literature. These values vary from 1.5 for reactor scale pipe breaks [13] to 25 for 4 mm diameter tubes with sharped entrance geometry. In the model of the LEAK code the flashing of the liquid in the crack channel is assumed to occur at Z = 12D irrespective of crack dimensions and thermodynamic properties of the upstream fluid. In the present work, the more realistic assumptions are made in modelling the critical flow through IGSCC as described in the next section.

3.1 Assumptions of the Present Model

The actual flow channel in an IGSCC (as shown in Figure 2.1) is approximated with a one dimensional convergent slit as shown in Figure 3.1. The convergence of the channel is determined by the specifications of inlet to exit area ratio and crack depth. Thus the flow area is assumed to vary linearly along the z-direction with the flow channel, while the slit gap is taken as uniform in transverse and in flow directions. As mentioned earlier, the fluid is considered homogeneous and in thermodynamic equilibrium. The entrance region is assumed to be smooth, hence frictionless. The gravitational effects

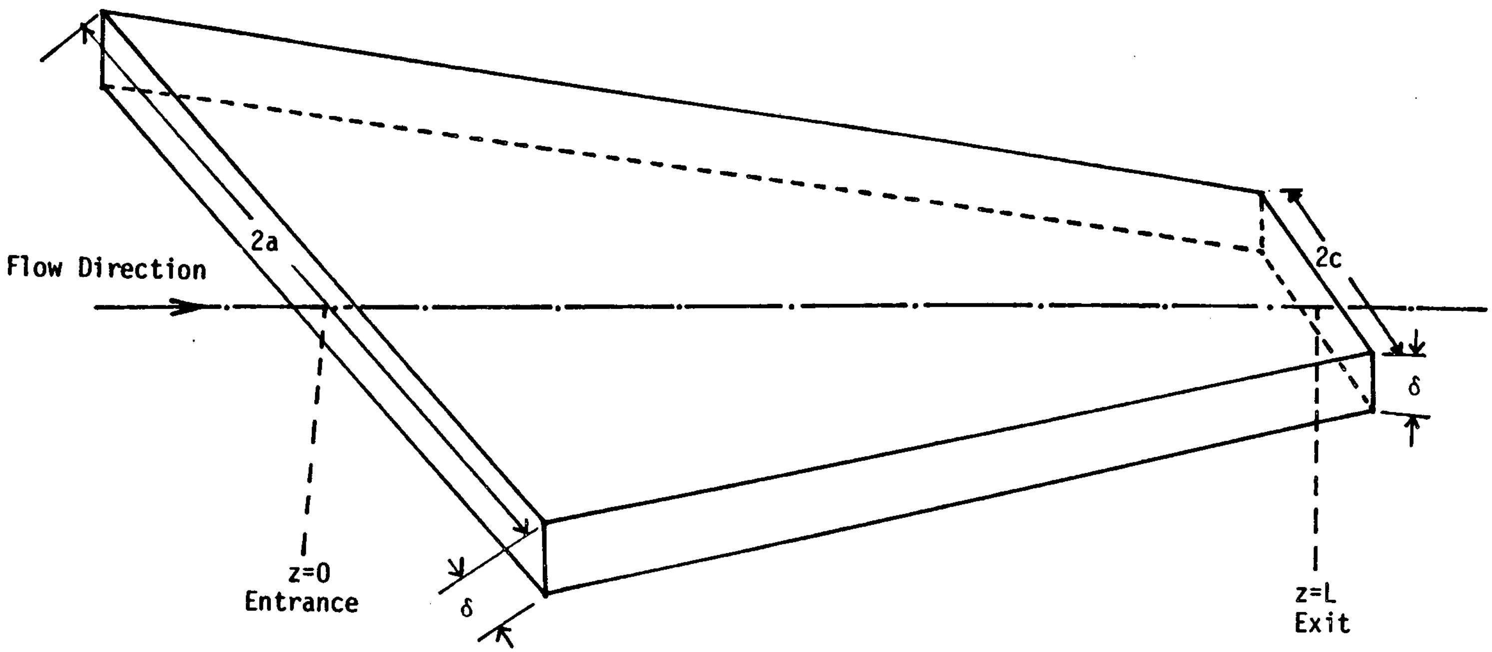

Figure 3.1 Idealized Geometry of the Crack

are neglected and the control surface of the geometry considered is assumed to be adiabatic. The flow is considered in steady state.

For subcooled stagnation conditions, the flow in the channel is divided into two regions, single phase and two-phase. The two phase region is assumed to begin at the plane where the liquid reaches the saturation pressure at T_0. Both single phase and two phase frictional pressure losses are calculated by assuming a single equivalent friction factor. Evaluation of the equivalent friction factor, which accounts for the tortuosity (bends, contractions, expansions) of the channel, is a key element in the modelling. In section 4.1 we present a parametric study of the BCL data to obtain optimized friction factors for each test section. In section 4.2 we present a generalized approach for estimating friction factors for IGSCC. This method is applied to the BCL test sections in Appendix A and the resulting friction factors used in an independent prediction of the BCL critical flow data.

3.2 Governing Equations

The continuity equation is

$$\frac{d}{dz}(\rho VA) = 0 \tag{3.1}$$

where $\dot{m} = \rho VA$.

The momentum equation is

$$-\frac{dP}{dz} = \rho V\frac{dV}{dz} + \frac{\tau_w P_m}{A} \quad . \tag{3.2}$$

The first term on right hand side of momentum equation is the acceleration pressure drop and the second term is the friction pressure drop.

The energy equation is

$$\frac{d}{dz}\left(h + \frac{V^2}{2}\right) = 0 \quad . \tag{3.3}$$

The state equations are

i) for two-phase mixture

$$v = (1 - x)v_f(P) + x\, v_g(P) = v_f(P) + x[v_g(P) - v_f(P)] \tag{3.4}$$

$$h = (1 - x)h_f(P) + x\, h_g(P) = h_f(P) + x\,[h_g(P) - h_f(P)] \tag{3.5}$$

ii) for single-phase liquid

$$v_\ell \simeq \text{constant} = v_f(T_o) \quad (3.6)$$

$$h_\ell \simeq h_f(T_o) \quad (3.7)$$

Critical Flow Criteria

Homogeneous equilibrium sound speed criterion was used to determine when the flow was critical. This is given as

$$V = V_a = \left\{ \left(\frac{\partial P}{\partial \rho} \right)_s \right\}^{1/2} \quad (3.8)$$

at the channel exit.

Using equations (3.2) to (3.5), equation (3.8) becomes

$$V_a = v \left[- \left\{ (1-x) \frac{dv_f}{dP} + x \frac{dv_g}{dP} + (v_g - v_f) \left(\frac{\partial x}{\partial P} \right)_s \right\} \right]^{1/2} \quad (3.9)$$

where

$$\left(\frac{\partial x}{\partial P} \right)_s = \frac{\left(\frac{ds_f}{dP} \right) (1-x) + x \left(\frac{ds_g}{dP} \right)}{(s_g - s_f)} \quad (3.10)$$

3.3 Development of Finite Difference Forms of Governing Equations

To achieve a numerical solution, the above equations are reduced to finite difference forms using a forward differencing scheme, which is numerically stable. The continuity and the energy equations, (3.1) and (3.3), are given in finite difference form as

$$\frac{\Delta}{\Delta z_i} (\rho A V)_i = \frac{\Delta \dot{m}_i}{\Delta z_i} = 0 \quad (3.11)$$

$$\frac{\Delta h_i}{\Delta z_i} + \frac{\Delta}{\Delta z_i} \left(\frac{1}{2} V^2 \right)_i = 0 \quad (3.12)$$

Here $\Delta z_i = z_{i+1} - z_i$, $\Delta h_i = h_{i+1} - h_i$,

and $\Delta\left(\frac{1}{2} V^2\right)_i = \frac{1}{2} V_{i+1}^2 - \frac{1}{2} V_i^2$.

The momentum equation (3.2) can be written as

$$-\left(\frac{dP}{dz}\right) = \frac{\dot{m}^2}{A^2}\left(\frac{dv}{dz}\right) - \frac{\dot{m}^2 v}{A^3}\left(\frac{dA}{dz}\right) + f\left(\frac{P_m}{A}\right)\frac{\dot{m}^2 v}{2A^2} \tag{3.13}$$

where f is an equivalent friction factor including effects of bends, contractions and expansions.

In equation (3.13) the first term on the right hand side is the pressure gradient due to phase change, the second term is the pressure gradient due to area change and the third term is pressure gradient due to friction in the crack channel. Equation (3.13) is integrated along the flow path to evaluate the overall pressure drop across the crack. The channel region is divided into two regions: a) entrance region; and b) main channel region.

a) Entrance region

i) Single phase entrance. (High stagnation subcooling)

With ideal flow assumed, the single phase pressure drop for flow between stagnation region and entrance region is obtained by using the Bernoulli equation (special case of equation (3.13))

$$\frac{P_o}{\rho_o} = \frac{P_1}{\rho_1} + \frac{V_1^2}{2}$$

or

$$P_{o-1} = \frac{1}{2}\rho_o V_1^2 = \frac{\dot{m}^2 v_o}{2A_1^2} \quad . \tag{3.14}$$

This case corresponds to $P_1 > P_{sat}(T_o)$. For the case with $P_1 = P_{sat}(T_o)$, there will be flashing at the entry. The entrance pressure drop is then

$$\Delta P_{o-1} = P_o - P_{sat}(T_o) \quad . \tag{3.15}$$

ii) Two phase entrance

In the case of very low stagnation subcooling the liquid may start to flash before entering the channel. In such cases the entrance pressure drop is calculated by the use of thermodynamic relationships for isentropic flow, i.e., both entropy and stagnation enthalpy remain constant. Thus we have

$$s_o = s_1 = s_{f1} + x_1 s_{fg1} \tag{3.16}$$

$$h_o = h_{f1} + x_1 h_{fg1} + \frac{V_1^2}{2} \tag{3.17}$$

and continuity

$$\dot{m} = \frac{A_1 V_1}{v_1} \tag{3.18}$$

where

$$v_1 = v_{f1} + x_1 v_{fg1} \quad .$$

With known values of A_1, $\dot{m}$, s_o, and h_o equations (3.16), (3.17) and (3.18) determine P_1, x_1 and V_1.

b) Main channel region.

i) Single phase flow

The single phase region ends at the point where the flashing occurs. The pressure drop between the entrance plane and the plane of flashing (where $P = P_{sat}$) is obtained from equation (3.13) neglecting the compressibility of the liquid, as

$$P_1 - P_{sat} = \frac{\dot{m}^2}{2} v_o \left(1 + \frac{\delta f}{\eta}\right) \left(\frac{1}{A_{f\ell}^2} - \frac{1}{A_1^2}\right) + \frac{\dot{m}^2 f v_o}{\delta \eta} \left(\frac{1}{A_{f\ell}} - \frac{1}{A_1}\right) \tag{3.19}$$

where $\eta \doteq \frac{2\delta}{L}(a-c)$.

Hence the flashing location is obtained in terms of the flashing area A_f

$$A_{f\ell} = \frac{1 + \left[1 + (\delta^2\eta^2 + \delta^3\eta f)/(\dot{m}^2 f^2 v_o)\right] C_1}{(\delta\eta/(\dot{m}^2 f\ v_o))\ C_1} \tag{3.20}$$

where

$$C_1 \doteq 2(P_1 - P_{sat}) + \frac{\dot{m}^2 v_o}{A_1{}^2}(1 + \frac{\delta f}{\eta}) + \frac{2\dot{m}^2 f\ v_o}{\delta\eta A_1} \ .$$

ii) Two-phase region

Now the pressure drop between two local points z_{i+1} and z_i in the channel can be written as

$$\Delta P_{(i+1-i)} = P_i - P_{i+1} = -\int_{z_i}^{z_{i+1}} \left(\frac{dP}{dz}\right) dz \qquad (3.21)$$

From equations (3.13) and (3.21) we have the pressure drop between two local points z_{i+1} and z_i as

$$\Delta P_{i+1-i} = \dot{m}^2 \int_{v_i}^{v_{i+1}} \frac{dv}{d^2} - \dot{m}^2 \int_{A_i}^{A_{i+1}} \frac{v}{A^3}\, dA + \frac{\dot{m}^2}{2} \int_{z_i}^{z_{i+1}} f\left(\frac{P_m}{A}\right)\left(\frac{v}{A^2}\right) dz \qquad (3.22)$$

Here

$$v_i = v(z = z_i)$$

$$v_{i+1} = v(z = z_{i+1})$$

$$A_i = A(z = z_i)$$

$$A_{i+1} = A(z = z_{i+1})$$

Now, the first integral in equation (3.22) is evaluated as follows

$$\dot{m}^2 \int_{v_i}^{v_{i+1}} \frac{dv}{A^2} = \frac{\dot{m}^2}{\bar{A}_i{}^2}(v_{i+1} - v_i) \qquad (3.23)$$

where

$$\bar{A}_i^2 = \frac{1}{2}(A_i{}^2 + A_{i+1}^2)$$

and the second integral is approximated by

$$\dot{m}^2 \int_{A_i}^{A_{i+1}} \frac{v}{A^3} (-dA) = \frac{\dot{m}^2 \bar{v}_i}{2} \left(\frac{L}{A_{i+1}^2} - \frac{1}{A_i^2} \right) \tag{3.24}$$

where

$$\bar{v}_i = \left(\frac{v_i + v_{i+1}}{2} \right) .$$

In order to evaluate third integral we have to evaluate (P_m/A) for the convergent crack geometry. A linear change in area of the crack channel is assumed in the present model. The local area A(z) is given as

$$A(z) = A_1 - \eta z \tag{3.25}$$

where

$$A_1 = 2a\delta \quad \text{and} \quad \eta \doteq \frac{2\delta}{L} (a-c) .$$

Hence

$$(P_m/A) = \frac{2}{A} \left(\frac{A}{\delta} + \delta\right) = 2\left(\frac{1}{\delta} + \frac{\delta}{A_1 - \eta z}\right) \tag{3.26}$$

Using equations (3.25) and (3.26) we have after simplifications

$$\frac{\dot{m}^2}{2} \int_{z_i}^{z_{i+1}} f\left(\frac{P_m}{A}\right)\left(\frac{v}{A^2}\right) dz = \frac{\dot{m}^2 f \bar{v}_i}{\delta \eta} \left[\left\{ \frac{1}{(A_1 - \eta z_{i+1})} - \frac{1}{(A_1 - \eta z_i)} \right\} + \frac{\delta^2}{2} \left\{ \frac{1}{(A_1 - z_{i+1})^2} - \frac{1}{(A_1 - \eta z_i)^2} \right\} \right] \tag{3.27}$$

Using equations (3.22), (3.23), (3.24) and (3.27) we have after some rearrangement

$$(\Delta P)_{i+1-i} = \frac{\dot{m}^2}{\bar{A}_i^2} (v_{i+1} - v_i) + \frac{\dot{m}^2 v_i}{2} \left(1 + \frac{\delta f}{\eta}\right) \times \left\{ \frac{1}{(A_1 - \eta z_{i+1})^2} - \frac{1}{(A_1 - \eta z_i)^2} \right\} + \frac{\dot{m}^2 f \bar{v}_i}{\delta \eta} \left\{ \frac{1}{(A_1 - \eta z_{i+1})} \quad \frac{1}{(A_1 - \eta z_i)} \right\} \tag{3.28}$$

The total pressure drop through the crack is then given as

$$(\Delta P)_T = (\Delta P)_{o-1} + (\Delta P)_{1-e} \tag{3.29}$$

The solution must simultaneously satisfy the continuity, energy and state equations.

The state equations (3.4) to (3.7) are given in difference form as

i) for two-phase homogeneous mixture

$$v_i = v_f(P_i) + x_i[v_g(P_i) - v_f(P_i)] \tag{3.30}$$

$$h_i = h_f(P_i) + x_i[h_g(P_i) - h_f(P_i)] \tag{3.31}$$

ii) for single-phase liquid

$$v_\ell = v_\ell(T_o) \simeq \text{constant} \tag{3.32}$$

$$h_\ell = h_\ell(T_o) \tag{3.33}$$

Using equations (3.30) to (3.31) the energy equation (3.12) becomes

$$h_o = h_f(P_i) + x_i[h_g(P_i) - h_f(P_i)] + \frac{\dot{m}^2}{2A_i^2}[v_f(P_i) + x_i\{v_g(P_i) - v_f(P_i)\}]^2 \tag{3.34}$$

Equation (3.34) can be rearranged to give the quality at mode i as

$$x_i = -C_2 + \left[C_2^{\,2} - \frac{2A_i^2(h_g - h_f)}{\dot{m}^2(v_g - v_f)} + \left(\frac{v_f}{v_g - v_f}\right)^2\right]^{1/2} \tag{3.35}$$

where

$$C_2 = \left[\frac{v_f}{v_g - v_f} + \frac{2A_i^2(h_g - h_f)}{\dot{m}^2(v_g - v_f)}\right]$$

and h and v are evaluated at P_i .

3.4 Computer Code (SOURCE) Logic

The difference equations presented in section 3.3 were programmed into a Fortran code called SOURCE. The logic of the code method is described in a SOURCE flow chart given in Appendix B. The SOURCE program listing is given in Appendix C. A brief description of the key features follows.

The governing steady equations are solved interatively marching downstream from the upstream stagnation region using an assumed mass flowrate. This develops the location of incipient flashing and the distribution of pressure and quality in the flow direction. At each node point the converged value of fluid velocity is compared with the HEM sound speed calculated for the local state. The marching procedure continues until either, a. the exit plane is reached at a subcritical flow state or b. a critical flow state is reached at a position upstream of the exit. In the first instance the assumed flowrate was too low, in second instance it was too high. The mass flowrate is adjusted systemmatically until a critical flow state is found at the exit plane within a small tolerance.

In principle any first guess flowrate will do, however, to reduce the number of iterations a simple approximate method of estimating the flowrate was built into SOURCE. The method uses the IHEM nozzle results tabulated by Hall [17] with a multiplier deduced from the BCL data. The multiplier is a linear function of L/D with subcooling as a parameter. As programmed this estimate may be made for stagnation temperature $480K \leq T_o \leq 550K$ and stagnation pressure $3 \leq P_o \leq 10$ MP_a.

The location of incipient flashing is found precisely using equation (3.20) for the case of incipient flashing within the channel. When flashing is initiated upstream of the channel equations (3.16) - (3.18) give the pressure and quality at the entrance. These results identify the region of two phase channel flow. Because the pressure gradient, in friction dominated critical flow, increases rapidly as the critical location is approached, a non-uniform axial discretization was chosen. Each successive distance $Dz(i) = (z_{i+1} - z_i)$ in just half the preceding one such that $Dz(i) = (DzT)2^{N-i}$. With the total two phase length given by $zTP = \sum_{i=1}^{N} Dz(i)$ the number of nodes N is fixed by the requirement that $DzT \leq 10^{-7}$ m.

The first node in the two phase region used a subroutine GUESS for an estimate of the pressure gradient, which changes stepwise at incipient flashing in the HEM model. GUESS uses the single phase pressure gradient to estimate the pressure P_{i+1} by forward extrapolation. This pressure is in turn used to evaluate an approximate quality x_{i+1} from equation (3.34). This quality is then used to evaluate the two phase friction multiplier with the aid of a linear fit to the result of Martinelli and Nelson [18].

$$\phi_{lo}^2 = 1.20\ (v_{fg}/v_f)(1.42 - 1.67 \times 10^{-4}P)\ x^{0.9} + 1\ . \qquad (3.36)$$

A second estimate of P_{i+1} is then obtained by extrapolating the two phase pressure gradient. The second estimate of x_{i+1} is then the first guess for iterative solution of equations (3.28) through (3.35).

For subsequent axial nodes the last evaluated pressure gradient is extrapolated forward to obtain a first estimate of P_{i+1}. Use of the energy equation (3.34) then gives the first guess x_{i+1} for iterative solution of equations (3.28) through (3.35).

After downstream marching is terminated by reaching a critical flow state or the channel exit, the flowrate is then corrected accordingly. When the exit is reached at a Mach number $M < 1.0$, the flowrate is corrected by

$\dot{m}_{new} = \dot{m}_{old}\ M^{-0.05}$ and a new solution is generated. If again the flow is subcritical at the exit the same correction is applied. This procedure is repeated until the new flowrate results in a critical flow state upstream of the exit. The desired solution is then bracketed by the last subcritical flow $\dot{m}_1$ and the last supercritical flow $\dot{m}_2$. The flowrate correction

$\dot{m} = \dfrac{\dot{m}_1 + \dot{m}_2}{2}$ is then used. If this flowrate gives a critical flow state upstream of the exit, it becomes the new $\dot{m}_2$. If instead it gives a subcritical flow at the exit it becomes the new $\dot{m}_1$. Successive corrections then converge rapidly and the solution is accepted when, for $M_e<1$, $(1-M_e) \leq 10^{-3}$ or when a critical flow state is reached at a position $\leq 10^{-7}$m upstream of the exit.

Thermodynamic properties of saturated liquid and vapor are evaluated using a subroutine STEAM which is described in Appendix D. This subroutine is very fast running and contributes to the efficiency of the numerical calculations.

The code was found to be very fast running. A typical computation required about 22 flowrate corrections and was completed in about 3 seconds of CPU time on an IBM 3081.

4. RESULTS

4.1 Parametric Study of BCL Data

Table 2.1 gives data of BCL phase II experiments carried out on IGSCC. In order to establish appropriate friction factors for the actual cracks all the BCL data except 21 were studied with SOURCE. These 21 tests (numbers 7, 8, 9, 10, 11, 13, 18, 41, 42, 43, 57, 58, 59, 60, 61, 62, 63, 73, 78, 79 and 80) were disqualified for the paramatric study, because they showed inconsistent measured mass flow rates in relation to the stagnation conditions, when compared with the main body of experimental data for their respective test sections. For initial SOURCE runs, certain values of friction factor were tried for each crack size so that the predicted mass flowrates compared well with the measured data. This process required running SOURCE least three friction factor values for each experimental test condition. Then an optimum value of friction factor was obtained for each crack size. This involved a graphical interpolation procedure. The optimum values of friction factor for each test section are given in Table 4.1. From the table we find that for the test section used for runs 1-6, the friction factor so obtained is quite high. For these test numbers the mass flow rate is in the range of 10^{-3} kg/s. The opening area of the crack was 0.268 mm which is quite high compared with the test section used for test numbers 41 to 68, for which the measured mass flow rates were in the range of 10^{-3} kg/s as well. Comparing the mass flow rates and crack geometry for tests 1-6 with other test sections, it is concluded that either the crack channel was blocked by particles during experimental measurements, as observed in destructive tests of pipes following BCL experiments, or the geometry of the crack is not properly given.

Once the optimum equivalent friction factor was obtained it was used again to run SOURCE for each test condition. When these results were compared it was apparent that a systematic deviation existed between the prediction and the measured data that was dependent upon the stagnation subcooling. It was found that the higher value of friction factor was necessary for smaller subcooling than at higher subcooling. This is physically plausible since at lower subcooling the two-phase region is longer than that with higher subcooling, and hence the effective friction factor for the case with longer two-phase region should be greater than for the case with smaller two-phase region. The subcooling for the BCL tests varied from 0.1C to 78C. A correction factor was developed to account for the subcooling effects. The subcooling correction factor is given by

$$\left.\begin{aligned} C &= 1.3015 - 5.3075 \times 10^{-3}\ \Delta T_{sub} \text{ for } \Delta T_{sub} < 60^{o}C \\ &= 1.0 \text{ for } \Delta T_{sub} > 60^{o}C \end{aligned}\right\} \quad (4.1)$$

Table 4.1 BCL Friction Factors from Parametric Study

Test Numbers	δ mm Average	L mm	A_e mm^2 Average	$\dot{m}$ Kg/s Range	f
1 - 6	0.074	19.27	0.268	10^{-3}	9.0
7 - 18	0.0205	18.63	0.0151	10^{-4}	0.8
19 - 40	0.108	19.27	1.026	10^{-2}	0.07
41 - 68	0.0488	18.63	0.0777	10^{-3}	0.02
69 - 82	0.220	19.27	6.133	10^{-1}	0.30

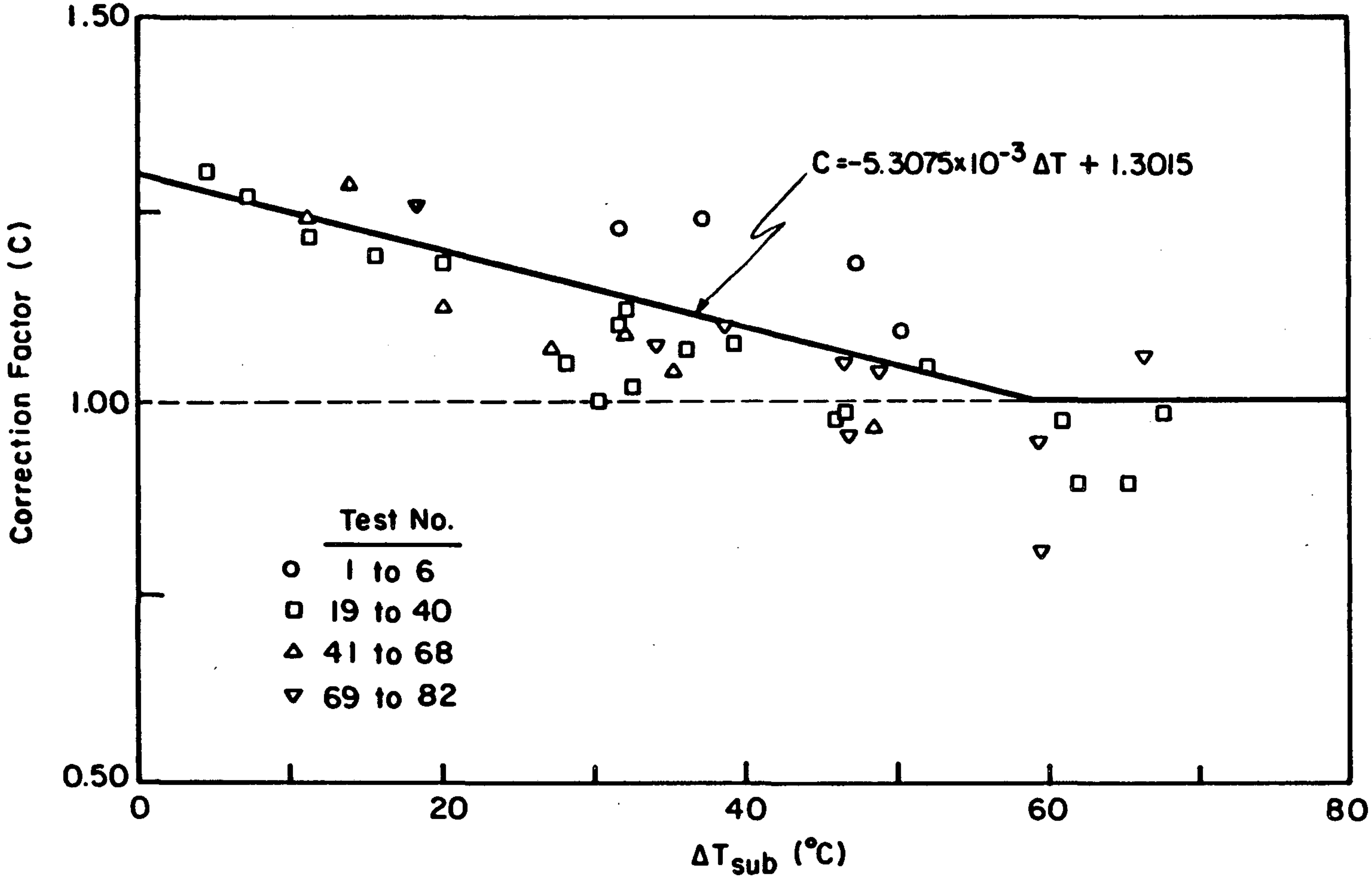

Figure 4.1 Subcooling Correction for SOURCE

In Table 4.2, the calculated mass flow rates, pressure and quality at the exit plane using SOURCE are presented for all the BCL phase II tests. These calculated values of mass flow rates when multiplied by the correction factor C, to account for the subcooling effect, then become the predicted mass flow rates. The predicted mass flow rates for 61 test numbers have been compared with BCL measured date in Figure 4.2. The comparison is remarkably good with standard deviation of 1.35%. When all the total 82 test number predictions were compared with BCL data, the standard deviation was 6.45%. Considering the evident lack of coherence in the basic BCL data, these comparisons show that the predictive method developed here offers an excellent capability to predict crack flows if the geometry is known.

4.2 Generalized Prediction of Equivalent Friction Factors

Choice of the optimum friction factor used to predict the results given in Table 4.2 was based on the parametric study of BCL data. For general use of SOURCE a methodology to estimate the equivalent friction factor from global features of IGSCCs is required. In this section we present a methodology which has been tested against the results of the parametric study of the BCL data in Appendix A.

The friction pressure drop in equation (3.13) was presented by an equivalent friction factor in the form

$$\left(\frac{dp}{dz}\right)_F = f\left(\frac{P_m}{A}\right) \cdot \frac{\dot{m}^2 v}{2A^2} \qquad (4.2)$$

and

$$f = f_p + D \sum_i n_i K_i \qquad (4.3)$$

where f_p represents "pipe" friction and the K_i represent the loss factors for specific effects such as bends, contractions, expansions and tortuosity and the n_i represents the number per unit length in the flow direction of the type i.

Assigning i = 1, for bends, i = 2 for contraction and i = 3 for expansions. The respective loss coefficients per unit length are given by [14].

For bends $n_i K_1 = (n_i - \frac{1}{L})(0.25\, f_p \cdot \pi \cdot (\frac{r}{D}) + 0.5\, K') + K'/L \qquad (4.4)$

when n_1 is number of bends per unit length, r is the radius of the bend D is the hydraulic diameter, f_p is the tube friction factor, and

Table 4.2 SOURCE Predictions Using Friction Factors from BCL Parametric Study

Test Number	Stagnation Conditions		Measured	Present Predictions		
	P_o, MPa	T_o, C	$\dot{m}$ Kg/sec	$\dot{m}$ Kg/sec	x_e	P_e MPa
1	7.316	272.8	1.02×10^{-3}	8.129×10^{-4}	2.297×10^{-1}	0.762
2	7.316	272.8	1.02×10^{-3}	8.129×10^{-4}	2.297×10^{-1}	0.762
3	8.667	267.2	1.10×10^{-3}	1.025×10^{-3}	1.984×10^{-1}	1.005
4	9.412	260.6	1.10×10^{-3}	1.153×10^{-3}	1.840×10^{-1}	0.952
5	9.412	260.6	1.10×10^{-3}	1.153×10^{-3}	1.840×10^{-1}	0.952
6	9.322	267.8	1.10×10^{-3}	1.000×10^{-3}	1.806×10^{-1}	1.278
7	9.301	284.4	5.49×10^{-5}	1.636×10^{-4}	2.495×10^{-1}	0.837
8	9.446	281.7	6.66×10^{-5}	1.676×10^{-4}	1.542×10^{-1}	2.371
9	9.467	278.3	3.08×10^{-5}	1.706×10^{-4}	1.420×10^{-1}	2.433
10	5.702	273.3	3.08×10^{-5}	8.809×10^{-4}	1.735×10^{-1}	1.604
11	5.971	262.8	1.34×10^{-4}	1.052×10^{-4}	1.415×10^{-1}	1.674
12	5.868	260.0	1.09×10^{-4}	1.043×10^{-4}	1.426×10^{-1}	1.525
13	5.854	268.3	1.51×10^{-4}	6.286×10^{-5}	4.817×10^{-1}	1.327
14	5.868	272.8	1.01×10^{-4}	9.394×10^{-5}	1.799×10^{-1}	1.445
15	3.523	251.7	9.30×10^{-5}	6.226×10^{-5}	1.560×10^{-1}	1.051
16	3.379	241.1	1.05×10^{-4}	5.483×10^{-5}	1.498×10^{-1}	0.858
17	5.861	278.9	1.01×10^{-4}	6.736×10^{-5}	3.503×10^{-1}	5.321
18	7.081	260.0	6.21×10^{-5}	-	-	-

Table 4.2 (continued)

Test Number	Stagnation Conditions		Measured	Present Predictions		
	P_0, MPa	T_0, C	$\dot{m}$ Kg/sec	$\dot{m}$ Kg/sec	x_e	P_e MPa
19	7.309	273.9	3.04×10^{-2}	2.506×10^{-2}	2.985×10^{-2}	4.998
20	7.309	282.2	2.90×10^{-2}	2.252×10^{-2}	6.109×10^{-2}	4.830
21	9.005	280.0	4.85×10^{-2}	3.120×10^{-2}	1.202×10^{-2}	6.070
22	9.005	273.3	4.62×10^{-2}	3.479×10^{-2}	0.0	5.796
23	8.964	256.7	4.52×10^{-2}	4.200×10^{-2}	0.0	4.448
24	8.888	256.7	4.44×10^{-2}	4.165×10^{-2}	0.0	4.448
25	7.164	256.1	3.67×10^{-2}	3.285×10^{-2}	0.0	4.404
26	7.164	256.7	3.59×10^{-2}	3.255×10^{-2}	0.0	4.448
27	5.571	260.6	2.51×10^{-2}	2.155×10^{-2}	2.011×10^{-2}	3.967
28	5.626	267.8	2.35×10^{-2}	1.805×10^{-2}	5.524×10^{-2}	3.852
29	5.592	241.7	3.01×10^{-2}	2.931×10^{-2}	0.0	3.449
30	5.592	243.9	2.98×10^{-2}	2.833×10^{-2}	0.0	3.584
31	7.219	242.8	3.96×10^{-2}	3.850×10^{-2}	0.0	3.516
32	7.219	238.3	3.94×10^{-2}	4.003×10^{-2}	0.0	3.249
33	8.812	241.7	4.51×10^{-2}	4.640×10^{-2}	0.0	3.449
34	8.812	235.0	4.73×10^{-2}	4.819×10^{-2}	0.0	3.074
35	7.129	226.1	3.84×10^{-2}	4.317×10^{-2}	0.0	2.603
36	7.129	222.8	3.92×10^{-2}	4.402×10^{-2}	0.0	2.447
37	5.592	220.0	3.84×10^{-2}	3.686×10^{-2}	0.0	2.320
38	5.440	223.2	2.97×10^{-2}	3.506×10^{-2}	0.0	2.465

Table 4.2 (continued)

Test Number	Stagnation Conditions		Measured	Present Predictions		
	P_0, MP_a	T_0, ^0C	$\dot{m}$ Kg/sec	$\dot{m}$ Kg/sec	x_e	P_e MPa
39	3.937	230.6	2.62×10^{-2}	2.224×10^{-2}	0.0	2.827
40	3.937	232.8	1.57×10^{-2}	2.010×10^{-2}	0.0	2.944
41	7.309	278.9	1.81×10^{-3}	2.344×10^{-3}	2.439×10^{-2}	5.586
42	8.060	277.2	1.98×10^{-3}	3.049×10^{-3}	0.0	6.153
43	8.722	276.7	2.19×10^{-3}	3.553×10^{-3}	0.0	6.103
44	9.377	274.4	2.37×10^{-3}	2.334×10^{-3}	0.0	5.895
45	7.350	278.3	3.62×10^{-4}	2.405×10^{-3}	1.912×10^{-2}	5.676
46	8.067	275.0	5.26×10^{-4}	3.161×10^{-3}	0.0	5.950
47	8.757	275.0	3.91×10^{-3}	3.658×10^{-3}	0.0	5.950
48	9.432	272.2	4.37×10^{-3}	4.207×10^{-3}	0.0	5.950
49	7.350	276.1	3.22×10^{-3}	2.510×10^{-3}	0.0	6.051
50	8.067	274.4	3.59×10^{-3}	3.197×10^{-3}	0.0	5.895
51	5.213	258.3	2.51×10^{-3}	1.689×10^{-3}	0.0	4.566
52	6.923	253.9	3.54×10^{-3}	3.257×10^{-3}	0.0	4.246
53	8.646	252.8	4.11×10^{-3}	4.260×10^{-3}	0.0	4.169
54	5.213	256.7	2.20×10^{-3}	1.777×10^{-3}	9.473×10^{-3}	4.203
55	6.902	254.4	2.61×10^{-3}	3.229×10^{-3}	0.0	4.282
56	8.646	253.3	3.17×10^{-3}	4.256×10^{-3}	0.0	4.204
57	3.413	233.9	7.57×10^{-4}	1.166×10^{-3}	9.002×10^{-3}	2.817
58	5.171	232.8	9.03×10^{-4}	2.706×10^{-3}	0.0	2.944
59	6.923	231.1	1.50×10^{-3}	3.644×10^{-3}	0.0	2.855

Table 4.2 (continued)

Test Number	Stagnation Conditions		Measured	Present Predictions		
	P_0, MP_a	T_0, °C	$\dot{m}$ Kg/sec	$\dot{m}$ Kg/sec	x_e	P_e MPa
60	8.646	228.9	1.85×10^{-3}	4.414×10^{-3}	0.0	2.742
61	8.646	231.7	1.75×10^{-3}	4.420×10^{-3}	0.0	2.886
62	7.033	228.3	1.76×10^{-3}	3.708×10^{-3}	0.0	2.712
63	5.206	225.0	1.53×10^{-3}	2.810×10^{-3}	0.0	2.550
64	3.448	222.8	1.33×10^{-3}	1.672×10^{-3}	0.0	2.447
65	3.461	235.0	1.84×10^{-3}	1.171×10^{-3}	1.050×10^{-2}	2.844
66	5.185	232.2	2.32×10^{-3}	2.688×10^{-3}	0.0	2.913
67	6.895	230.0	2.69×10^{-3}	3.640×10^{-3}	0.0	2.797
68	8.646	228.3	2.69×10^{-3}	4.418×10^{-3}	0.0	2.712
69	8.626	241.7	1.51×10^{-1}	1.797×10^{-1}	0.0	3.449
70	6.936	236.8	1.39×10^{-1}	1.455×10^{-1}	0.0	3.163
71	6.861	236.7	1.57×10^{-1}	1.440×10^{-1}	0.0	3.158
72	8.536	241.1	1.75×10^{-1}	1.741×10^{-1}	0.0	3.413
73	5.109	252.8	1.41×10^{-1}	5.656×10^{-2}	7.546×10^{-2}	2.447
74	6.861	253.9	1.69×10^{-1}	1.339×10^{-1}	2.205×10^{-2}	3.709
75	8.605	254.4	1.91×10^{-1}	1.731×10^{-1}	0.0	4.282
76	8.598	250.6	2.00×10^{-1}	1.747×10^{-1}	0.0	4.018
77	6.861	248.3	1.78×10^{-1}	1.371×10^{-1}	1.995×10^{-3}	3.818
78	5.192	246.1	1.51×10^{-1}	6.733×10^{-2}	5.056×10^{-2}	2.606
79	3.937	240.6	1.28×10^{-1}	3.762×10^{-2}	6.916×10^{-2}	1.985
80	5.089	236.1	1.55×10^{-1}	6.793×10^{-2}	2.330×10^{-2}	2.643

Table 4.2 (continued)

Test Number	Stagnation Conditions		Measured	Present Predictions		
	P_0, MP_a	T_0, ^oC	$\dot{m}$ Kg/sec	$\dot{m}$ Kg/sec	x_e	P_e MPa
81	6.771	237.2	1.76×10^{-1}	1.422×10^{-1}	0.0	3.186
82	8.577	234.4	1.99×10^{-1}	1.777×10^{-1}	0.0	3.030

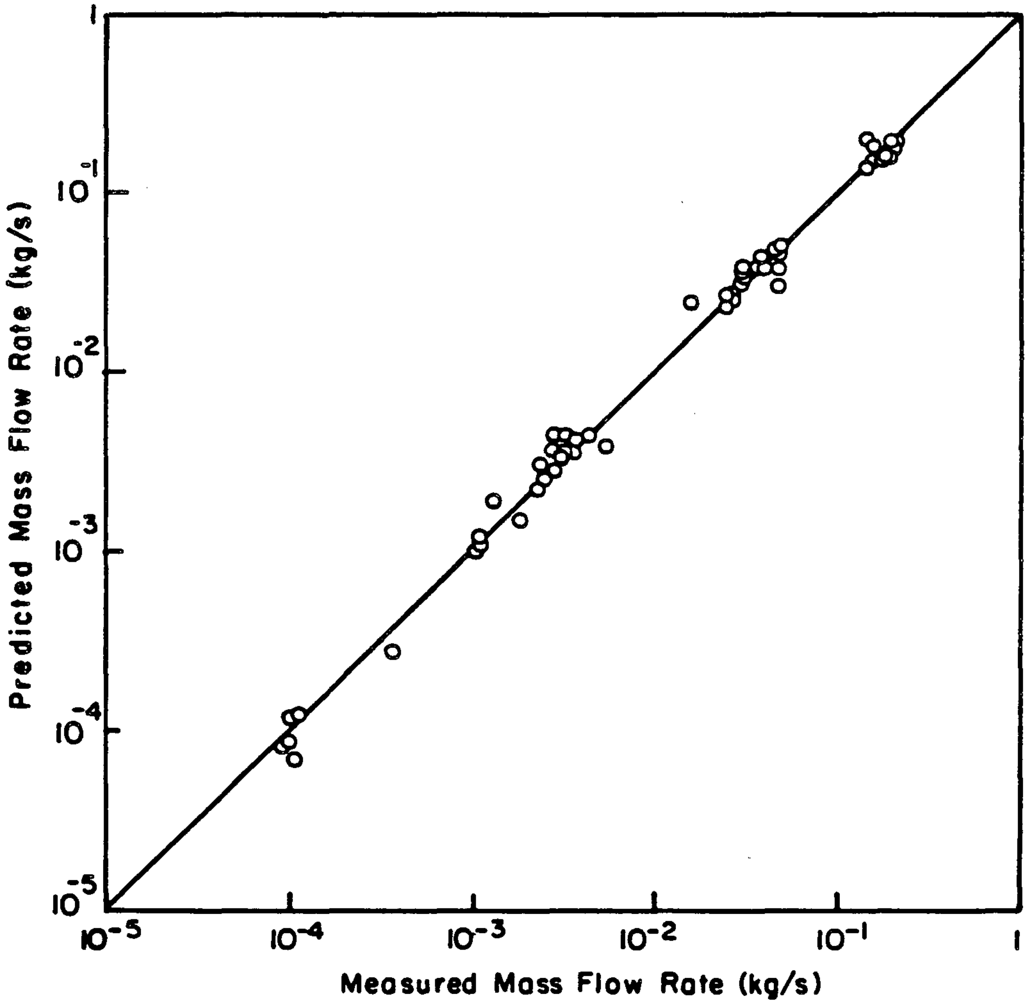

Figure 4.2 Corrected SOURCE Predictions (Based on Optimum Friction Factor) Compared with BCL Data

$K' \doteq 15\ f_p$ for 45^0 bends $K' \doteq 30\ f_p$ for 90^0 bends.

For contractions $n_2K_2 = (0.8 \sin \frac{\alpha}{2} (1-\beta^2))n_2$ (4.5)

For expansions $n_3K_3 = (2.6 \sin \frac{\alpha}{2} (1-\beta^2)^2)\cdot n_3$. (4.6)

Here n_2, n_3 are respectively, number per unit length of contractions and expansions, α is the angle of convergence, and β is the ratio of lower to higher diameter.

Close observation of photomicrographs of the IGSCC reveals that the bends, contractions and expansions each appear in the crack channel at intervals of approximately 10δ. For evaluating the loss coefficients K_i, the bends in the crack were approximated on the average as 45^0 bends. The ratio r/D was approximated a constant 0.60. Then the loss coefficient K_1 for bends can be calculated as

$$K_1 = 8f_p + \frac{7f_p}{n_1L_1} \quad (4.7)$$

To evaluate the loss coefficient due to contraction and expansions, the angle of convergence was approximated to be 45 degrees and $\beta = 0.5$ was used.

The number of bends per unit length was evaluated as the

$$n_1 = \frac{1}{10\delta} \quad (4.8)$$

The number of contractions or expansions per unit length was evaluated as

$$n_2 + n_3 = \frac{1}{10\delta} \quad \text{with } n_2 = n_3 \ . \quad (4.9)$$

The method of evaluating the equivalent friction factor involves determining the friction f_p for the crack and then the loss coefficients are determined using equations (4.5) through (4.7). Then using the equation (4.3) the equivalent frcition factor f is determined.

To determine the friction factor f_p, Reynolds number has to be evaluated. As the inlet and outlet area are different the Reynolds number was taken as the average value of the Reynolds numbers at inlet and outlet plane of the crack. The surface roughness was taken as ε = 1.78μ. This value for surface roughness was used in the BCL LEAK 00 code. Depending on the relative surface roughness ε/D and Re the friction factor was determined from the standard charts.

The above methodology was applied for all the test cases of BCL test sections to evaluate the equivalent friction factor (see Appendix A). Using these values of equivalent friction factor the mass flow rate predictions were obtained for the 61 tests. SOURCE predictions using these friction factors, corrected for subcooling, are compared with BCL data in Table 4.3 and in Figure 4.3. Except for the prediction for Tests 1-6, the results compare well with BCL data, with a standard derivation of 15.90%. These predictions appear to be better than the prediction by Chexal et al.[16] with LEAK-01, which is shown in Figure 4.4.

As already noted, the test section used for Test 1-6 was evidently partially plugged probably during the machining. As a result the friction factor given by the generalized method does not represent that test section and the predicted flow rate is about 4 times the measured value. Although there is no conclusive evidence, it seems unlikely that such extensive plugging value, could occur in an actual IGSCC. If it does, the extent of the crack would be under-estimated by the observed leak rate. Further experimental investigation is needed using improved techniques to produce test cracks.

4.3 Quality and Pressure Profiles

SOURCE calculations develop predictions of the profile of fluid state along the flow path, including the state (critical state) at the point of choking, as well as the critical flow rate. In Appendix E we present graphs of the quality and pressure profiles predicted for 20 of the BCL test conditions. Negative quality characterizes the subcooled liquid region so that flashing starts at the point where $x = o$.

The very steep slopes at the exit point up the need for very fine noding near the exit to avoid error in the numerical computations.

Table 4.3 SOURCE Predictions Using Friction Factors from Generalized Methodology

Test Number	Stagnation Conditions P_o, MPa	T_o, C	Measured $\dot{m}$ Kg/sec	Present Prediction $\dot{m}$ Kg/sec
1	7.316	272.8	$1.02x10^{-3}$	$4.386x10^{-3}$
2	7.316	272.8	$1.02x10^{-3}$	$4.386x10^{-3}$
3	8.667	267.2	$1.10x10^{-3}$	$4.785x10^{-3}$
4	9.412	260.6	$1.10x10^{-3}$	$5.005x10^{-3}$
5	9.412	260.6	$1.10x10^{-3}$	$5.005x10^{-3}$
6	9.322	267.8	$1.10x10^{-3}$	$4.895x10^{-3}$
12	5.868	260.0	$1.09x10^{-4}$	$1.482x10^{-4}$
14	5.868	272.8	$1.01x10^{-4}$	$1.343x10^{-4}$
15	3.523	251.7	$9.30x10^{-5}$	$9.486x10^{-5}$
16	3.379	241.1	$1.05x10^{-4}$	$8.715x10^{-5}$
17	5.681	278.9	$1.01x10^{-4}$	$1.020x10^{-4}$
19	7.309	273.9	$3.04x10^{-2}$	$2.067x10^{-2}$
20	7.309	282.2	$2.90x10^{-2}$	$1.682x10^{-2}$
21	9.005	280.0	$4.85x10^{-2}$	$2.619x10^{-2}$
22	9.005	273.3	$4.62x10^{-2}$	$2.910x10^{-2}$
23	8.694	256.7	$4.52x10^{-2}$	$3.026x10^{-2}$
24	8.888	256.7	$4.44x10^{-2}$	$2.931x10^{-2}$
25	7.164	256.1	$3.67x10^{-2}$	$2.312x10^{-2}$
26	7.164	256.7	$3.59x10^{-2}$	$2.297x10^{-2}$
27	5.571	260.6	$2.51x10^{-2}$	$1.456x10^{-2}$
28	5.626	267.8	$2.35x10^{-2}$	$1.245x10^{-2}$
29	5.592	241.7	$3.01x10^{-2}$	$2.062x10^{-2}$
30	5.592	243.9	$2.98x10^{-2}$	$1.996x10^{-2}$
31	7.219	242.8	$3.96x10^{-2}$	$2.853x10^{-2}$
32	7.219	238.3	$3.94x10^{-2}$	$2.916x10^{-2}$
33	8.812	241.7	$4.51x10^{-2}$	$3.382x10^{-2}$
34	8.812	235.0	$4.73x10^{-2}$	$3.263x10^{-2}$
35	7.129	226.1	$3.84x10^{-2}$	$2.957x10^{-2}$
36	7.129	222.8	$3.92x10^{-2}$	$2.942x10^{-2}$

Table 4.3 (continued)

Test Number	Stagnation Conditions P_o, MPa	T_o, C	Measured $\dot{m}$ Kg/sec	Present Prediction $\dot{m}$ Kg/sec
37	5.592	220.0	3.84×10^{-2}	2.573×10^{-2}
38	5.440	223.2	2.97×10^{-2}	2.435×10^{-2}
39	3.937	230.6	2.62×10^{-2}	1.546×10^{-2}
40	3.937	232.8	1.57×10^{-2}	1.316×10^{-2}
43	8.722	276.7	2.19×10^{-3}	1.664×10^{-3}
44	9.377	274.4	2.37×10^{-3}	1.848×10^{-3}
47	8.757	275.0	3.91×10^{-3}	1.603×10^{-3}
48	9.432	272.2	4.37×10^{-3}	1.857×10^{-3}
49	7.350	276.1	3.22×10^{-3}	1.385×10^{-3}
50	8.067	274.4	3.59×10^{-3}	1.436×10^{-3}
51	5.213	258.3	2.51×10^{-3}	0.978×10^{-3}
52	6.923	253.9	3.54×10^{-3}	1.451×10^{-3}
53	8.646	252.8	4.11×10^{-3}	1.891×10^{-3}
54	5.213	256.7	2.20×10^{-3}	0.910×10^{-3}
55	6.902	254.4	2.61×10^{-3}	1.409×10^{-3}
56	8.646	253.3	3.17×10^{-3}	1.933×10^{-3}
62	7.033	228.3	1.76×10^{-3}	1.487×10^{-3}
63	5.206	225.0	1.53×10^{-3}	1.117×10^{-3}
64	3.448	222.8	1.33×10^{-3}	0.731×10^{-3}
65	3.461	235.0	1.84×10^{-3}	0.717×10^{-3}
66	5.185	232.2	2.32×10^{-3}	1.206×10^{-3}
67	6.895	230.0	2.69×10^{-3}	1.614×10^{-3}
68	8.646	228.3	2.69×10^{-3}	2.313×10^{-3}
69	8.626	241.7	1.51×10^{-1}	2.219×10^{-1}
70	6.936	236.8	1.39×10^{-1}	1.876×10^{-1}
71	6.861	236.7	1.57×10^{-1}	1.931×10^{-1}
72	8.536	241.1	1.75×10^{-1}	2.275×10^{-1}
74	6.861	253.9	1.69×10^{-1}	1.690×10^{-1}
75	8.605	254.4	1.91×10^{-1}	2.421×10^{-1}
76	8.598	250.6	2.00×10^{-1}	2.344×10^{-1}

Table 4.3 (continued)

Test Number	Stagnation Conditions P_o, MPa	T_o,C	Measured $\dot{m}$ Kg/sec	Present Prediction $\dot{m}$ Kg/sec
77	6.861	248.3	1.78×10^{-1}	2.344×10^{-1}
81	6.771	237.2	1.76×10^{-1}	1.901×10^{-1}
82	8.577	234.4	1.99×10^{-1}	2.328×10^{-1}

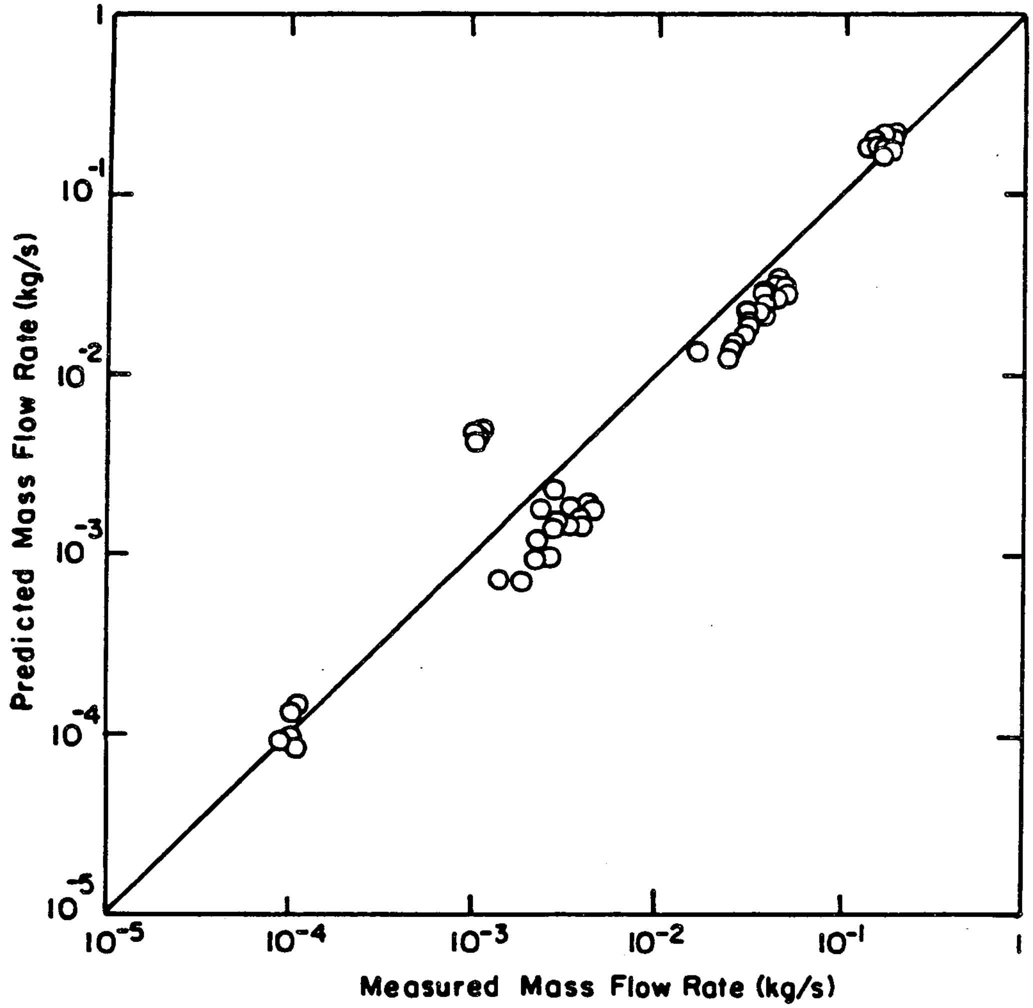

Figure 4.3 Corrected SOURCE Predictions (Based on Friction Factor from Generalized Method) Compared with BCL Data

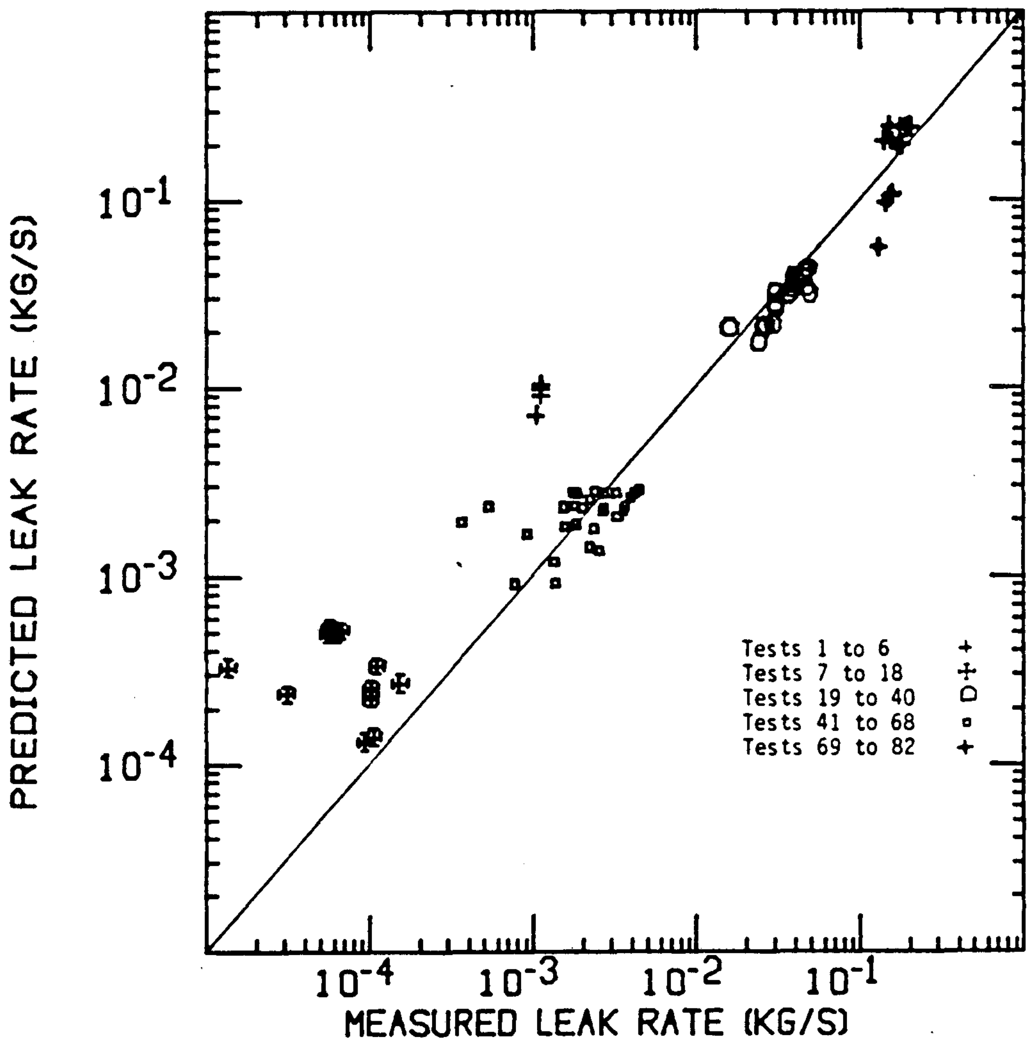

Figure 4.4 Chexal et al.[16] Predictions Compared with BCL Data

5. CONCLUSIONS

A computer code (SOURCE) has been developed to estimate leak rates through IGSCC cracks. The basis of the code is the steady state Homogeneous Equilibrium Model with friction and area change. A general method was developed to estimate the equivalent friction factor, lumping the effects of wall friction, tortuosity of the flow path and expansions and contractions, from physical features of IGSCC. Experimental results of Collier et al. (BCL) were used to develop a subcooling dependent correction factor to apply to SOURCE critical flow predictions. Using optimum friction factors deduced from BCL data for each test section, corrected SOURCE predictions agree with the BCL measured flowrates for 61 qualified tests with a standard deviation of 1.35% and for all 82 tests with a standard deviation of 6.5%. Using the independently estimated friction factor (from the generalized method) the predictions agree with qualified data with a standard deviation of 15.9%. This is an improvement as compared with Chexal's method.

The code SOURCE is very fast running and should be adaptable to large systems codes without significant sacrifice in cost. The method developed is recommended for estimating leak rates through IGSCC.

6. REFERENCES

1. Walker, W. L. and Higgins, J. P., "Performance of 304 Stainless Steel Structural Components in General Electric Company Boiling Water Reactor," Paper No. 103, NACE Corrosion Conference, Anaheim, CA, 1973.

2. Klepfer, H. H., et al., "Investigation of Cause of Cracking in Austenitic Stainless Steel Piping," General Electric Report NEDO-21,000, July 1975.

3. Agostinelli, A., Salemann, V. and Harrison, N. J., "Predictions of Flashing Water Flow Through Fine Annular Clearances," ASME Transactions, Vol. 80, 1958, pp. 1138-1142.

4. Hendricks, R. C., Simoneau, R. J. and Hsu, Y. Y., "A Visual Study of Radial Inward Flow of Subcooled Nitrogen," in: Advanced in Cryogenic Engineering, Vol. 20, K. D. Timmehaus, ed., Plenum Press, New York, p. 370, 1975.

5. Simoneau, R. J., "Two-Phase Choked Flow of Subcooled Nitrogen Through a Slit," NASA Lewis Research Center, NASA TM-71516, 1974.

6. Amos, C. N. and Schrock, V. E., "Critical Discharge of Initially Subcooled Water Through Slits," NUREG/CR-3475, LBL-16363, 1983.

7. Collier, R. P., Stulen, F. B., Mayfield, M. E., Pope, D. B. and Scott, P. M., "Two-Phase Flow Through Intergranular Stress Corrosion Cracks and Resulting Acoustic Emission," EPRI Final Report NP-3540-LD, RP-T118-2, 1980.

8. Mayfield, M. E., et al., "Cold Leg Integrity Evaluation - Final Report," NUREG/CR-1319, Battelle Columbus Laboratories, 1980.

9. Henry, R. E., "The Two-Phase Critical Discharge of Initially Saturated or Subcooled Liquid," Nuclear Science and Engineering Vol. 41, p. 336, 1970.

10. Abdollahian, D. and Chexal, D., "Calculation of Leak Rates Through Cracks in Pipes and Tubes," EPRI Final Report NP-3395 RP-1757-19, December 1983.

11. General Electric Report NEDC-24750-4.

12. S. Ranganath, G. E. San Jose, private communication (1984).

13. D. Abdollahian, et al., "Critical Flow Data Review and Analysis," EPRI Report NP-2192, January 1982.

14. Engineering Div. of Crane Co., "Flow of Fluids Through Valves Fittings and Pipe," Crane Co. Technical Paper No. 410, 1976.

15. Ishimoto, S., Uematsu, M., Tanishita, I., "New Equations for the Thermodynamic Properties of Saturated Water and Steam," Bulletin of the JSME, Vol. 15, No. 88, p. 1278, 1972.

16. Chexal, B., Abdollahian, D., Norris, D., "Analytical Prediction of Single Phase and Two-Phase Flow Through Cracks in Pipes and Tubes," AIChE Symp. Series-Heat Transfer, Niagara Falls, 236, Vol. 80, p. 19, 1984.

17. Hall, D. G. and Czapary, L. S., "Tables of Homogeneous Equilibrium Critical Flow Parameters for Water in SI Units," EGG-2056, September 1980.

18. Martinelli, R. C. and Nelson, D. B., "Prediction of Pressure Drop During Forced Circulation Boiling of Water," Trans. ASME, Vol. 70, pp 695-702, 1948.

APPENDIX A

Here we estimate the equivalent friction factor for each BCL test section using the generalized method described in Section 4.2.

i) Test section with δ = 0.074 mm:

$$\text{the hydraulic diameter } D = \frac{4A}{P} = 0.145 \text{ mm.}$$

The grain sizes for thermally stressed steel pipes are around $\sim$2 µm = 2×10^{-3} mm. This grain size is taken to yield surface roughness ε = 1.78 µ = 1.78×10^{-3} mm. Hence the relative roughness is

$$\varepsilon/D = 1.78\times10^{-3}/0.145 = 0.0122$$

The Reynolds number at the exit is 5.4×10^{5}. Here we have evaluated the hydraulic diameter and the relative surface roughness at the exit. According to the present modelling of the crack geometry with constant δ, these parameters will be the same throughout the crack channel. However, the Reynolds number is smaller at the upstream of the crack exit. Hence an average Reynolds number is used. For relative surface roughness of 0.0122 the friction factor f is independent of Reynolds number and is given as

$$f_p = 8[2.46 \ln(D/\varepsilon) + 3.22]^{-2}$$

Hence for G/D = 0.0122 we have f = 0.048.

Now we evaluate the loss coefficients $K_i n_i$ for various bends and expansion along the crack channel.

For this test section, δ = 0.074, we have an average number of bends, 1.35 per mm and the average number of contraction and expansion, each of 0.67 per mm.

Hence for 45° bends $K_1 n_1$ = 0.535/mm

for contraction $K_2 n_2$ = 0.135/mm and

for expansion $K_3 n_3$ = 0.272/mm .

$$\therefore f = f_p + D \sum_i K_i n_i$$

$$= 0.184$$

ii) Test section with δ = 0.022 mm:

Hydraulic diameter D = 0.041 mm.

Relative roughness $\varepsilon/D = 1.78\times10^{-3}/0.041 = 0.043$.

Reynolds number range 2×10^{5} to 2×10^{4}.

$$\therefore f_p = 0.07$$

Loss coefficients: Here $n_1 = 4.87$ $n_2 = n_3 = 2.43$.

$K_1 n_1 = 2.75/mm$

$K_2 n_2 = 0.476/mm$

$K_3 n_3 = 0.989/mm$

$\therefore f = f_p + D \sum_i K_i n_i$

$= 0.243$

iii) Test section with $\delta = 0.108$

Hydraulic diameter D = 0.212

Relative roughness $\varepsilon/D = 1.78 \times 10^{-2}/0.212 = 0.0084$.

Exit Reynolds number range 8.7×10^6 to 2.7×10^6

Hence friction factor $f_p = 0.038$

Loss coefficients: Here $n_1 = 0.925$ $n_2 = n_3 = 0.46$

$K_1 n_1 = 0.303/mm$

$K_2 n_2 = 0.098/mm$

$K_3 n_3 = 0.203/mm$

Hence $f = f_p + D \sum_i K_i n_i$

$= 0.166$

iv) Test section with $\delta = 0.048$ mm:

Hydraulic diameter D = 0.092

Relative roughness $\varepsilon/D = 0.0193$

Exit Reynolds number range 5×10^6 to 1×10^6

Hence friction factor $f_p = 0.05$

Loss coefficients: Here $n_1 = 2.08$ $n_2 = n_2 = 1.04$

$K_1 n_1 = 0.851/mm$

$K_2 n_2 = 0.203/mm$

$K_3 n_3 = 0.423/mm$

Hence $f = f_p + D \sum_i K_i n_i$

$= 0.186$

v) Test section with δ = 0.22 mm:

Hydraulic diameter D = 0.441

Relative roughness ε/D = 0.00403

Exit Reynolds number range: 1×10^7 to 2×10^7.

Hence friction factor f_p = 0.030

Loss coefficients: Here $n_1 = 0.45$ $n_2 = n_3 = 0.227$

$K_1 n_1$ = 0.119/mm

$K_2 n_2$ = 0.045/mm

$K_3 n_3$ = 0.092/mm

Hence $f = f_p + D \sum_i K_i n_i$

$= 0.143$

Table A.1 compares the friction factors obtained from the present generalized method with those obtained from parametric study.

Table A.1

Comparison of friction factors calculated based on generalized methodology with those from parametric study

(mm)	D(mm)	Re (average)	f_p	$D \sum_i K_i n_i$	f Generalized Methodology	f Parametric Study
0.074	0.144	5.483×10^3	0.048	0.136	0.184	9.0
0.022	0.041	1.684×10^3	0.070	0.173	0.243	0.80
0.108	0.212	6.675×10^4	0.038	0.128	0.166	0.07
0.048	0.092	1.476×10^4	0.050	0.136	0.186	0.02
0.22	0.441	9.550×10^4	0.030	0.113	0.143	0.30

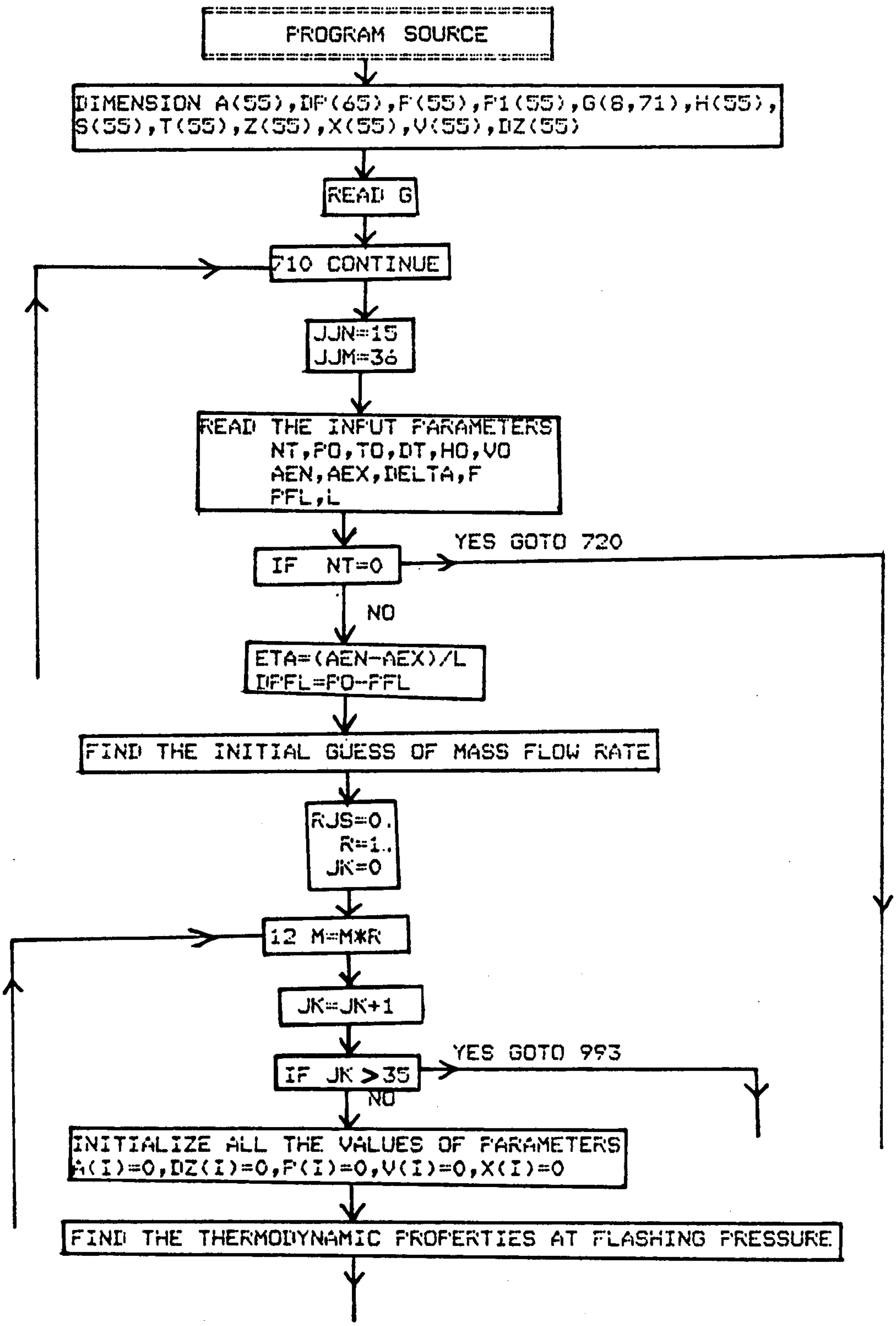
PROGRAM SOURCE
DIMENSION A(55),DP(65),F(55),P1(55),G(8,71),H(55),
S(55),T(55),Z(55),X(55),V(55),DZ(55)
READ G
710 CONTINUE
JJN=15
JJM=36
READ THE INPUT PARAMETERS
NT,PO,TO,DT,HO,VO
AEN,AEX,DELTA,F
PFL,L
IF NT=0
YES GOTO 720
NO
ETA=(AEN-AEX)/L
DPFL=PO-PFL
FIND THE INITIAL GUESS OF MASS FLOW RATE
RJS=0.
R=1.
JK=0
12 M=M*R
JK=JK+1
IF JK > 35
YES GOTO 993
NO
INITIALIZE ALL THE VALUES OF PARAMETERS
A(I)=0,DZ(I)=0,P(I)=0,V(I)=0,X(I)=0
FIND THE THERMODYNAMIC PROPERTIES AT FLASHING PRESSURE

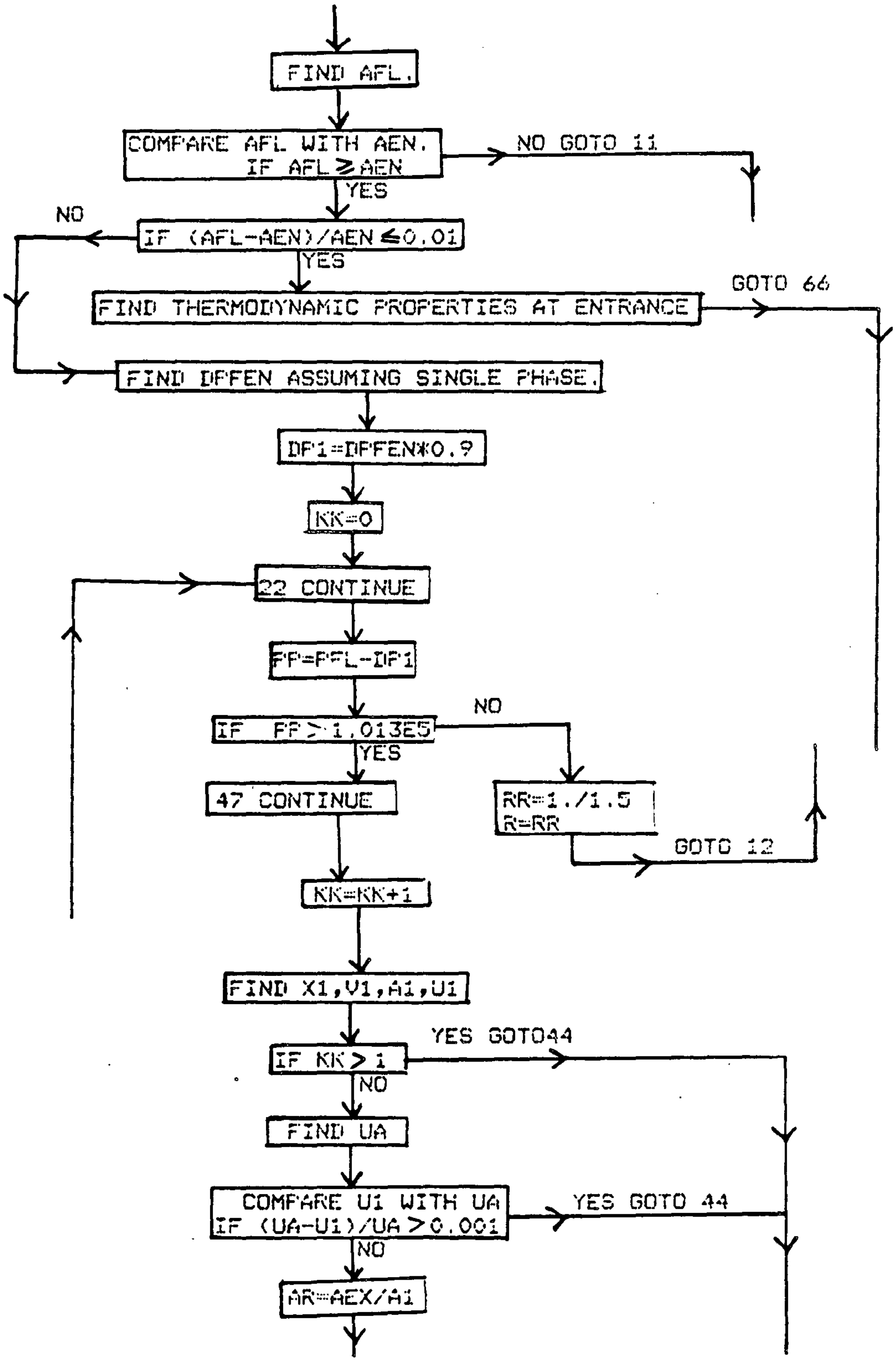
FIND AFL.
COMPARE AFL WITH AEN.
IF AFL ≥ AEN
NO GOTO 11
YES
NO
IF (AFL-AEN)/AEN ≤ 0.01
YES
GOTO 66
FIND THERMODYNAMIC PROPERTIES AT ENTRANCE
FIND DPFEN ASSUMING SINGLE PHASE.
DP1=DPFEN*0.9
KK=0
22 CONTINUE
PP=PFL-DP1
NO
IF PP > 1.013E5
YES
47 CONTINUE
RR=1./1.5
R=RR
GOTO 12
KK=KK+1
FIND X1,V1,A1,U1
YES GOTO44
IF KK > 1
NO
FIND UA
COMPARE U1 WITH UA
IF (UA-U1)/UA > 0.001
YES GOTO 44
NO
AR=AEX/A1

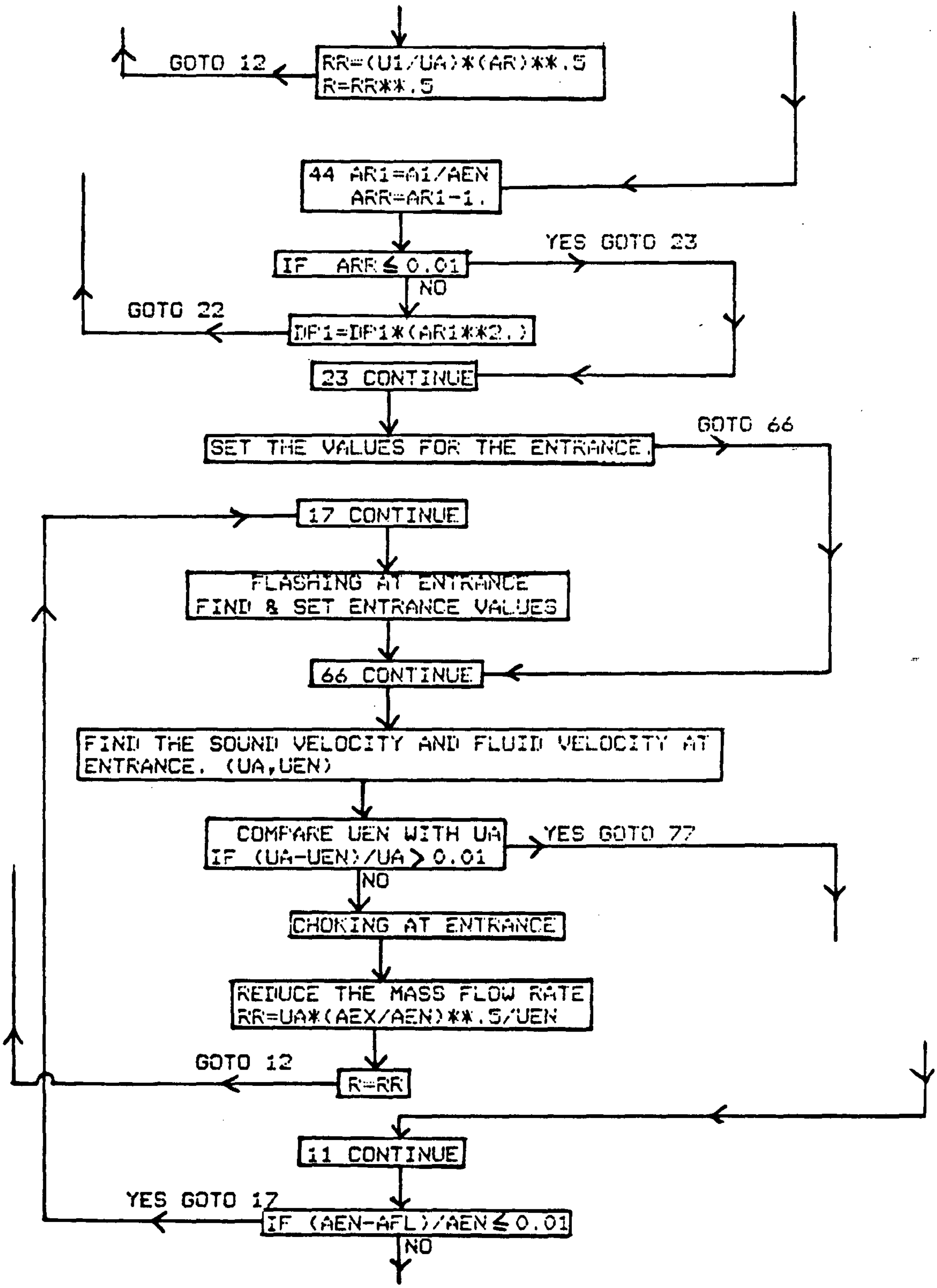
GOTO 12
RR=(U1/UA)*(AR)**.5
R=RR**.5
44 AR1=A1/AEN
ARR=AR1-1.
IF ARR ≦ 0.01
YES GOTO 23
NO
GOTO 22
DP1=DP1*(AR1**2.)
23 CONTINUE
SET THE VALUES FOR THE ENTRANCE
GOTO 66
17 CONTINUE
FLASHING AT ENTRANCE
FIND & SET ENTRANCE VALUES
66 CONTINUE
FIND THE SOUND VELOCITY AND FLUID VELOCITY AT ENTRANCE. (UA,UEN)
COMPARE UEN WITH UA
IF (UA-UEN)/UA > 0.01
YES GOTO 77
NO
CHOKING AT ENTRANCE
REDUCE THE MASS FLOW RATE
RR=UA*(AEX/AEN)**.5/UEN
GOTO 12
R=RR
11 CONTINUE
YES GOTO 17
IF (AEN-AFL)/AEN ≦ 0.01
NO

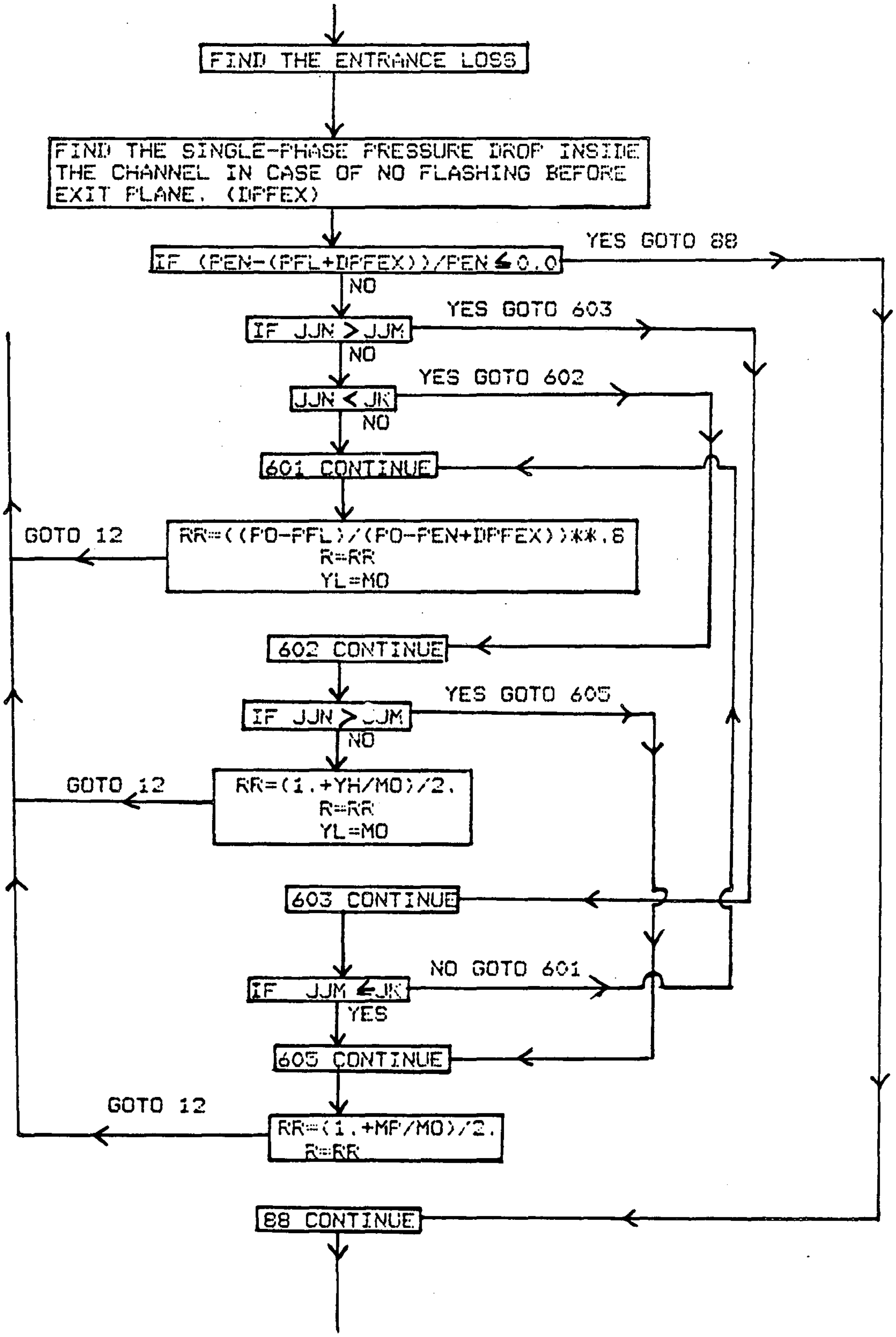
FIND THE ENTRANCE LOSS
FIND THE SINGLE-PHASE PRESSURE DROP INSIDE THE CHANNEL IN CASE OF NO FLASHING BEFORE EXIT PLANE. (DPFEX)
IF (PEN-(PFL+DPFEX))/PEN ≤ 0.0
YES GOTO 88
NO
IF JJN > JJM
YES GOTO 603
NO
JJN < JK
YES GOTO 602
NO
601 CONTINUE
RR=((PO-PFL)/(PO-PEN+DPFEX))**.8
R=RR
YL=MO
GOTO 12
602 CONTINUE
IF JJN > JJM
YES GOTO 605
NO
RR=(1.+YH/MO)/2.
R=RR
YL=MO
GOTO 12
603 CONTINUE
IF JJM ≤ JK
NO GOTO 601
YES
605 CONTINUE
RR=(1.+MF/MO)/2.
R=RR
GOTO 12
88 CONTINUE

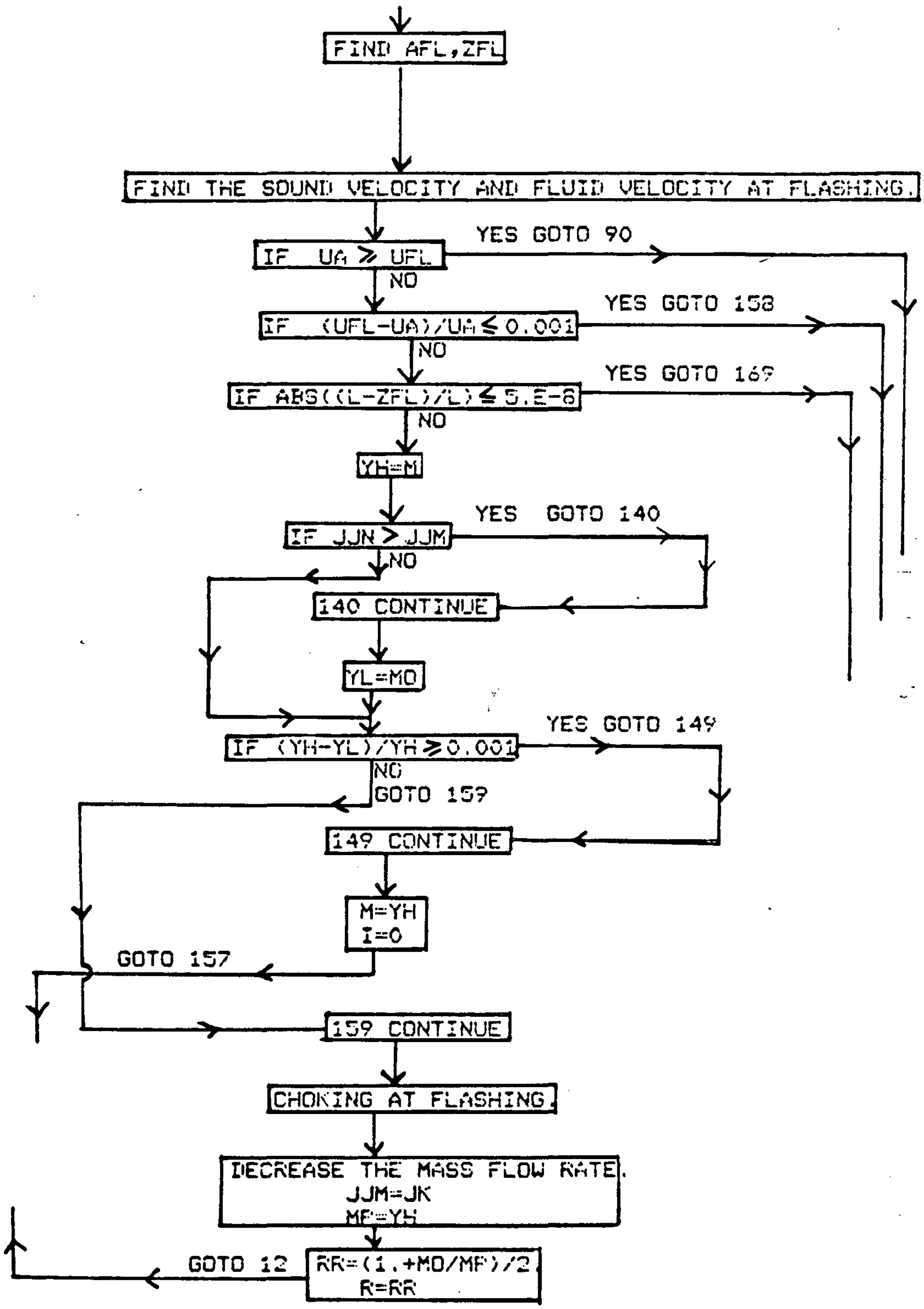
FIND AFL,ZFL
FIND THE SOUND VELOCITY AND FLUID VELOCITY AT FLASHING.
IF UA ≥ UFL
YES GOTO 90
NO
IF (UFL-UA)/UA ≤ 0.001
YES GOTO 158
NO
IF ABS((L-ZFL)/L) ≤ 5.E-8
YES GOTO 169
NO
YH=M
IF JJN > JJM
YES GOTO 140
NO
140 CONTINUE
YL=MO
IF (YH-YL)/YH ≥ 0.001
YES GOTO 149
NO
GOTO 159
149 CONTINUE
M=YH
I=0
GOTO 157
159 CONTINUE
CHOKING AT FLASHING.
DECREASE THE MASS FLOW RATE.
JJM=JK
MP=YH
GOTO 12
RR=(1.+MO/MP)/2
R=RR

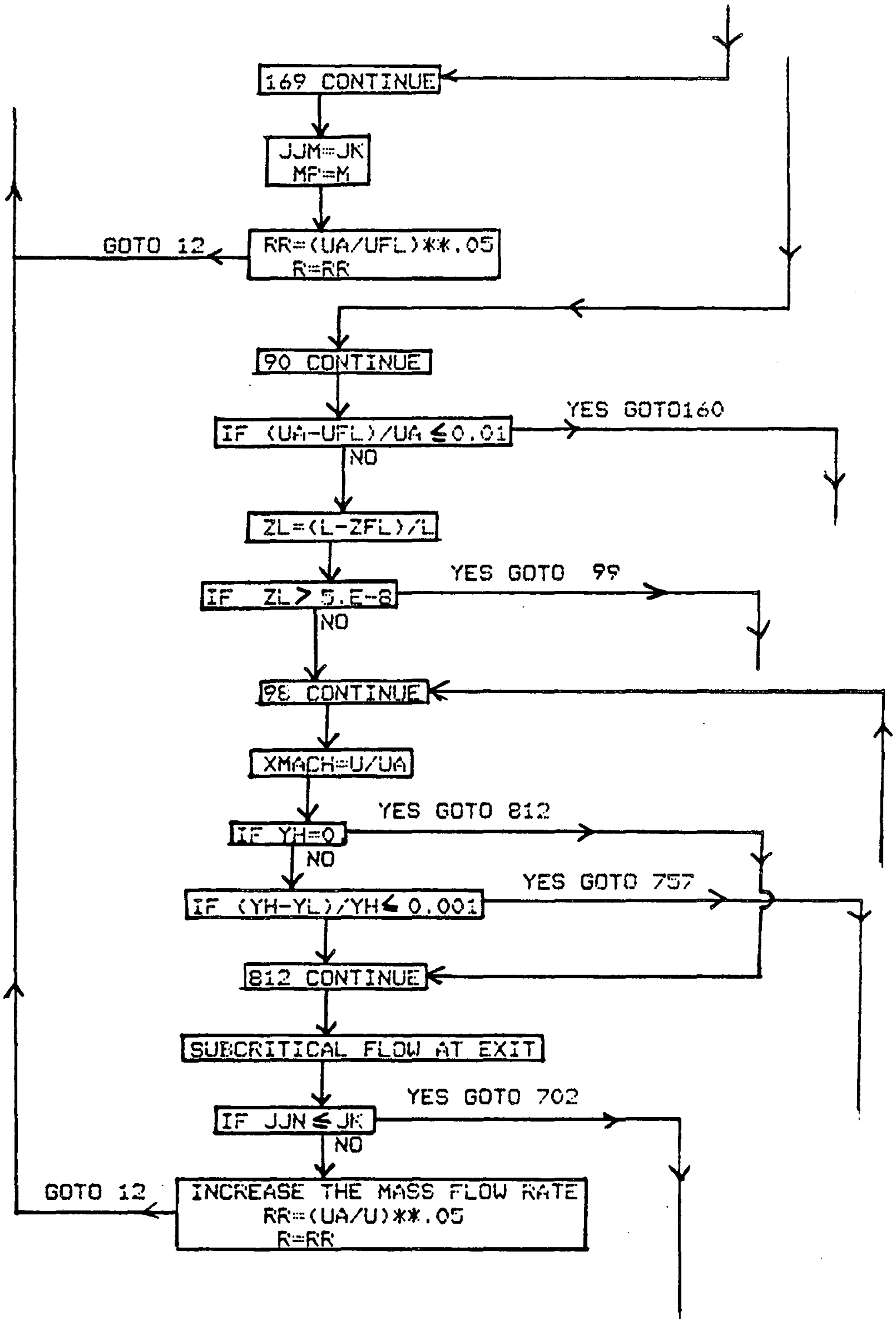
169 CONTINUE
JJM=JK
MP=M
GOTO 12
RR=(UA/UFL)**.05
R=RR
90 CONTINUE
IF (UA-UFL)/UA ≦0.01
YES GOTO160
NO
ZL=(L-ZFL)/L
IF ZL > 5.E-8
YES GOTO 99
NO
98 CONTINUE
XMACH=U/UA
IF YH=0
YES GOTO 812
NO
IF (YH-YL)/YH≦ 0.001
YES GOTO 757
812 CONTINUE
SUBCRITICAL FLOW AT EXIT
IF JJN≦JK
YES GOTO 702
NO
GOTO 12
INCREASE THE MASS FLOW RATE
RR=(UA/U)**.05
R=RR

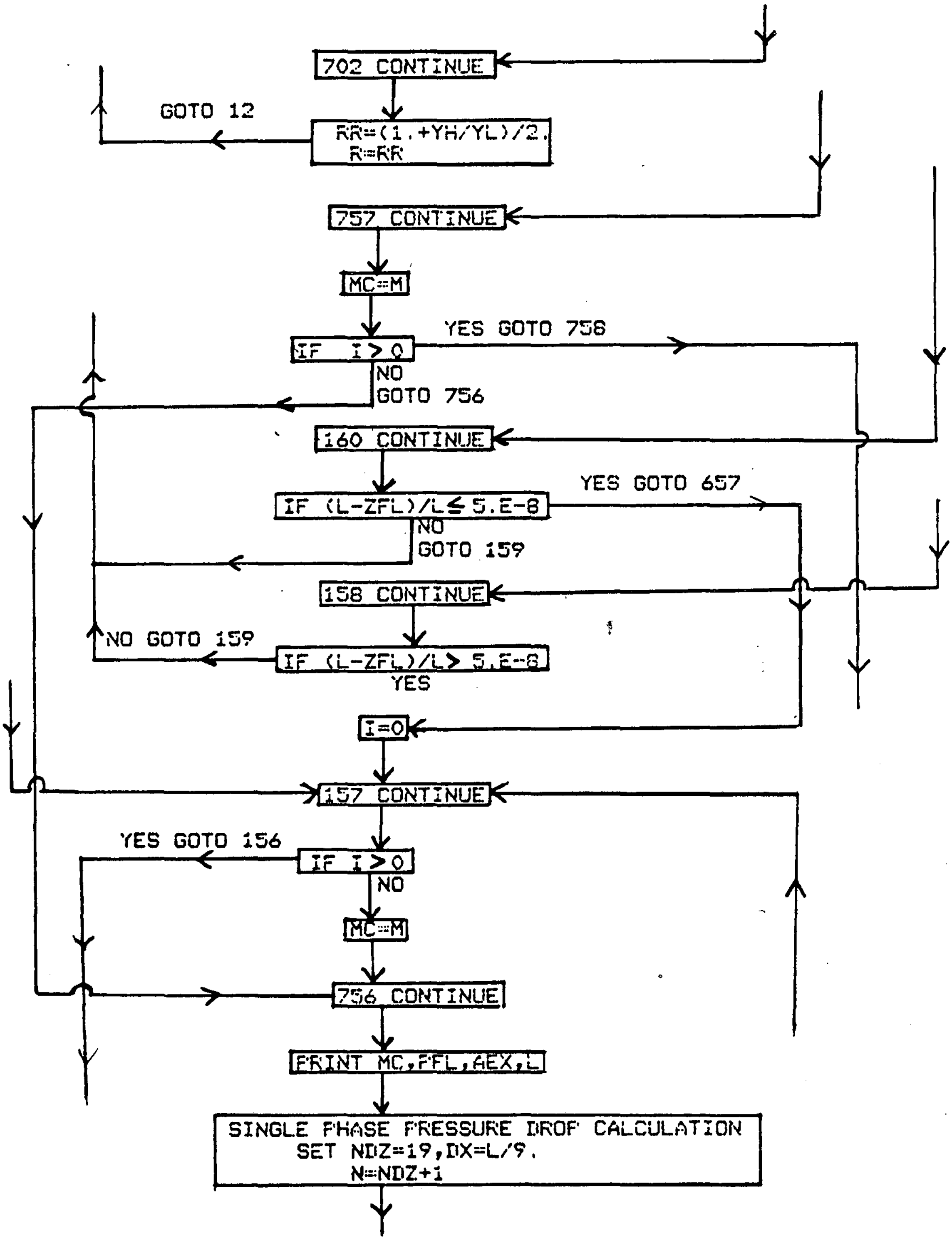
702 CONTINUE
GOTO 12
RR=(1.+YH/YL)/2.
R=RR
757 CONTINUE
MC=M
YES GOTO 758
IF I > 0
NO
GOTO 756
160 CONTINUE
YES GOTO 657
IF (L-ZFL)/L ≤ 5.E-8
NO
GOTO 159
158 CONTINUE
NO GOTO 159
IF (L-ZFL)/L > 5.E-8
YES
I=0
157 CONTINUE
YES GOTO 156
IF I > 0
NO
MC=M
756 CONTINUE
PRINT MC,PFL,AEX,L
SINGLE PHASE PRESSURE DROP CALCULATION
SET NDZ=19,DX=L/9.
N=NDZ+1

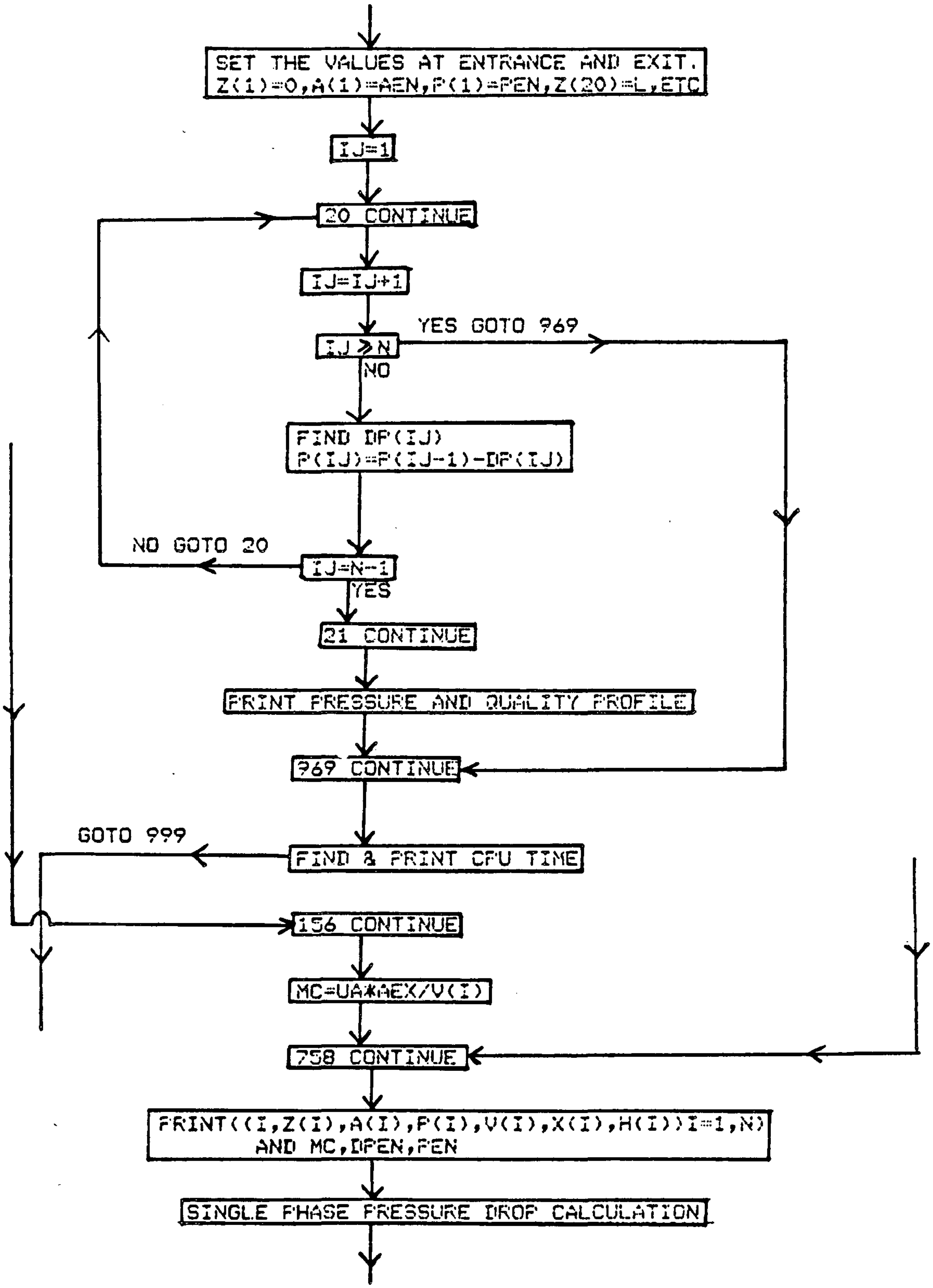
SET THE VALUES AT ENTRANCE AND EXIT.
Z(1)=0,A(1)=AEN,P(1)=PEN,Z(20)=L,ETC
IJ=1
20 CONTINUE
IJ=IJ+1
IJ ≥ N
YES GOTO 969
NO
FIND DP(IJ)
P(IJ)=P(IJ-1)-DP(IJ)
NO GOTO 20
IJ=N-1
YES
21 CONTINUE
PRINT PRESSURE AND QUALITY PROFILE
969 CONTINUE
GOTO 999
FIND & PRINT CPU TIME
156 CONTINUE
MC=UA*AEX/V(I)
758 CONTINUE
PRINT((I,Z(I),A(I),P(I),V(I),X(I),H(I))I=1,N)
AND MC,DPEN,PEN
SINGLE PHASE PRESSURE DROP CALCULATION

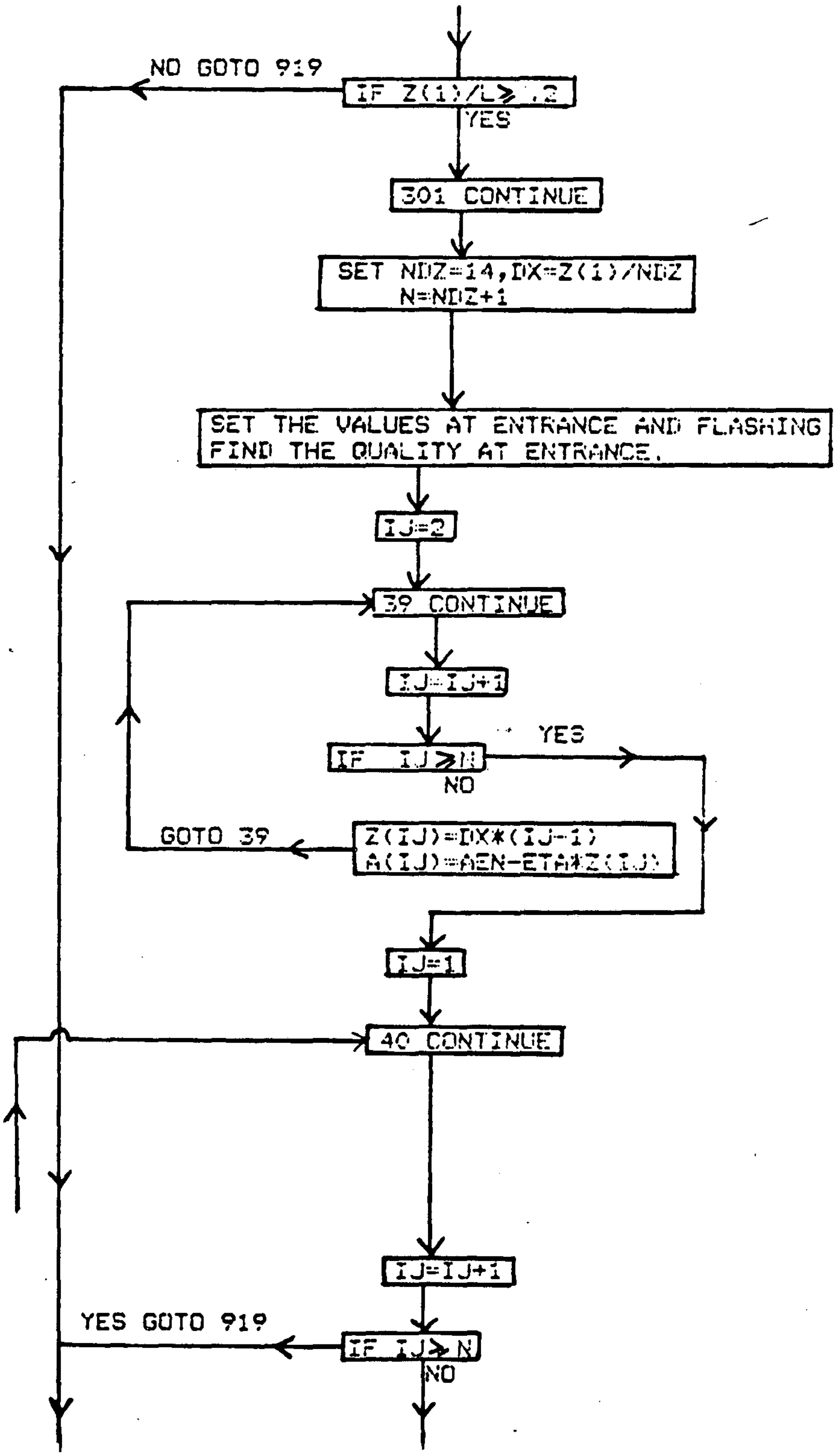
NO GOTO 919
IF Z(1)/L≥ .2
YES
301 CONTINUE
SET NDZ=14,DX=Z(1)/NDZ
N=NDZ+1
SET THE VALUES AT ENTRANCE AND FLASHING
FIND THE QUALITY AT ENTRANCE.
IJ=2
39 CONTINUE
IJ=IJ+1
YES
IF IJ≥N
NO
GOTO 39
Z(IJ)=DX*(IJ-1)
A(IJ)=AEN-ETA*Z(IJ)
IJ=1
40 CONTINUE
IJ=IJ+1
YES GOTO 919
IF IJ≥N
NO

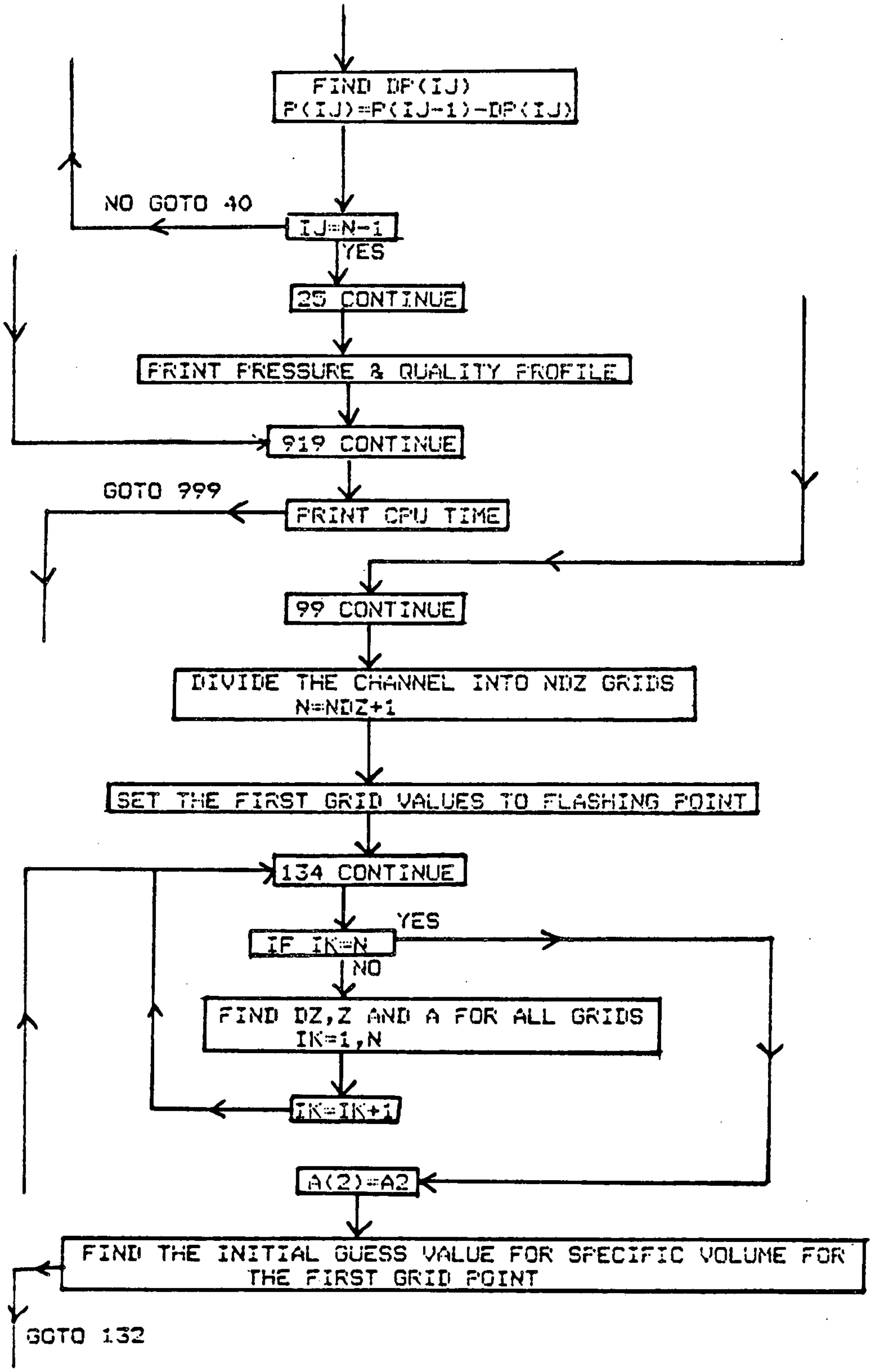
FIND DP(IJ)
P(IJ)=P(IJ-1)-DP(IJ)
NO GOTO 40
IJ=N-1
YES
25 CONTINUE
PRINT PRESSURE & QUALITY PROFILE
919 CONTINUE
GOTO 999
PRINT CPU TIME
99 CONTINUE
DIVIDE THE CHANNEL INTO NDZ GRIDS
N=NDZ+1
SET THE FIRST GRID VALUES TO FLASHING POINT
134 CONTINUE
YES
IF IK=N
NO
FIND DZ,Z AND A FOR ALL GRIDS
IK=1,N
IK=IK+1
A(2)=A2
FIND THE INITIAL GUESS VALUE FOR SPECIFIC VOLUME FOR
THE FIRST GRID POINT
GOTO 132

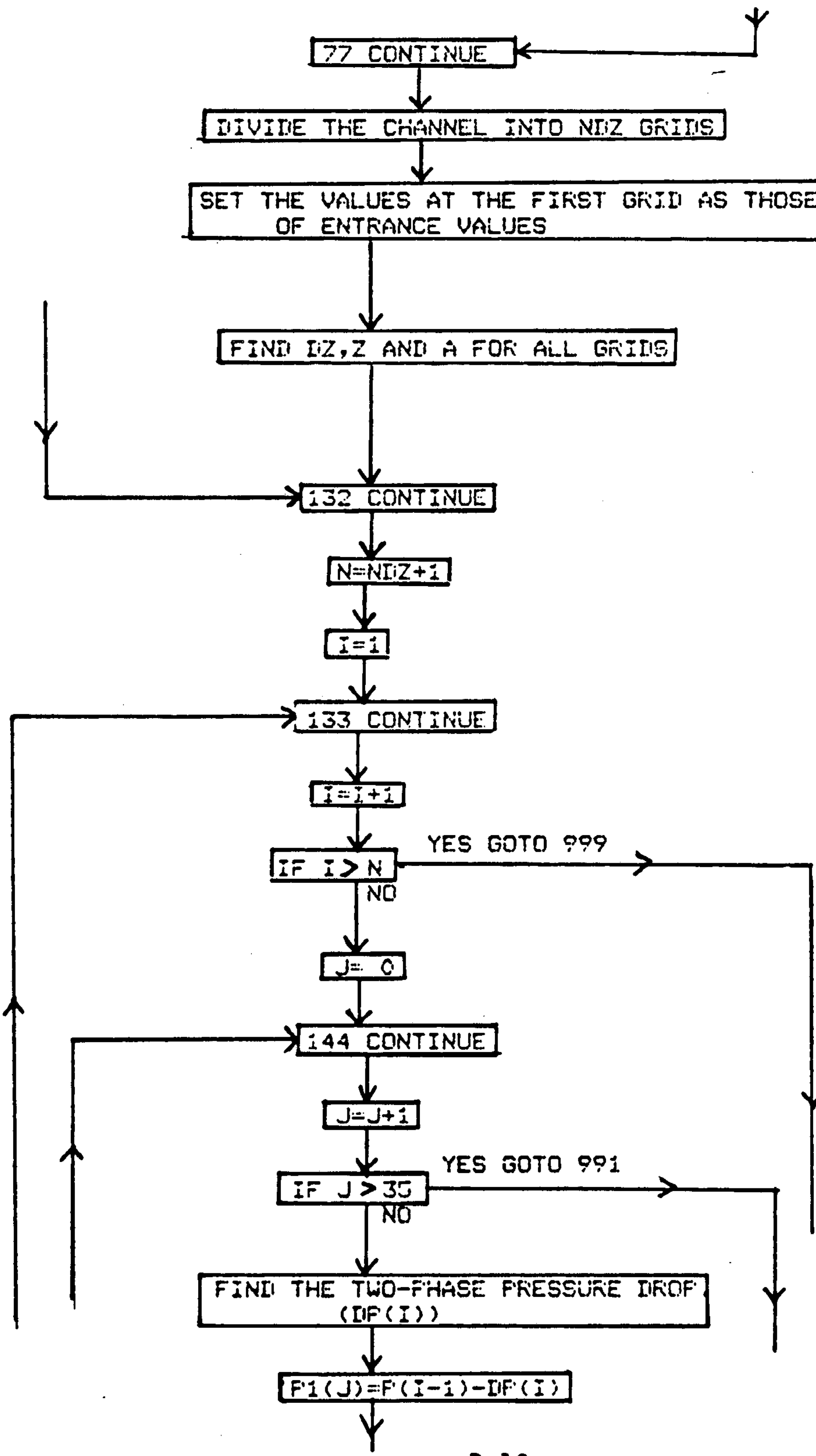
77 CONTINUE
DIVIDE THE CHANNEL INTO NDZ GRIDS
SET THE VALUES AT THE FIRST GRID AS THOSE OF ENTRANCE VALUES
FIND DZ,Z AND A FOR ALL GRIDS
132 CONTINUE
N=NDZ+1
I=1
133 CONTINUE
I=I+1
IF I > N
YES GOTO 999
NO
J= 0
144 CONTINUE
J=J+1
IF J > 35
YES GOTO 991
NO
FIND THE TWO-PHASE PRESSURE DROP (DP(I))
P1(J)=P(I-1)-DP(I)

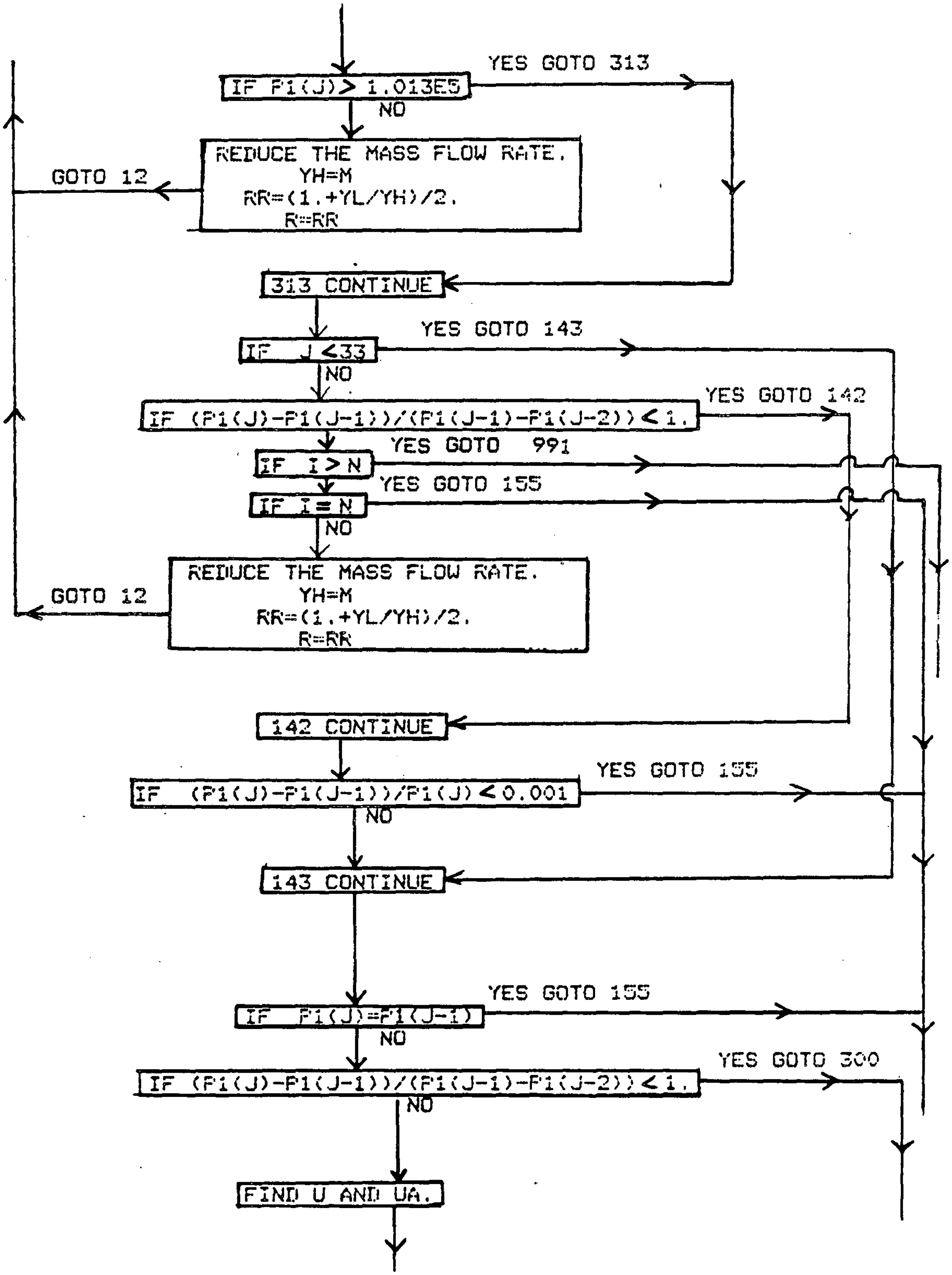
IF P1(J) > 1.013E5
YES GOTO 313
NO
REDUCE THE MASS FLOW RATE.
YH=M
RR=(1.+YL/YH)/2.
R=RR
GOTO 12
313 CONTINUE
IF J < 33
YES GOTO 143
NO
IF (P1(J)-P1(J-1))/(P1(J-1)-P1(J-2)) < 1.
YES GOTO 142
IF I > N
YES GOTO 991
IF I = N
YES GOTO 155
NO
REDUCE THE MASS FLOW RATE.
YH=M
RR=(1.+YL/YH)/2.
R=RR
GOTO 12
142 CONTINUE
IF (P1(J)-P1(J-1))/P1(J) < 0.001
YES GOTO 155
NO
143 CONTINUE
IF P1(J)=P1(J-1)
YES GOTO 155
NO
IF (P1(J)-P1(J-1))/(P1(J-1)-P1(J-2)) < 1.
YES GOTO 300
NO
FIND U AND UA.

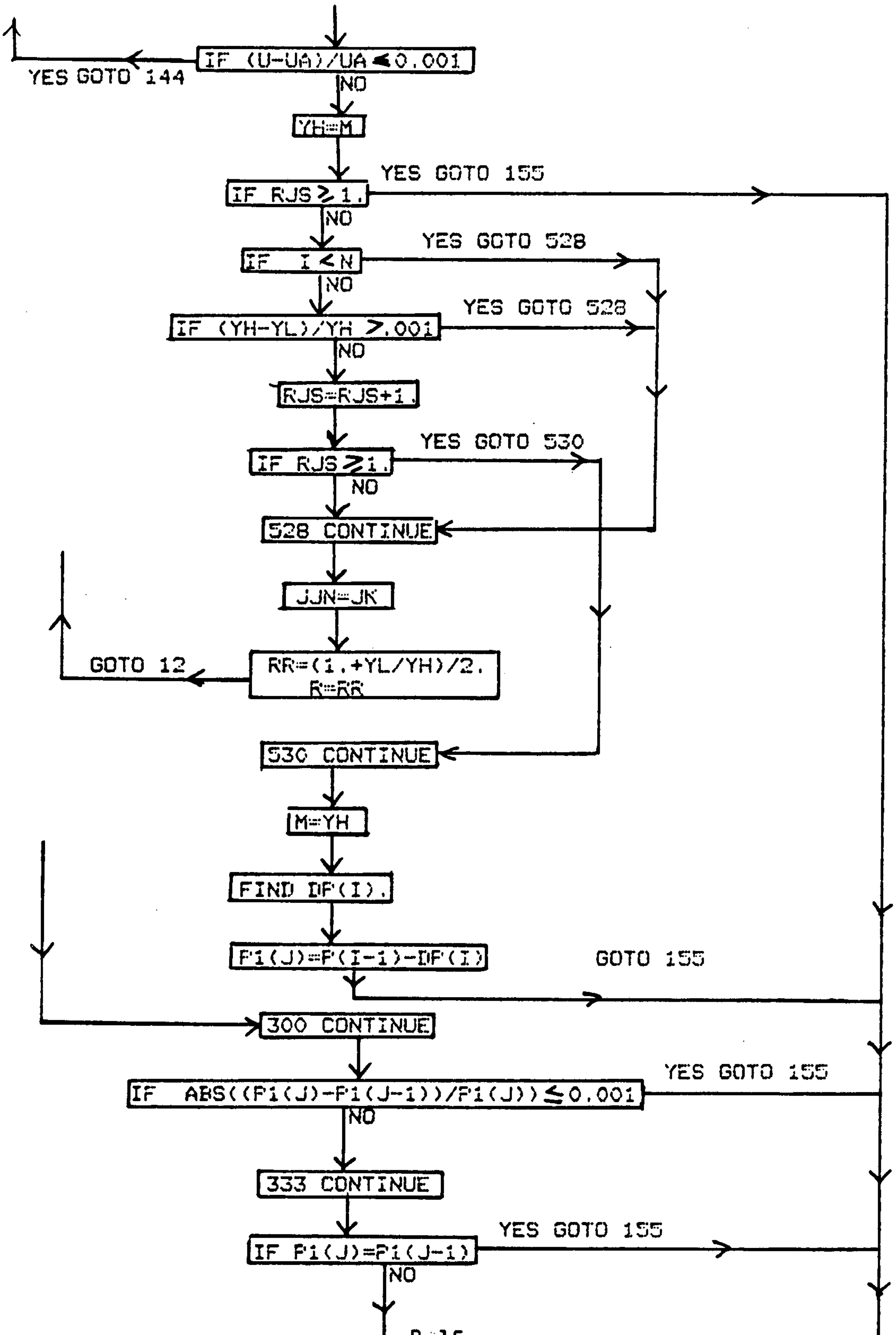
IF (U-UA)/UA ≤ 0.001
YES GOTO 144
NO
YH=M
IF RJS ≥ 1.
YES GOTO 155
NO
IF I < N
YES GOTO 528
NO
IF (YH-YL)/YH ≥ .001
YES GOTO 528
NO
RJS=RJS+1.
IF RJS ≥ 1.
YES GOTO 530
NO
528 CONTINUE
JJN=JK
RR=(1.+YL/YH)/2.
R=RR
GOTO 12
530 CONTINUE
M=YH
FIND DF(I).
F1(J)=F(I-1)-DF(I)
GOTO 155
300 CONTINUE
IF ABS((F1(J)-F1(J-1))/F1(J)) ≤ 0.001
YES GOTO 155
NO
333 CONTINUE
IF F1(J)=F1(J-1)
YES GOTO 155
NO

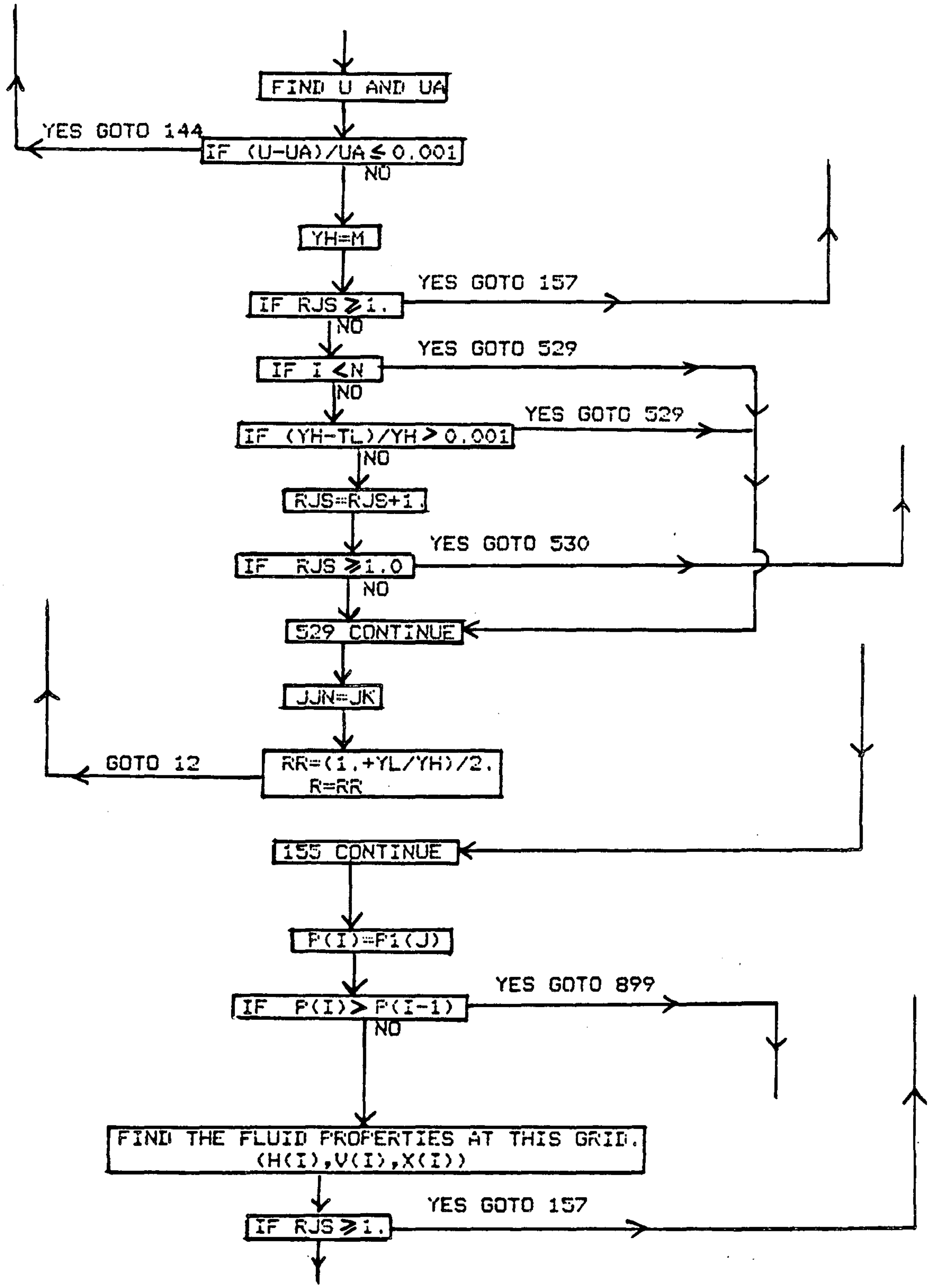
FIND U AND UA
YES GOTO 144
IF (U-UA)/UA ≤ 0.001
NO
YH=M
YES GOTO 157
IF RJS ≥ 1.
NO
YES GOTO 529
IF I < N
NO
YES GOTO 529
IF (YH-TL)/YH > 0.001
NO
RJS=RJS+1.
YES GOTO 530
IF RJS ≥ 1.0
NO
529 CONTINUE
JJN=JK
GOTO 12
RR=(1.+YL/YH)/2.
R=RR
155 CONTINUE
P(I)=P1(J)
YES GOTO 899
IF P(I) > P(I-1)
NO
FIND THE FLUID PROPERTIES AT THIS GRID.
(H(I),V(I),X(I))
YES GOTO 157
IF RJS ≥ 1.

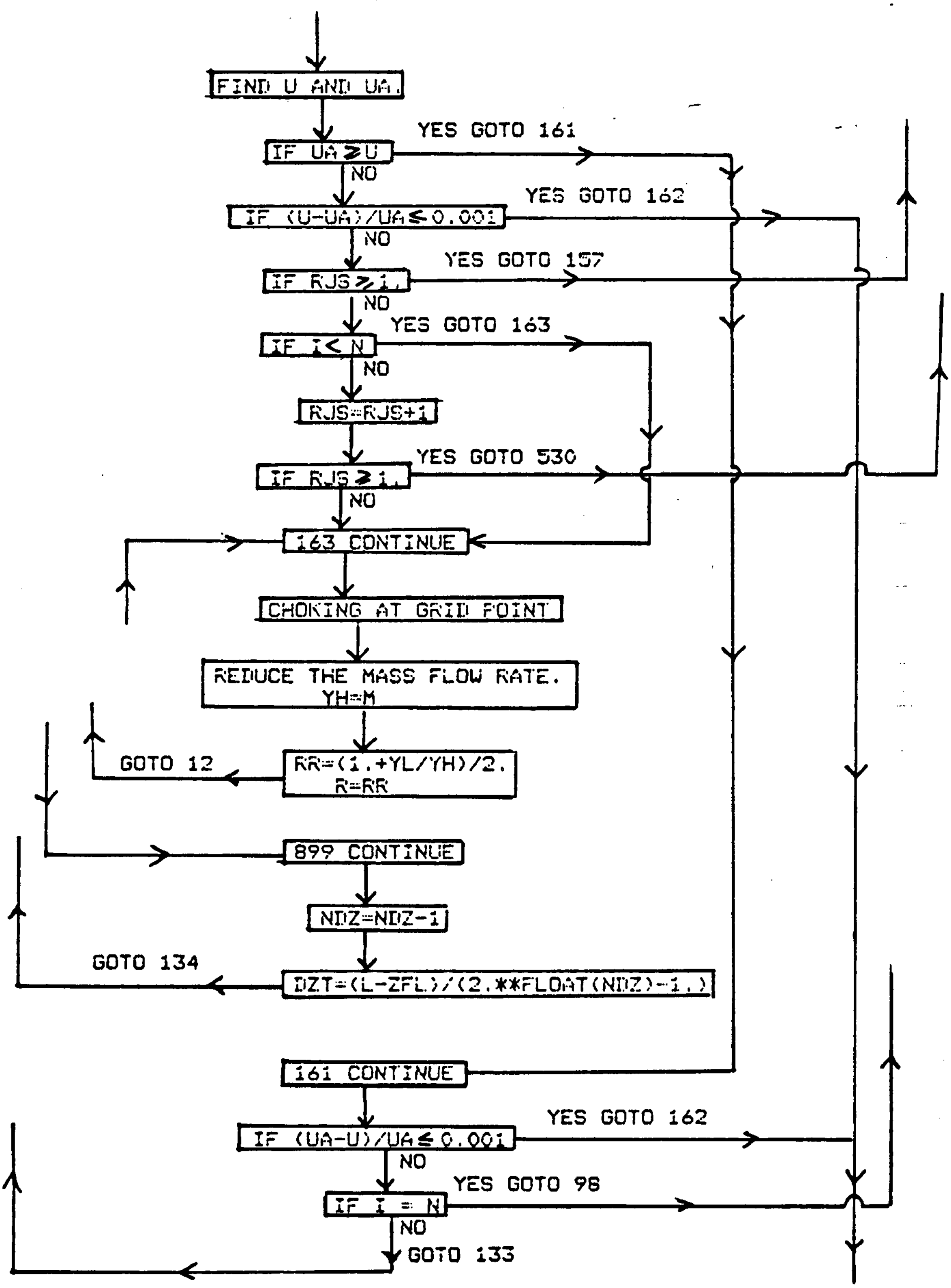
FIND U AND UA.
IF UA ≥ U
YES GOTO 161
NO
IF (U-UA)/UA ≤ 0.001
YES GOTO 162
NO
IF RJS ≥ 1.
YES GOTO 157
NO
IF I < N
YES GOTO 163
NO
RJS=RJS+1
IF RJS ≥ 1.
YES GOTO 530
NO
163 CONTINUE
CHOKING AT GRID POINT
REDUCE THE MASS FLOW RATE. YH=M
RR=(1.+YL/YH)/2. R=RR
GOTO 12
899 CONTINUE
NDZ=NDZ-1
DZT=(L-ZFL)/(2.**FLOAT(NDZ)-1.)
GOTO 134
161 CONTINUE
IF (UA-U)/UA ≤ 0.001
YES GOTO 162
NO
IF I = N
YES GOTO 98
NO
GOTO 133

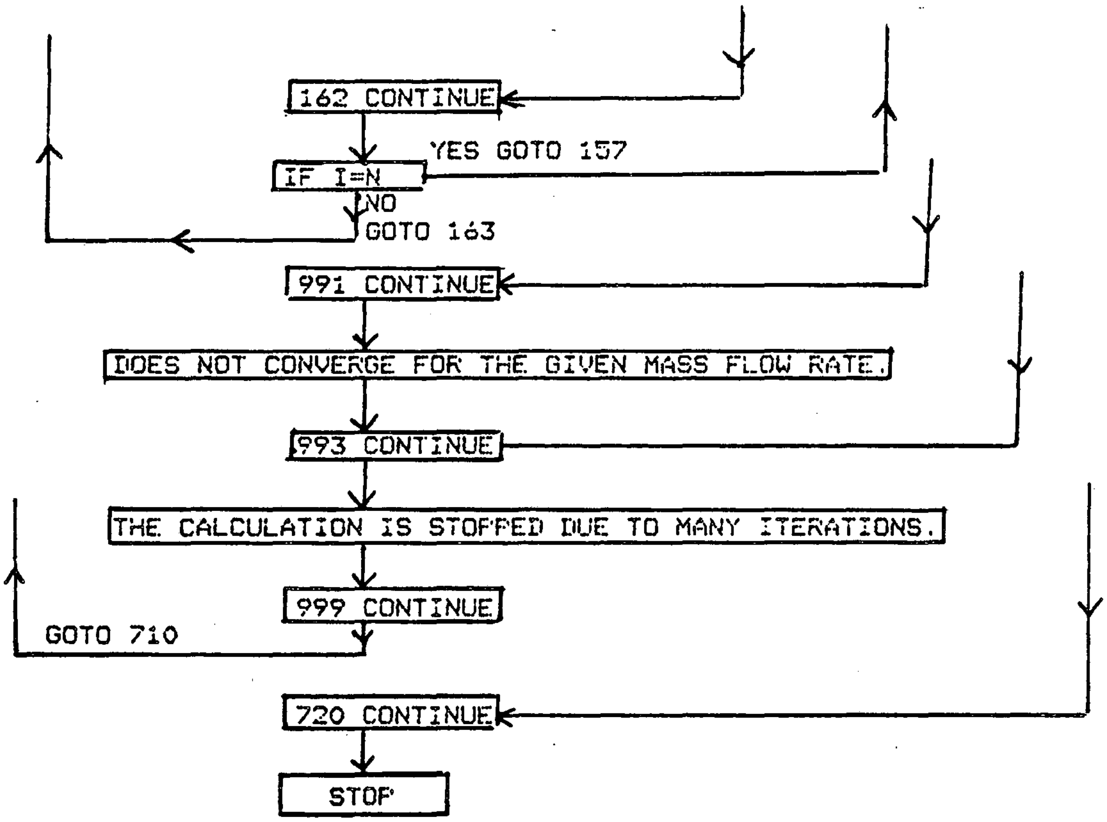
162 CONTINUE
YES GOTO 157
IF I=N
NO
GOTO 163
991 CONTINUE
DOES NOT CONVERGE FOR THE GIVEN MASS FLOW RATE.
993 CONTINUE
THE CALCULATION IS STOPPED DUE TO MANY ITERATIONS.
999 CONTINUE
GOTO 710
720 CONTINUE
STOP

```
C*****************************************************************
C
C        THIS IS A SOURCE PROGRAM
C
      PROGRAM SOURCE
C
C ----------------------------------------------------------------
C PURPOSE
C THE PROGRAM CALCULATES THE CRITICAL MASS FLOW RATE THROUGH A INTER-
C GRANULAR STRESS COROSION CRACKS ON PIPES SUCH AS FOUND IN THE
C PRIMARY COOLANT SYSTEM OF NUCLEAR REACTOR PIPES.
C ----------------------------------------------------------------
C
      IMPLICIT REAL*8(A,L,M)
      REAL*4 ECPU, ETIME, ETCPU
      CHARACTER*23 DATTIM
      DIMENSION A(55),DP(55),P(55),P1(65),G(8,71),H(55),S(55),T(55),
     &DZ(55),X(55),V(55),Z(55)
C
C
      COMMON/BLOCK1/VF,DVFDP,VG,DVGDP,HF,DHFDP,HG,DHGDP,SF,DSFDP,SG,
     &DSGDP
      COMMON/BLOCK2/M,VFL,ETA,DELTA,F,AFL,ZFL,NDZ,DZT,PFL,HFL
      OPEN(10,FILE='HEMD.DATA',STATUS='OLD',FORM='UNFORMATTED')
C
C        VARIABLES USED IN THE PROGRAM
C ----------------------------------------------------------------
C  VARIABLE                DESCRIPTION
C ----------------------------------------------------------------
C  A(I)     CROSS SECTIONAL AREA OF CRACK AT LOCATION Z(I)
C  AEN      ENTRANCE AREA
C  AEX      EXIT AREA
C  AAV      AVERAGE AREA BETWEEN TWO NODES
C  A1       DUMMY AREA BEFORE ENTRANCE
C  AR1      AREA RATIO AT TWO PHASE ENTRANCE A1/AEN
C  AFL      AREA AT FLASHING
C  AR       AREA RATIO AEX/A1
C
C  C3       TOLARANCE FOR LENTGH
C
C  SA       HALF WIDTH OF CRACK CHANNEL AT ENTRANCE
C  SB       HALF WIDTH OF CRACK CHANNEL AT EXIT
C
C  DELTA    CRACK CHANNEL THICKNESS
C  DP       PRESSURE DROP BETWEEN TWO NODE POINTS
C  DPEN     ENTRANCE PRESSURE LOSS
C  DP1      DUMMY PRESSURE LOSS BETWEEN STAGN AND ENTRANCE
C  DH       HYDRAULIC DIAMETER OF CRACK
C  DPFEX    PRESSURE DROP FOR NO FLASH BEFORE EXIT
C  DPFL     PRESSURE DROP BETWEEN FLASH AND STAGN
C  DPFEN    PRESSURE DROP BETWEEN FLASH AND ENTRANCE TWO PHASE ENTRANCE
C  DPSP     SINGLE PHASE PRESSURE DROP AT ENTRANCE
C  DPSP1    SINGLE PHASE PRESSURE DROP BETWEEN FLASH AND FIRST GRID
C  DX       STEP SIZE IN SINGLE IN SINGLE-PHASE REGION
C  DZ(I)    STEP SIZE AT ITH GRID
C  DT       SUBCOOLING  OF LIQUID
C  DZT      TERMINAL GRID SIZE
C
C  ETA      AREA SLOPE
C
```

```
C  F        FRICTION FACTOR                                    SOU00610
C                                                             SOU00620
C  G        MASS FLUX                                          SOU00630
C                                                             SOU00640
C  H(I)     ENTHALPY AT GRID I                                 SOU00650
C  HO       STAGNATION ENTHALPY                                SOU00660
C  HF       LIQUID SATURATED ENTHALPY                          SOU00670
C  HG       GAS SATURATED ENTHALPY                             SOU00680
C  HEN      ENTRANCE LOCAL ENTHALPY                            SOU00690
C  HFL      ENTHALPY AT FLASH                                  SOU00700
C                                                             SOU00710
C  IJ       SPATIAL INDEX FOR SINGLE-PHASE REGION              SOU00720
C  I        SPATIAL INDEX FOR CHANNEL STEPS                    SOU00730
C                                                             SOU00740
C  J        INDEX FOR ITERATION ON MOMENTUM EQN                SOU00750
C                                                             SOU00760
C  L        CHANNEL LENGTH                                     SOU00770
C                                                             SOU00780
C  M        MASS FLOW RATE  ASSUMED                            SOU00790
C  MC       CRITICAL MASS FLOW RATE                            SOU00800
C                                                             SOU00810
C  NDZ      NUMBER OF SPATIAL STEPS                            SOU00820
C  NT       TEST NUMBER                                        SOU00830
C                                                             SOU00840
C  P(I)     LOCAL PRESSURE AT GRID I                           SOU00850
C  PO       STAGN PRESSURE                                     SOU00860
C  PFL      PRESSURE AT FLASH                                  SOU00870
C  PEX      PRESSURE AT EXIT PLANE                             SOU00880
C  PEN      PRESSURE AT ENTRANCE PLANE                         SOU00890
C  PP       DUMMY LOCAL PRESSURE BEFORE ENTRANCE               SOU00900
C  PHI      MARTINNELI-NELSON FRICTION MULTIFLIER              SOU00910
C                                                             SOU00920
C  R        CHANGE FACTOR ON MASS FLOW RATE                    SOU00930
C  RR       INTENDED CHANGE FACTOR ON MASS FLOW RATE           SOU00940
C                                                             SOU00950
C  S(I)     LOCAL ENTROPY AT GRID I                            SOU00960
C  SO       STAGN ENTROPY                                      SOU00970
C  SFL      ENTROPY AT FLASH                                   SOU00980
C  SF       SATURATED LIQUID ENTROPY                           SOU00990
C  SG       SATURATED  GAS ENTROPY                             SOU01000
C                                                             SOU01010
C  T(I)     LOCAL SAT. TEMPERATURE                             SOU01020
C  TFL      SATURATED TEMPERATURE                              SOU01030
C  TO       STAGN TEMPERATURE                                  SOU01040
C                                                             SOU01050
C  U        LOCAL FLUID VELOCITY                               SOU01060
C  UFL      FLUID VELOCITY AT FLASH                            SOU01070
C  UA       SONIC VELOCITY                                     SOU01080
C                                                             SOU01090
C  V(I)     LOCAL SPECIFIC VOLUME                              SOU01100
C  VO       STAGN SP. VOLUME                                   SOU01110
C  VF       SATURATED  SP. VOLUME OF LIQUID                    SOU01120
C  VG       SATURATED GAS SPECIFIC VOLUME                      SOU01130
C  VFL      SP VOLUME AT FLASH                                 SOU01140
C  VEN      SP VOLUME AT ENTRANCE                              SOU01150
C  VEX      SP VOLUME AT EXIT                                  SOU01160
C                                                             SOU01170
C  X(I)     QUALITY AT GRID I                                  SOU01180
C  XEN      ENTRANCE QUALITY                                   SOU01190
C  XEX      EXIT QUALITY                                       SOU01200
```

```
C
C   YH      THE HIGHEST MASS FLOW RATE FOR ITERATION
C   YL      THE LOWEST MASS FLOW RATE FOR ITERATION
C
C   Z(I)    SPATIAL DISTANCE AT GRID I
C   ZFL     FLASHING LOCATION
C
C-----------------------------------------------------------------------
C   ALL  UNITS USED ARE IN STANDARD MKS  AND TEMPERATURE IN DEG KELVIN
C-----------------------------------------------------------------------
C
C   READ MASS FLUX DATA
      READ(10) G
  710 CONTINUE
      JJN=15
      JJM=36
C   READ INPUT PARAMETERS
      READ(5,*)NT,PO,TO,DT,HO,VO
      READ(5,*)AEN,AEX,DELTA,F
      READ(5,*)PFL,L
      IF(NT.EQ.0)GOTO 720
      ETA=(AEN-AEX)/L
      DPFL=PO-PFL
C   PRINT INPUT PARAMETERS
      WRITE(6,100)NT
      WRITE(6,101)PO,TO,DT
      WRITE(6,102)AEX,AEN,L
      WRITE(6,103)F
      PRINT*,'ETA=',ETA
  100 FORMAT(1H1,///T25,'TEST  NUMBER  = ',I5,/)
  101 FORMAT(//T5,'PO=',E15.7,2X,'TO=',E15.7,2X,'DT=',E15.7)
  102 FORMAT(1H+,T65,'AEX=',E15.7,2X,'AEN=',E15.7,2X,'L=',E15.7)
  103 FORMAT(/T30,'    F  =',E15.7)
C   TO FIND THE INITIAL GUESS VALUE OF M
      TRE=480.
      PRE=2.900E6
C   FIRST FIND THE G(I,J)
      S1=(TO-TRE)/10.+0.5
      K1=IFIX(S1)
      S2=(PO-PRE)/100000.+0.5
      K2=IFIX(S2)
      S3=G(K1,K2)
C   FIND L/DH AND THEN THE INITIAL GUESS M
      S4=L/(DELTA*2.)
      S5=DT/(TO-273.1)
      Q1=-0.0013506
      Q2=-0.0013663
      Q3=-0.0018824
      IF(S5.GT.0.2)THEN
      M=S3*AEX*(Q1*S4+0.52)
      ELSE IF(S5.GT.0.1)THEN
      M=S3*AEX*(Q2*S4+0.69)
      ELSE
      M=S3*AEX*(Q3*S4+0.97)
      END IF
      IF(M.GT.0.)GOTO 391
      IF(NT.LT.7)THEN
      M=1.0E-3
      ELSE IF(NT.LT.19)THEN
      M=1.0E-4
```

```
      ELSE IF(NT.LT.41)THEN
      M=2.E-2
      ELSE IF(NT.LT.69)THEN
      M=1.E-3
      ELSE
      M=1.0E-1
      END IF
  391 CONTINUE
      RJS=0.
      R=1.
      JK=0
   12 M=M*R
C  IF ITERATION ON MASS FLOW RATE ADJUSTMENT GOES MORE THAN N TIMES
C  STOP
      JK=JK+1
      IF(JK.GT.35)GOTO 993
C  FIND THE FLASHING AREA ASSUMING SINGLE PHASE LIQUID AND HENCE FIND
C  UFL
C  INITIALISE ALL THE ARRAYS
      DO 5 I=1,55
      A(I)=0.
      DZ(I)=0.
      P(I)=0.
      P1(I)=0.
      V(I)=0.
      X(I)=0.
    5 CONTINUE
C  FIND THE THERODYNAMIC PROPERTIES AT FLASH PRESSURE
      CALL STEAM(PFL)
C  SET THE VALUES AT FLASH
      HFL=HF
      VFL=VF
      SFL=SF
      AFL=(M**2.*V0*0.5/DPFL)**0.5
C  COMPARE AFL WITH AEN TO SEE IF SINGLE PHASE ENTRANCE IF YES GO TO 11
      IF(AFL.LT.AEN)GOTO 11
C  COMPARE THE TOLARENCE
      IF((AFL-AEN)/AEN.LE.0.01)GOTO 17
C  FIND PRESSURE DROP BETWEEN FLASH AND ENTRANCE
      DPFEN=(M**2.*VFL*0.5/AEN**2.)*(1.-(AEN/AFL)**2.)
      DP1=DPFEN*0.9
C  SET FOR ITERATION AND FIND THERMODYNAMIC PROPERTIES AT PP
      KK=0
   22 CONTINUE
      PP=PFL-DP1
      IF(PP.GT.1.013E5)GOTO 47
      RR=1./1.5
      R=RR
      GOTO 12
   47 CONTINUE
      KK=KK+1
      CALL STEAM(PP)
      X1=(S0-SF)/(SG-SF)
      V1=VF+X1*(VG-VF)
      H1=HF+X1*(HG-HF)
      U1=(2.*(HFL-H1)+UFL**2.)**0.5
      A1=M*V1/U1
      IF(KK-1)42,42,44
   42 CONTINUE
C  FIND SOUND VELOCITY
```

```
      DX1DP=-((DSFDP)*(1.-X1)+X1*DSGDP)/(SG-SF)
      UA=V1*((-((1.-X1)*DVFDP+X1*DVGDP+(VG-VF)*DX1DP))**(-0.5))
C  COMPARE U1 AND UA
      IF((UA-U1)/UA.GT.0.001)GOTO 44
      AR=AEX/A1
C  REDUCE MASS FLOW RATE
      RR=U1*(AR**.5)/UA
      R=RR**.5
      GOTO 12
   44 CONTINUE
C  CHECK FOR THE CONVERGENCE FOR AREA AT ENTRANCE
      AR1=A1/AEN
      ARR=AR1-1.
      IF(ARR.LE.0.01)GOTO 23
      DP1=DP1*(AR1**2.0)
      GOTO 22
   23 CONTINUE
C  SET THE ENTRANCE VALUES FOR THEY ARE NOW DETERMINED
      PEN=PP
      HEN=H1
      VEN=V1
      UEN=U1
      XEN=X1
      SEN=SF+X1*(SG-SF)
      GOTO 66
C  THE FOLLOWING CORRESPOND TO THE CASE OF FLASH AT ENTRANCE PLANE
   17 CONTINUE
      CALL STEAM(PFL)
      PEN=PFL
      HEN=HFL
      VEN=VF
      SEN=SF
      UEN=M*VEN/AEN
      XEN=0.
   66 CONTINUE
C  FIND THE SOUND VELOCITY AT ENTRANCE PLANE
      DX1DP=-((DSFDP)*(1.-XEN)+XEN*DSGDP)/(SG-SF)
      UA=VEN*((-((1.-XEN)*DVFDP+XEN*DVGDP+(VG-VF)*DX1DP))**(-0.5))
C  COMPARE UEN WITH UA. IT'S TWO-PHASE ENTRANCE IF YES ON GOTO 77.
      IF((UA-UEN)/UA.GT.0.001)GOTO 77
C  REDUCE MASS FLOW RATE
      RR=UA*((AEX/AEN)**0.5)/UEN
      R=RR
      GOTO 12
   11 CONTINUE
      IF((AEN-AFL)/AEN.LE.0.01)GOTO 17
C  DESIGNATE SINGLE PHASE AS TP=0.
      TP=0.
C  FIND ENTRANCE LOSS
      DPEN=M**2.*V0*0.5/AEN**2.
      PEN=P0-DPEN
C  FIND PRESSURE DROP FOR NO FLASH BEFORE EXIT PLANE
      AEXS=AEN*AEN+AEX*AEX
      V1=2.*M*M*(VFL-V0)/(AEXS)
      V2=M*M*0.25*(VFL+V0)*(1.+F*DELTA/ETA)*(1./AEX**2.-1./AEN**2.)
      V3=M*M*0.5*F*(VFL+V0)*(1./AEX-1./AEN)/(ETA*DELTA)
      DPFEX=V1+V2+V3
C  CHECK FOR FLASH POSITION INSIDE CHANNEL IF YES GOTO 88
      IF((PEN-(PFL+DPFEX))/PEN.LE.0.000)GOTO 88
C  INCREASE MASS FLOW RATE
```

```
      MO=M
      IF(JJN.GT.JJM)GOTO 603
      IF(JJN-JK)602,602,601
  601 CONTINUE
      RR=((PO-PFL)/(PO-PEN+DPFEX))**.8
      R=RR
      YL=MO
      GOTO 12
  602 CONTINUE
      IF(JJN.GT.JJM)GOTO 605
      RR=(1.+YH/MO)/(2.)
      R=RR
      YL=MO
      GOTO 12
  603 CONTINUE
      IF(JJM-JK)605,605,601
  605 CONTINUE
      RR=(1.+MP/MO)/(2.)
      R=RR
      GOTO 12
   88 CONTINUE
C  FLASH INSIDE THE CHANNEL
      AFF=2.*(PEN-PFL)+M*M*VFL*(1.+DELTA*F/ETA)/AEN**2.+(2.*M*M*F*VFL/
     &(ETA*DELTA*AEN))
      AFL=(1.+(1.+((ETA**2.*DELTA**2.+DELTA**3.*ETA*F)/(M*M*F*F*VFL))*
     &AFF)**0.5)/((ETA*DELTA/(M*M*F*VFL))*AFF)
      ZFL=(AEN-AFL)/ETA
C  WRITE ZFL AND   AFL AT PFL
C  FIND THE SOUND VELOCITY AND FLUID VELOCITY
      CALL STEAM(PFL)
      XFL=0.
      VFL=VF
      HFL=HF
      SFL=SF
      DXDP=-(DSFDP)/(SG-SF)
      UA=VFL*((-(DVFDP+(VG-VF)*DXDP))**(-0.5))
      UFL=(M*VFL)/AFL
C  COMPARE THE SOUND VELOCITY AND THE FLUID VELOCITY
      IF(UA.GE.UFL)GOTO 90
      IF((UFL-UA)/UA.LE.0.001)GOTO 158
      IF(ABS((L-ZFL)/L).LE.0.5E-7)GOTO 169
      YH=M
      IF(JJN.GT.JJM)GOTO 140
      GOTO 141
  140 CONTINUE
      YL=MO
  141 CONTINUE
      IF((YH-YL)/YH.LE.0.001)GOTO 149
      GOTO 159
  149 CONTINUE
      M=YH
      I=0
      GOTO 157
  159 CONTINUE
C  DECREASE THE MASS FLOW RATE
      JJM=JK
      MP=YH
      RR=(1.+MO/MP)/(2.)
      R=RR
      GOTO 12
```

```
  169 CONTINUE
      JJM=JK
      MP=M
      RR=(UA/UFL)**.05
      R=RR
      GOTO 12
   90 CONTINUE
      IF((UA-UFL)/UA.LE.0.001)GOTO 160
C  CHECK FOR LENGTH
      ZL=(L-ZFL)/L
      IF(ZL.GT.0.5E-7)GOTO 99
      U=UFL
   98 CONTINUE
      XMACH=U/UA
      IF(YH.EQ.0.)GOTO 812
      IF((YH-YL)/YH.LE.0.001)GOTO 757
  812 CONTINUE
      YL=M
      XMACH=U/UA
C  INCREASE MASS FLOW RATE
      IF(JJN-JK)702,702,701
  701 CONTINUE
      RR=(UA/U)**0.05
      R=RR
      GOTO 12
  702 CONTINUE
      RR=(1.+YH/YL)/(2.)
      R=RR
      GOTO 12
  757 CONTINUE
      MC=M
      IF(I.GT.0)GOTO 758
      GOTO 756
C  CONTINUE FOR STEP 158
  160 CONTINUE
      IF((L-ZFL)/L.LE..50E-7)GOTO 657
      GOTO 159
  158 CONTINUE
C  FIRST CHECK FOR LENGTH WHEATHER AT EXIT
      IF((L-ZFL)/L.GT.0.50E-7)GOTO 159
  657 I=0
  157 CONTINUE
C  WRITE CHOKE EXACTLY AT EXIT AND FIND CRITICAL MASS FLOW RATE
      IF(I.GT.0)GOTO 156
      MC=M
  756 CONTINUE
      PRINT*,'THE FINAL CRITICAL MASS FLOW RATE IS',MC
      PRINT*,'***********************************************************
     &***'
      WRITE(6,113)L,AEX,PFL,MC
  113 FORMAT(///T25,'RIGHT CONDITIONS ATTAINED AT EXIT FLASHING',//T5
     &,'Z(I)=',E15.7,'AEX=',E15.7,'PFL=',E15.7,2X,'MC=',E15.7)
C FIND THE PRESSURE DISTRIBUTION IN SINGLE-PHASE REGION.
      NDZ=19
      N=NDZ+1
      DX=L/19.
      Z(1)=0.0
      A(1)=AEN
      P(1)=PEN
      P(20)=PFL
```

```
      Z(20)=L
      A(20)=AEX
      X(20)=0.0
      DO 19 IJ=2,19
      Z(IJ)=DX*(IJ-1)
      A(IJ)=AEN-ETA*Z(IJ)
   19 CONTINUE
      CALL STEAM(PEN)
      X(1)=(HO-HF)/(HG-HF)
      M=MC
      IJ=1
   20 CONTINUE
      IJ=IJ+1
      IF(IJ.GE.N)GOTO 969
      DP(IJ)=M*M*0.5*VO*(1.+DELTA*F/ETA)*(1./A(IJ)**2.-1./A(IJ-1)**2.)
     &+M*M*F/(2.*DELTA*ETA)*(2.*VO)*(1./A(IJ)-1./A(IJ-1))
      P(IJ)=P(IJ-1)-DP(IJ)
      CALL STEAM(P(IJ))
      X(IJ)=(HO-HF)/(HG-HF)
      IF(IJ.EQ.(N-1))GOTO 21
      GOTO 20
   21 CONTINUE
      WRITE(6,478)
  478 FORMAT(///T6,'I',7X,'Z(I)',15X,'A(I)',15X,'P(I)',15X,'X(I)')
      DO 248 IJ=1,N
  248 WRITE(6,249)IJ,Z(IJ),A(IJ),P(IJ),X(IJ)
  249 FORMAT(//6X,I2,4(2X,E15.7))
  969 CONTINUE
      CALL DATETM(DATTIM,23,VCPU,CTIME,TCPU)
      WRITE(6,801)DATTIM,VCPU,CTIME,TCPU
      GOTO 999
  156 CONTINUE
      MC=UA*AEX/V(I)
  768 CONTINUE
      WRITE(6,114)I,P(I),I,X(I),I,V(I),MC
  114 FORMAT(//T25,'RIGHT CONDITIONS ATTAINED AT EXIT PLANE',//T5,'P(',
     &I2,')=',E15.7,'X(',I2,')=',E15.7,'V(',I2,')=',E15.7,'MC =',E15.7)
      PRINT*,'THE FINAL CRITICAL MASS FLOW RATE IS',MC
      PRINT*,'*********************************************************
     &***'
      PRINT*,'DPEN=',DPEN,'PEN=',PEN
      WRITE(6,477)
  477 FORMAT(///T6,'I',7X,'Z(I)',15X,'A(I)',15X,'P(I)',15X,'V(I)',12X,'
     &X(I)',12X,'H(I)')
      Z(1)=ZFL
      A(1)=AFL
      DO 662 KKK=2,N
      DZ(KKK)=DZT*2.**(FLOAT(N-KKK))
      Z(KKK)=Z(KKK-1)+DZ(KKK)
      A(KKK)=AEN-ETA*Z(KKK)
  662 CONTINUE
      DO 246 I=1,N
  246 WRITE(6,247)   I,Z(I),A(I),P(I),V(I),X(I),H(I)
  247 FORMAT(//6X,I2,6(2X,E15.7))
      IF(Z(1)/L.GE.0.2)GOTO 301
      GOTO 919
C FIND THE PRESSURE DISTRIBUTION IN SINGLE-PHASE REGION.
  301 CONTINUE
      NDZ=14
      N=NDZ+1
```

```
      DX=(Z(1))/14.
      P(15)=P(1)
      P(1)=PEN
      A(15)=A(1)
      A(1)=AEN
      Z(15)=Z(1)
      Z(1)=0.0
      X(15)=0.0
      CALL STEAM(PEN)
      X(1)=(HO-HF)/(HG-HF)
      DO 39 IJ=2,14
      Z(IJ)=DX*(IJ-1)
      A(IJ)=AEN-ETA*Z(IJ)
   39 CONTINUE
      M=MC
      IJ=1
   40 CONTINUE
      IJ=IJ+1
      IF(IJ.GE.N)GOTO 919
      DP(IJ)=M*M*0.5*VO*(1.+DELTA*F/ETA)*(1./A(IJ)**2.-1./A(IJ-1)**2.)
     &+M*M*F/(2.*DELTA*ETA)*(2.*VO)*(1./A(IJ)-1./A(IJ-1))
      P(IJ)=P(IJ-1)-DP(IJ)
      CALL STEAM(P(IJ))
      X(IJ)=(HO-HF)/(HG-HF)
      IF(IJ.EQ.(N-1))GOTO 25
      GOTO 40
   25 CONTINUE
      PRINT*,'**THE FOLLOWING ARE THE PRESSURE AND QUALITY DISTRIBUTION
     &IN SINGLE-PHASE REGION**'
      WRITE(6,478)
      DO 48 IJ=1,N
   48 WRITE(6,249)IJ,Z(IJ),A(IJ),P(IJ),X(IJ)
  919 CONTINUE
C WRITE CPU TIME FOR THE CALCULATIONS
      CALL DATETM (DATTIM,23,VCPU,CTIME,TCPU)
      WRITE(6,801)DATTIM,VCPU,CTIME,TCPU
  801 FORMAT('DATE/TIME:',A23/,'VCPU=',F10.3,'SEC.','CONNECT TIME=',F
     &10.3,'SEC.','TCPU=',F10.3,'SEC.')
      GOTO 999
C  CONTINUE FOR SINGLE PHASE CALCULATIONS FROM STEP 92 TO 99
   99 CONTINUE
C  DIVIDE THE CHANNEL IN GRIDS
      C3=0.01E-5
      IF((L-ZFL).GT.C3)GOTO 966
      NDZ=1
      DZT=(L-ZFL)
      GOTO 96
  966 CONTINUE
      IF(ZL.GE.0.01)GOTO 511
      NDZ=15
      GOTO 398
  511 CONTINUE
      NDZ=25
  398 CONTINUE
      DZT=(L-ZFL)/(2.**(FLOAT(NDZ))-1.)
      IF(DZT.GT.C3)GOTO 96
      NDZ=NDZ-1
      GOTO 398
   96 CONTINUE
C  SUBROUTINUE GRID DOES THE DIVISION OF GRIDS INTO NDZ GRIDS WITH A(I)
```

```
C  Z(I) DETERMINED
      N=NDZ+1
C  SET THE FLASH AS THE ZERO POINT
      Z(1)=ZFL
      P(1)=PFL
      A(1)=AFL
      V(1)=VFL
      X(1)=0.
      H(1)=HFL
  134 CONTINUE
      DO 6 IK=2,N
      DZ(IK)=DZT*2.**(FLOAT(N-IK))
      Z(IK)=Z(IK-1)+DZ(IK)
      A(IK)=AEN-ETA*Z(IK)
    6 CONTINUE
      A2=A(2)
C  GUESS DOES THE INITIAL GUESS FOR SPECIFIC VOLUME AT FIRST GRID POINT
      CALL GUESS(A2,O,Q)
      V(2)=O
      X(2)=Q
      GOTO 132
C  THE STEP COMING FROM THE TWO PHASE ENTRANCE IS THE FOLLOWING IE 77
   77 CONTINUE
C  DIVIDE THE CHANNEL IN TO GRID POINTS
      NDZ=15
   75 CONTINUE
      DZT=L/(2.**(FLOAT(NDZ))-1.)
      IF(DZT.GT.C3)GOTO 76
      NDZ=NDZ-1
      GOTO 75
   76 CONTINUE
C  SET THE ENTRANCE AS THE ZERO TH GRID
      Z(1)=0.
      A(1)=AEN
      V(1)=VEN
      P(1)=PEN
      X(1)=XEN
      V(2)=V(1)
      DO 7 II=2,N
      DZ(II)=DZT*2.**(FLOAT(N-II))
      Z(II)=Z(II-1)+DZ(II)
      A(II)=AEN-ETA*Z(II)
    7 CONTINUE
  132 CONTINUE
      N=NDZ+1
      I=1
C  NOW START CALCULATING THE PRESSURE DROP FOR SUCESSIVE GRID POINT
  133 CONTINUE
      I=I+1
C     PRINT*,'I =',I
C  STOP IF END POINT IS REACHED
      IF(I.GT.N)GOTO 999
      J=0
C  LOOP FOR THE CONVERGENCE OF PRESSURE AT NEXT GRID POINT
  144 CONTINUE
      J=J+1
C  IF ITERATION GOES MORE THAN 35 TIMES THEN STOP
      IF(J.GT.35)GOTO 991
C  FIND PRESSURE DROP USING TWO-PHASE MOMENTUM EQUATION
      DP(I)=2.*M*M/(A(I)**2.+A(I-1)**2.)*(V(I)-V(I-1))+M*M*0.25*(V(I-1)+
```

```
     &V(I))*(1.+DELTA*F/ETA)*(1./A(I)**2.-1./A(I-1)**2.)+M*M*F/(2.*DELTA
     &*ETA)*(V(I-1)+V(I))*(1./A(I)-1./A(I-1))
C      PRINT*,'DP(I) =',DP(I)
C  FIND THE PRESSURE AT THE I TH GRID POINT
      P1(J)=P(I-1)-DP(I)
      IF(P1(J).GT.1.013E5)GOTO 313
C  REDUCE THE MASS FLOW RATE
      YH=M
      RR=(1.+YL/YH)/(2.)
      R=RR
      GOTO 12
  313 CONTINUE
      IF(J.LT.33)GOTO 143
C  CHEK FOR CONVERGENCE IF ITERATION IS MORE THAN 30 TIMES
      IF((P1(J)-P1(J-1))/(P1(J-1)-P1(J-2)).LT.1.)GOTO 142
      IF(I.GT.N)GOTO 991
      IF(I.EQ.N)GOTO 155
      YH=M
      RR=(1.+YL/YH)/(2.)
      R=RR
      GOTO 12
  142 CONTINUE
C  SEE FOR CONVERGENCE
      IF((P1(J)-P1(J-1))/P1(J).LE.0.001)GOTO 155
  143 CONTINUE
      IF(J-3) 333,333,600
  600 CONTINUE
      IF(P1(J).EQ.P1(J-1))GOTO 155
      IF((P1(J)-P1(J-1))/(P1(J-1)-P1(J-2)).LT.1.)GOTO 300
      CALL STEAM(P1(J))
      VC=A(I)*A(I)*(HO-HF)/(M*M*(VG-VF)**2.)
      VA=VF/(VG-VF)
      VB=A(I)*A(I)*(HG-HF)/(M*M*(VG-VF)**2.)
      X(I)=-(VA+VB)+((VA+VB)**2.+2.*VC-VA**2.)**(0.5)
      V(I)=VF+X(I)*(VG-VF)
      U=M*V(I)/A(I)
      DXDP=-(DSFDP*(1.-X(I))+X(I)*DSGDP)/(SG-SF)
      UA=V(I)*((-((1.-X(I))*DVFDP+X(I)*DVGDP+(VG-VF)*DXDP))**(-.5))
      XMACH=U/UA
      IF((U-UA)/UA.LE.0.001)GOTO 144
C REDUCE THE MASS FLOW RATE.
      YH=M
      IF(RJS.GE.1)GOTO 157
      IF(I.LT.N)GOTO 528
      IF((YH-YL)/YH.GT.0.001)GOTO 528
      RJS=RJS+1.
      IF(RJS.GE.1.)GOTO 530
  528 CONTINUE
      JJN=JK
      RR=(1.+YL/YH)/(2.)
      R=RR
      GOTO 12
  530 CONTINUE
      M=YH
      DP(I)=2.*M*M/(A(I)**2.+A(I-1)**2.)*(V(I)-V(I-1))+M*M*0.25*(V(I-1)
     &+V(I))*(1.+DELTA*F/ETA)*(1./A(I)**2.-1./A(I-1)**2.)+M*M*F/(2.*
     &DELTA*ETA)*(V(I-1)+V(I))*(1./A(I)-1./A(I-1))
      P1(J)=P(I-1)-DP(I)
      GOTO 155
  300 CONTINUE
```

```
      IF(ABS((P1(J)-P1(J-1))/P1(J)).LE.0.001)GOTO 155
  333 CONTINUE
      IF(P1(J).EQ.P1(J-1))GOTO 155
C  FIND THE VALUEES OF PROPERTIES AT NEW VALUE OF P1(J)
      CALL STEAM(P1(J))
C  FIND QUALITY USING ENERGY EQUATION
      VC=A(I)*A(I)*(HO-HF)/(M*M*(VG-VF)**2.)
      VA=VF/(VG-VF)
      VB=A(I)*A(I)*(HG-HF)/(M*M*(VG-VF)**2.)
      X(I)=-(VA+VB)+((VA+VB)**2.+2.*VC-VA**2.)**(0.5)
      V(I)=VF+X(I)*(VG-VF)
      H(I)=HF+X(I)*(HG-HF)
C FIND FLUID VELOCITY AND SOUND VELOCITY AT DRID POINTS
      U=M*V(I)/A(I)
      DXDP=-(DSFDP*(1.-X(I))+X(I)*DSGDP)/(SG-SF)
      UA=V(I)*((-((1.-X(I))*DVFDP+X(I)*DVGDP+(VG-VF)*DXDP))**(-.5))
      XMACH=U/UA
      IF((U-UA)/UA.LE.0.001)GOTO 144
C REDUCE THE MASS FLOW RATE.
      YH=M
      IF(RJS.GE.1.)GOTO 157
      IF(I.LT.N)GOTO 529
      IF((YH-YL)/YH.GT.0.001)GOTO 529
      RJS=RJS+1.
      IF(RJS.GE.1.)GOTO 530
  529 CONTINUE
      JJN=JK
      RR=(1.+YL/YH)/(2.)
      R=RR
      GOTO 12
  155 CONTINUE
      P(I)=P1(J)
      IF(P(I).GT.P(I-1))GOTO 899
C WRITE THE CONVERGED VALUES AT THIS GRID POINT.
C  FIND THE FLUID PROPERTIES
      CALL STEAM(P(I))
C FIND THE QUALITY
      VC=A(I)*A(I)*(HO-HF)/(M*M*(VG-VF)**2.)
      VA=VF/(VG-VF)
      VB=A(I)*A(I)*(HG-HF)/(M*M*(VG-VF)**2.)
      X(I)=-(VA+VB)+((VA+VB)**2.+2.*VC-VA**2.)**0.5
      V(I)=VF+X(I)*(VG-VF)
      H(I)=HF+X(I)*(HG-HF)
C  WRITE THE FLUID STATE AT THE GRID I
      IF(RJS.GE.1.)GOTO 157
C  FIND SOUND VELOCITY AND FLUID VELOCITY
      U=M*V(I)/A(I)
      DXDP=-(DSFDP*(1.-X(I))+X(I)*DSGDP)/(SG-SF)
      UA=V(I)*((-((1.-X(I))*DVFDP+X(I)*DVGDP+(VG-VF)*DXDP))**(-0.5))
      XMACH=U/UA
C  COMPARE THE SOUND AND FLUID VELOCITIES
      IF(UA.GE.U)GOTO 161
      IF((U-UA)/UA.LE.0.001)GOTO 162
      IF(RJS.GE.1.)GOTO 157
      IF(I.LT.N)GOTO 163
      RJS=RJS+1.
      IF(RJS.GE.1.)GOTO 530
  163 CONTINUE
C  DECREASE MASS FLOW RATE
      YH=M
```

```
      RR=(1.+YL/YH)/(2.)                                                SOU07210
      R=RR                                                              SOU07220
      GOTO 12                                                           SOU07230
  899 CONTINUE                                                          SOU07240
      NDZ=NDZ-1                                                         SOU07250
      N=NDZ+1                                                           SOU07260
      DZT=(L-ZFL)/(2.**(FLOAT(NDZ))-1.)                                 SOU07270
      GOTO 134                                                          SOU07280
  161 CONTINUE                                                          SOU07290
      IF((UA-U)/UA.LE.0.001)GOTO 162                                    SOU07300
C  CHECK FOR THE LENGTH                                                 SOU07310
      IF(I.EQ.N)GOTO 98                                                 SOU07320
      GOTO 133                                                          SOU07330
C  CONTINUE FOR STEP 162                                                SOU07340
  162 CONTINUE                                                          SOU07350
C FIRST CHECK FOR LENGTH WHEATHER AT EXIT                               SOU07360
      IF(I.EQ.N)GOTO 157                                                SOU07370
      GOTO 163                                                          SOU07380
  991 CONTINUE                                                          SOU07390
      WRITE(6,119)P1(J),P1(J-1),P1(J-2),P1(J-3),P1(J-4)                 SOU07400
  119 FORMAT(//T10,'DOES NOT CONVERGE FOR THE GIVEN MASS FLOW RATE',//, SOU07410
     &5(2X,E15.7))                                                      SOU07420
  993 CONTINUE                                                          SOU07430
      PRINT*,'THE CALCULATION IS STOPPED DUE TO MANY ITERATIONS'        SOU07440
  999 CONTINUE                                                          SOU07450
      GOTO 710                                                          SOU07460
  720 CONTINUE                                                          SOU07470
      STOP                                                              SOU07480
      END                                                               SOU07490
C                                                                       SOU07500
C***********************************************************************SOU07510
C                                                                       SOU07520
C-----------------------------------------------------------------------SOU07530
C                                                                       SOU07540
C  THE FOLLOWING ARE SUBROUTINES                                        SOU07550
C-----------------------------------------------------------------------SOU07560
      SUBROUTINE GUESS(AA,C,D)                                          SOU07570
C  THIS SUBROUTINE DETERMINES FIRST GUESS VALUE FOR SP VOLUME AT FIRST  SOU07580
C  GRID POINT AFTER THE FLASHING POINT                                  SOU07590
      IMPLICIT REAL*8(A,L,M)                                            SOU07600
      COMMON/BLOCK1/VF,DVFDP,VG,DVGDP,HF,DHFDP,HG,DHGDP,SF,DSFSP,SG,    SOU07610
     &DSGDP                                                             SOU07620
      COMMON/BLOCK2/M,VFL,ETA,DELTA,F,AFL,ZFL,NDZ,DZT,PFL,HFL           SOU07630
C  FIND SINGLE PHASE PRESSURE DROP BETWEEN FLASH AND FIRST GRID         SOU07640
      DPSP1=M*M*0.5*VFL*(1.+DELTA*F/ETA)*(1./AA**2.-1./AFL**2.)+M*M*F   SOU07650
     &*VFL/ETA/DELTA*(1./AA-1./AFL)                                     SOU07660
C  FIND PRESSURE AT FIRST GRID                                          SOU07670
      PS1=PFL-DPSP1                                                     SOU07680
C  FIND PROPERTIES OF FLUID AT PS1                                      SOU07690
      IF(PS1.LT.100.)GOTO 10                                            SOU07700
      CALL STEAM(PS1)                                                   SOU07710
C  FIND QUALITY AT FIRST GRID                                           SOU07720
      X1=(HFL-HF)/(HG-HF)                                               SOU07730
C  FIND MARTINELLI-NELSON FRICTION  MULTIFLIER                          SOU07740
C                                                                       SOU07750
      PS1=PS1*1.45041E-4                                                SOU07760
C                                                                       SOU07770
      PHI=EXP((1.65E-10*PS1**4.-8.9E-7*PS1**3.+1.79E-3*PS1**2.-1.63*PS1+SOU07780
     &6.02E2)*X1)                                                       SOU07790
C  FIND TWO-PHASE PRESSURE DROP                                         SOU07800
```

```
      P2P=PHI*DPSP1
      PP2=PFL-P2P
C  FIND FLUID PROPERTIES WITH THIS VALUE OF PP2
      CALL STEAM(PP2)
      D=(HFL-HF)/(HG-HF)
      C=VF+D*(VG-VF)
C
   10 CONTINUE
      RETURN
      END
C
C-----------------------------------------------------------------------
      SUBROUTINE STEAM(P)
      COMMON/BLOCK1/VF,DVFDP,VG,DVGDP,HF,DHFDP,HG,DHGDP,SF,DSFDP,SG,
     &DSGSP
C
C_______________________________________________________________________
C THIS IS A SUBROUTINE TO CALCULATE THE THERMODYNAMIC PROPERTIES OF
C SATURATED WATER AND STEAM AND THE DERIVATIVES OF SPECIFIC VOLUME V,
C ENTROPY,S,ENTHALPY H,ETC AS REQUIRED.
C THE UNITS WE ARE USING ARE FOR P KG/CM**2.,FOR T DEG. K , FOR V,
C CM**3/GM,FOR ENTHALPY H KCAL/KG AND FOR S KCAL/KG K.
C THE INPUT AND OUTPUT FROM THIS SUBROUTINE GIVE THE CALCULATED FLUID
C PROPERTIES IN MKS UNITS
C----------------------------------------------------------------------
C
C DEFINE THE CRITICAL PRESSURE,TEMPERATURE,SPECIFIC VOLUME,ENTHALPY
C AND THE ENTROPY WITH THE UNITS ALREADY SAID ABOVE
C
      PC=2.2119256D7
      TC=647.27
      VC=3.1698D-3
      HC=2.107209D6
      SC=4.4427222D3

      Z=-ALOG(P/PC)
C CONSTANTS FOR SATURATION TEMPERATURE
      A1=0.1295426849D0
      A2=0.4513602436D0
      A3=0.2122378436D0
      A4=-0.3581437096D-2
      A5=0.9090316283D-4
      A6=0.3338530622D1
      A7=0.1426558985D1
C EQUATION FOR SATURATION TEMPERATURE
      A8=1.+A6*Z+A7*Z*Z
      A9=A1*Z+A2*Z*Z+A3*(Z**3.)+A4*(Z**4.)+A5*(Z**5.)
      TA=TC*(A8/(A8+A9))
      THETA=TA/TC
C DERIVATIVE DT/DP
      A10=A6+2.*A7*Z
      A11=A10+A1+2.*A2*Z+3.*A3*Z*Z+4.*A4*(Z**3.)+5.*A5*(Z**4.)
      A12=A10/A8
      A13=A11/(A8+A9)
      DTDP=-TA*(A12-A13)/P
C CONSTANTS FOR SPECIFIC VOLUME OF WATER VF
      B1=0.1030837042D5
      B2=0.5538426569D7
      B3=0.1799772193D9
      B4=-0.4743843407D9
```

```
      B5=0.2019749779D10
      B6=-0.6258564009D10
      B7=0.1230937510D11
      B8=-0.1351160480D11
      B9=0.6353769714D10
      B10=0.1163268984D5
      B11=.7686775534D7
      B12=0.3694089380D9
C
      Y=1.-THETA
C EQUATION FOR SPECIFIC VOLUME OF WATER VF
      B13=1.+B1*Y+B2*Y*Y+B3*(Y**3.)+B4*(Y**4.)
      B14=B5*(Y**5.)+B6*(Y**6.)+B7*(Y**7.)+B8*(Y**8.)+B9*(Y**9.)
      B15=B13+B14
      B16=1.+B10*Y+B11*Y*Y+B12*Y**3.
C
      VF=VC*B15/B16
C DERIVATIVE DVF/DP   : DVFDP
      B17=B1+2.*B2*Y+3.*B3*Y*Y+4.*B4*Y**3.
      B18=5.*B5*Y**4.+6.*B6*Y**5.+7.*B7*Y**6.+8.*B8*Y**7.+9.*B9*Y**8.
      B19=B17+B18
      B20=B19/B15
      B21=B10+2.*B11*Y+3.*B12*Y*Y
      B22=B21/B16
C
      DVFDP=-VF*DTDP*(B20-B22)/TC
C
C
C CONSTANTS FOR THE SPECIFIC VOLUME OF STEAM VG
      C1=0.4116876614D4
      C2=0.8824691596D6
      C3=0.4332657100D7
      C4=-0.2835427189D8
      C5=0.3658875474D8
      C6=0.1299835973D7
      C7=-0.1729496423D8
      C8=0.4780391119D4
      C9=0.1436268862D7
      C10=0.2732195974D8
      C11=-0.8611392578D8
      C12=0.8981196903D8
C EQUATION FOR THE SPECIFIC VOLUME OF STEAM VG
      C13=1.+C8*Y+C9*Y*Y+C10*Y**3.+C11*Y**4.+C12*Y**5.
      C14=1.+C1*Y+C2*Y*Y+C3*Y**3.+C4*Y**4.
      C15=C5*Y**5.+C6*Y**6.+C7*Y**7.
      C16=C14+C15
      C17=C16*THETA**6.
C
      VG=VC*C13/C17
C
C DERIVATIVE DVGDP
      C18=C8+2.*C9*Y+3.*C10*Y*Y+4.*C11*Y**3.+5.*C12*Y**4.
      C19=C18/C13
      C20=C1+2.*C2*Y+3.*C3*Y*Y+4.*C4*Y**3.
      C21=5.*C5*Y**4.+6.*C6*Y**5.+7.*C7*Y**6.
      C22=C20+C21
      C23=C22/C16
C
      DVGDP=VG*DTDP*(-6./THETA-C19+C23)/TC
C
```

```
C
C CONSTANTS FOR SPECIFIC ENTHALPY OF WATER HF
      D1=0.5035888418D4
      D2=0.8529880310D6
      D3=0.3975661294D7
      D4=-0.1321212174D8
      D5=0.7472567358D7
      D6=-0.1690034753D7
      D7=0.5288733377D4
      D8=0.9824212891D6
      D9=0.7825906288D7
      D10=-0.4620228177D7
C
C EQUATION FOR SPECIFIC ENTHALPY OF WATER HF
      D11=1.+D1*Y+D2*Y*Y+D3*Y**3.+D4*Y**4.+D5*Y**5.+D6*Y**6.
      D12=1.+D7*Y+D8*Y*Y+D9*Y**3.+D10*Y**4.
      HF=HC*D11/D12
C DERIVATIVE DHF/DP ; DHFDP
      D13=D1+2.*D2*Y+3.*D3*Y*Y+4.*D4*Y**3.+5.*D5*Y**4.+6.*D6*Y**5.
      D14=D7+2.*D8*Y+3.*D9*Y*Y+4.*D10*Y**3.
      D15=D13/D11
      D16=D14/D12
      DHFDP=-HF*(D15-D16)*DTDP/TC
C CONSTANTS  FOR SPECIFIC ENTHALPY OF STEAM HG
      E1=0.4981303137D4
      E2=0.1557966611D7
      E3=0.3218710689D8
      E4=0.9584965114D7
      E5=-0.4398959523D8
      E6=0.2724983908D8
      E7=0.4802965641D4
      E8=0.1385876104D7
      E9=0.2323566205D8
      E10=0.8134541110D6
C EQUATIN FOR SPECIFIC ENTHALPY OF STEAM HG
      E11=1.+E1*Y+E2*Y*Y+E3*Y**3.+E4*Y**4.+E5*Y**5.+E6*Y**6.
      E12=1.+E7*Y+E8*Y*Y+E9*Y**3.+E10*Y**4.
      HG=HC*E11/E12
C DERIVATIVE DHGDP
      E13=E1+2.*E2*Y+3.*E3*Y*Y+4.*E4*Y**3.+5.*E5*Y**4.+6.*E6*Y**5.
      E14=E7+2.*E8*Y+3.*E9*Y*Y+4.*E10*Y**3.
      E15=E13/E11
      E16=E14/E12
      DHGDP=-HG*(E15-E16)*DTDP/TC
C CONSTANTS FOR SPECIFIC ENTROPY OF WATER SF
      F1=0.5003614305D4
      F2=0.8273857898D6
      F3=0.3893852407D7
      F4=-0.1159666364D8
      F5=0.3369640365D7
      F6=0.1226506021D7
      F7=0.5187295813D4
      F8=0.9168034019D6
      F9=0.6319591884D7
      F10=-0.676264517D7
C
C EQUATION FOR THE SPECIFIC ENTROPY OF WATER SF
      F11=1.+F1*Y+F2*Y*Y+F3*Y**3.+F4*Y**4.+F5*Y**5.+F6*Y**6.
      F12=1.+F7*Y+F8*Y*Y+F9*Y**3.+F10*Y**4.
      SF=SC*F11/F12
```

```
C DERIVATIVE DSF/DP ; DSFDP                                              SOU09610
      F13=F1+2.*F2*Y+3.*F3*Y*Y+4.*F4*Y**3.+5.*F5*Y**4.+6.*F6*Y**5.       SOU09620
      F14=F7+2.*F8*Y+3.*F9*Y*Y+4.*F10*Y**3.                              SOU09630
      F15=F13/F11                                                        SOU09640
      F16=F14/F12                                                        SOU09650
      DSFDP=-SF*(F15-F16)*DTDP/TC                                        SOU09660
C CONSTANTS FOR SPECIFIC ENTROPY OF STEAM SG                              SOU09670
      G1=0.5922502679D4                                                  SOU09680
      G2=0.2121506453D7                                                  SOU09690
      G3=0.4367159918D8                                                  SOU09700
      G4=-0.1755438026D8                                                 SOU09710
      G5=-0.3706247525D8                                                 SOU09720
      G6=0.4303459784D8                                                  SOU09730
      G7=0.5782905801D4                                                  SOU09740
      G8=0.1950840259D7                                                  SOU09750
      G9=0.3351957025D8                                                  SOU09760
      G10=-0.3604330231D8                                                SOU09770
C EQUATION FOR THE SPECIFIC ENTROPY OF STEAM SG                           SOU09780
      G11=1.+G1*Y+G2*Y*Y+G3*Y**3.+G4*Y**4.+G5*Y**5.+G6*Y**6.             SOU09790
      G12=1.+G7*Y+G8*Y*Y+G9*Y**3.+G10*Y**4.                              SOU09800
      SG=SC*G11/G12                                                      SOU09810
C DERIVATIVE DSG/DP ; DSGDP                                              SOU09820
      G13=G1+2.*G2*Y+3.*G3*Y*Y+4.*G4*Y**3.+5.*G5*Y**4.+6.*G6*Y**5.       SOU09830
      G14=G7+2.*G8*Y+3.*G9*Y*Y+4.*G10*Y**3.                              SOU09840
      G15=G13/G11                                                        SOU09850
      G16=G14/G12                                                        SOU09860
      DSGDP=-SG*(G15-G16)*DTDP/TC                                        SOU09870
      RETURN                                                             SOU09880
      END                                                                SOU09890
```

APPENDIX D

Pressure and Quality Profiles

In this appendix the pressure and quality profiles obtained with SOURCE for some BCL tests are given. The choice of test numbers is based on highest and lowest subcoolings for each of the five BCL crack test sections. Hence total of 10 test numbers are chosen for presentation. The test parameters associated with each test are illustrated in each figure.

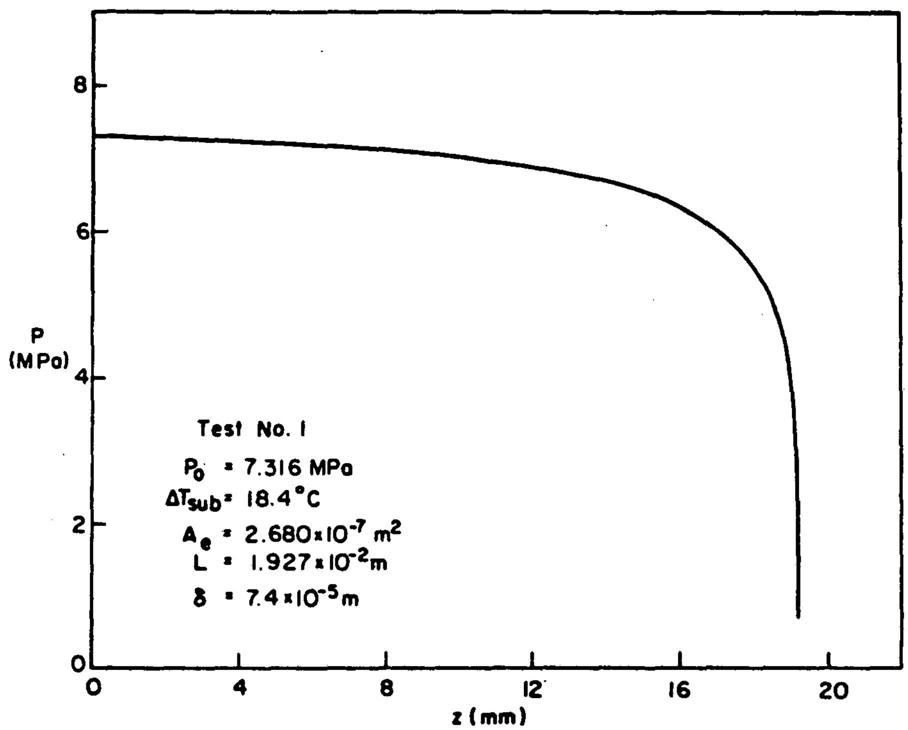

8
6
P
(MPa)
4
2
0
Test No. 1
P_o = 7.316 MPa
ΔT_{sub} = 18.4°C
A_e = 2.680×10^{-7} m^2
L = 1.927×10^{-2}m
δ = 7.4×10^{-5}m
0
4
8
12
16
20
z (mm)

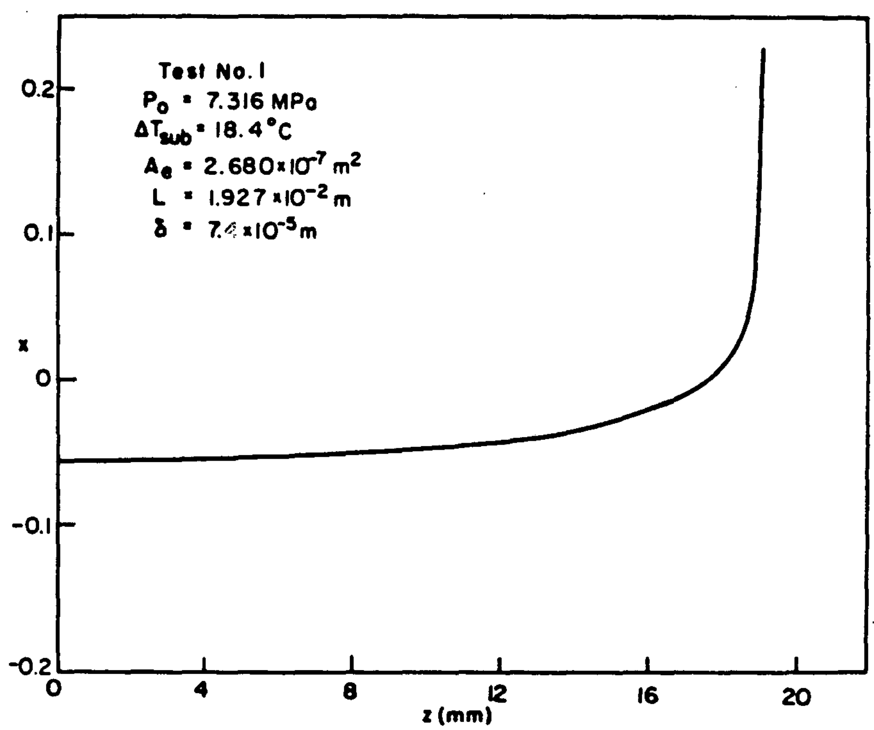

Test No. 1
P_o = 7.316 MPa
ΔT_{sub} = 18.4°C
A_e = 2.680×10^{-7} m^2
L = 1.927×10^{-2} m
δ = 7.4×10^{-5}m
0.2
0.1
x
0
-0.1
-0.2
0
4
8
12
16
20
z (mm)

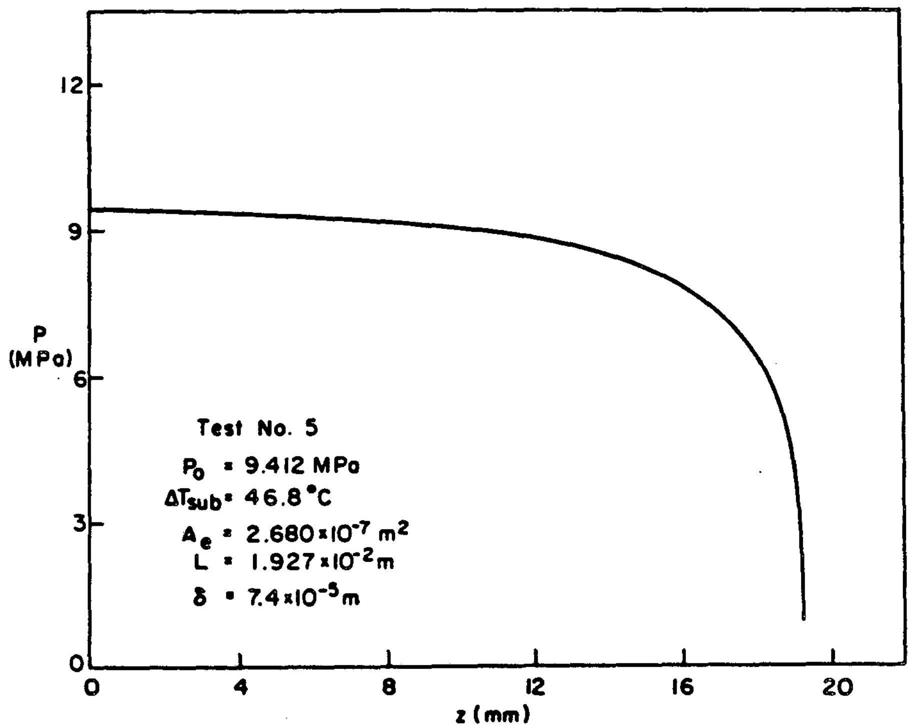
P
(MPa)
12
9
6
3
0
Test No. 5
P_o = 9.412 MPa
ΔT_{sub} = 46.8°C
A_e = 2.680 × 10^{-7} m^2
L = 1.927 × 10^{-2} m
δ = 7.4 × 10^{-5} m
0
4
8
12
16
20
z (mm)

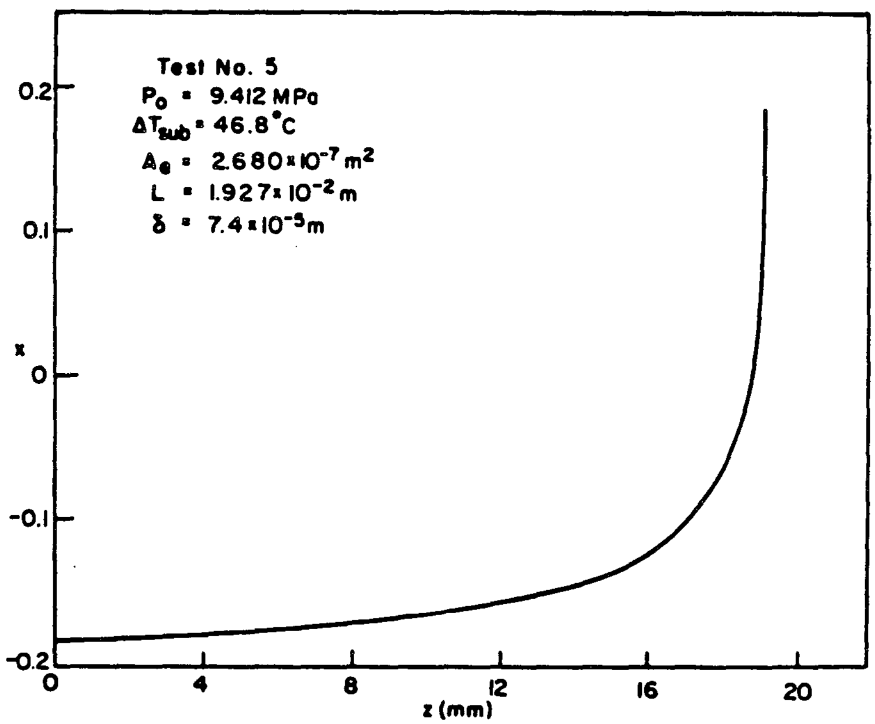
Test No. 5
P_o = 9.412 MPa
ΔT_{sub} = 46.8°C
A_e = 2.680 × 10^{-7} m^2
L = 1.927 × 10^{-2} m
δ = 7.4 × 10^{-5} m
x
0.2
0.1
0
-0.1
-0.2
0
4
8
12
16
20
z (mm)

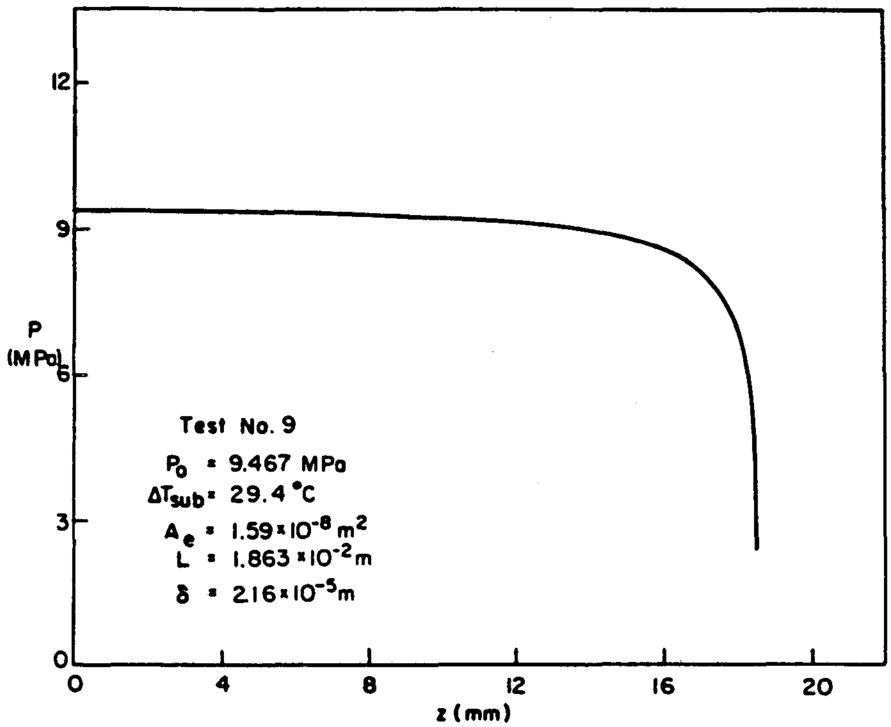

P
(MPa)
12
9
6
3
0
0
4
8
12
16
20
z (mm)
Test No. 9
P_o = 9.467 MPa
ΔT_{sub} = 29.4 °C
A_e = 1.59×10^{-8} m^2
L = 1.863×10^{-2} m
δ = 2.16×10^{-5} m

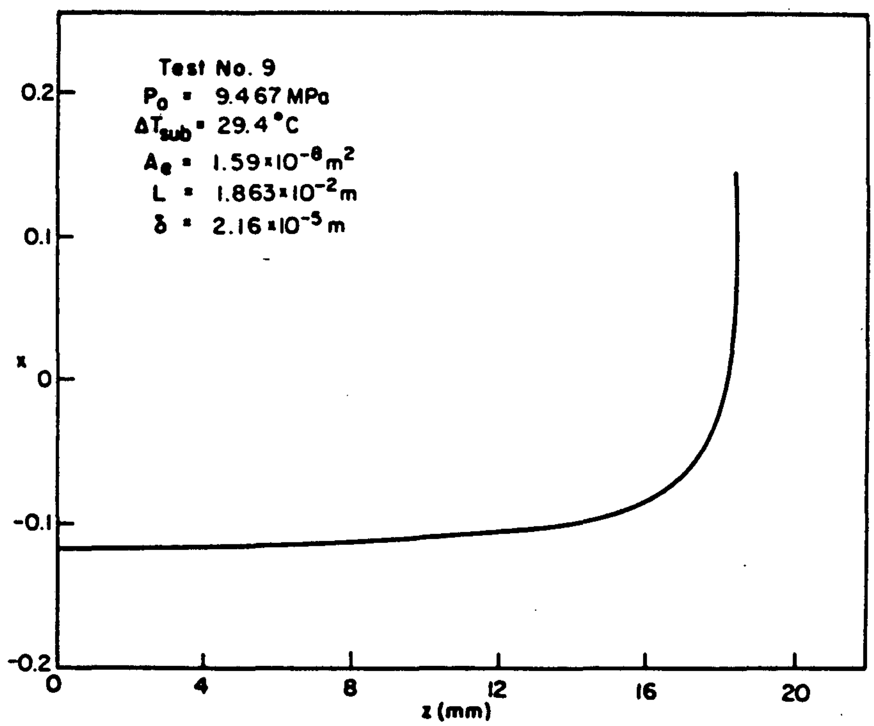

x
0.2
0.1
0
-0.1
-0.2
0
4
8
12
16
20
z (mm)
Test No. 9
P_o = 9.467 MPa
ΔT_{sub} = 29.4 °C
A_e = 1.59×10^{-8} m^2
L = 1.863×10^{-2} m
δ = 2.16×10^{-5} m

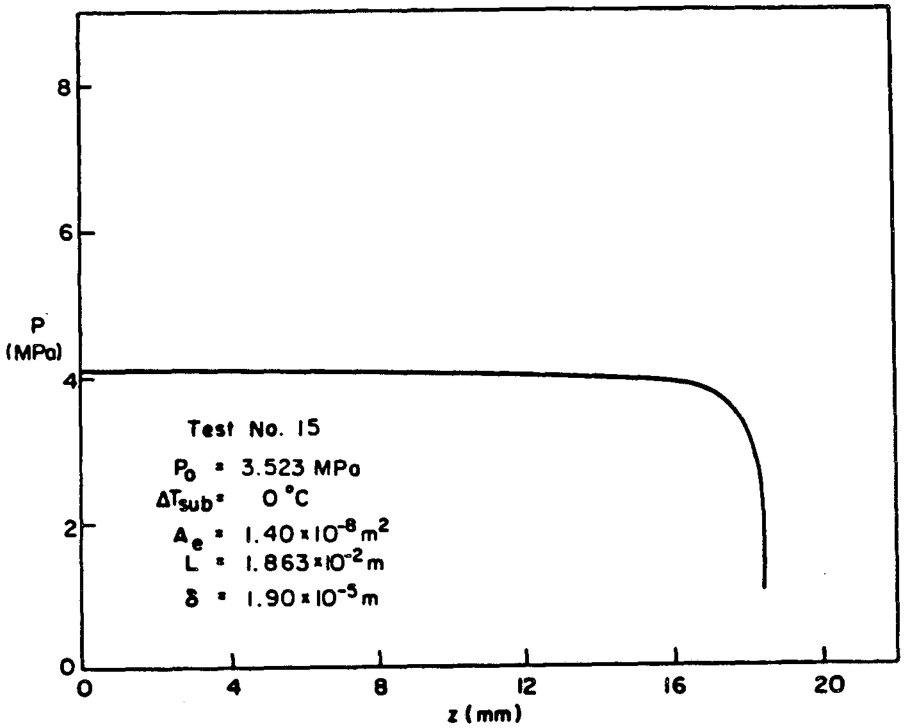
P
(MPa)
8
6
4
2
0
0
4
8
12
16
20
z (mm)
Test No. 15
P_o = 3.523 MPa
ΔT_{sub} = 0 °C
A_e = 1.40×10^{-8} m^2
L = 1.863×10^{-2} m
δ = 1.90×10^{-5} m

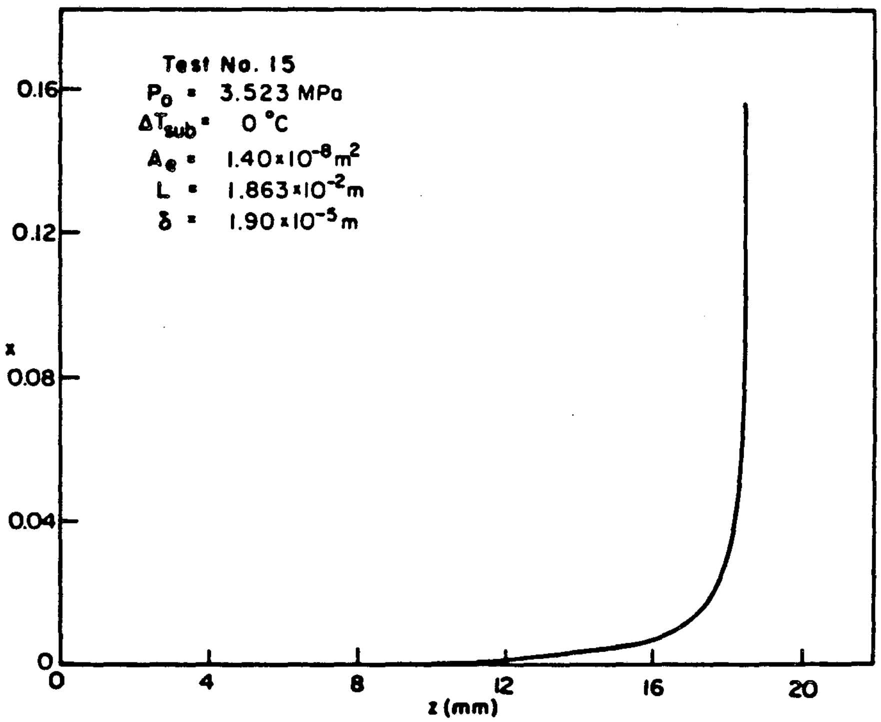
x
0.16
0.12
0.08
0.04
0
0
4
8
12
16
20
z (mm)
Test No. 15
P_o = 3.523 MPa
ΔT_{sub} = 0 °C
A_e = 1.40×10^{-8} m^2
L = 1.863×10^{-2} m
δ = 1.90×10^{-5} m

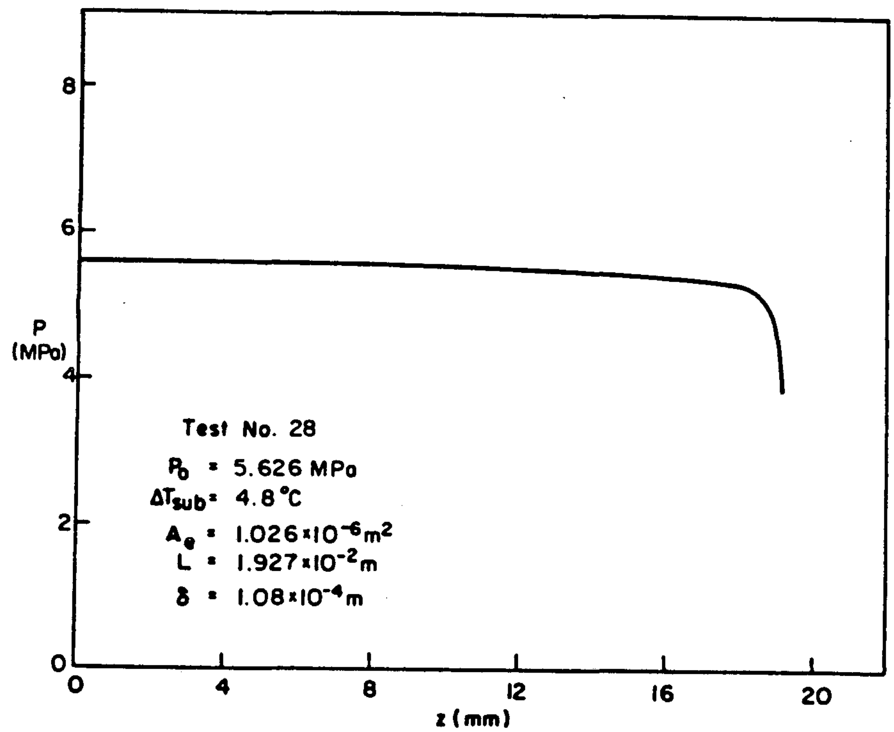
P
(MPa)
8
6
4
2
0
0
4
8
12
16
20
z (mm)
Test No. 28
P_0 = 5.626 MPa
ΔT_{sub} = 4.8 °C
A_e = $1.026 \times 10^{-6} m^2$
L = $1.927 \times 10^{-2} m$
δ = $1.08 \times 10^{-4} m$

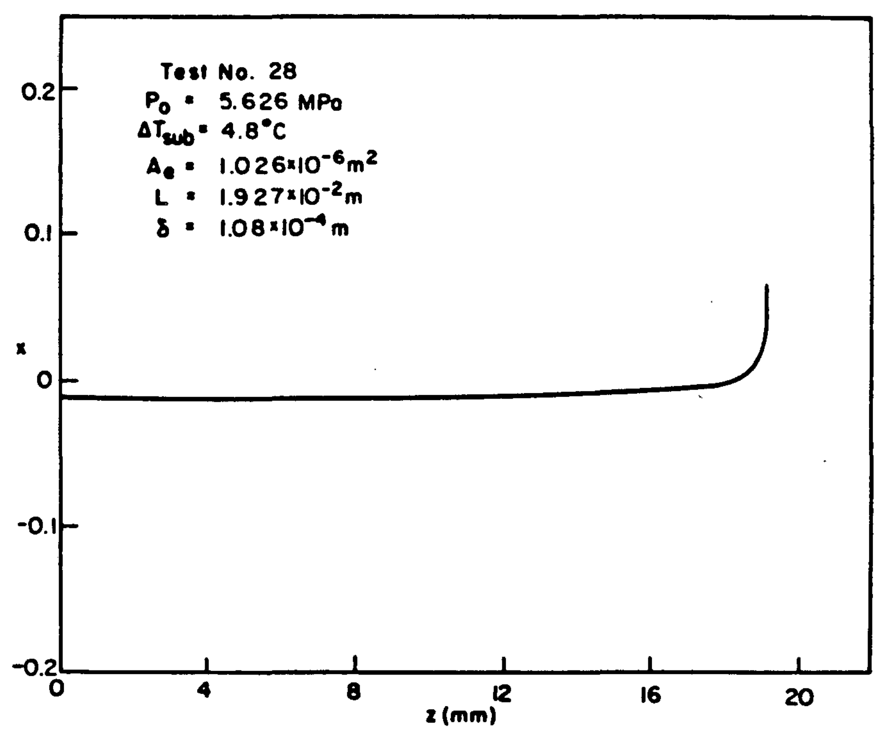
x
0.2
0.1
0
-0.1
-0.2
0
4
8
12
16
20
z (mm)
Test No. 28
P_0 = 5.626 MPa
ΔT_{sub} = 4.8 °C
A_e = $1.026 \times 10^{-6} m^2$
L = $1.927 \times 10^{-2} m$
δ = $1.08 \times 10^{-4} m$

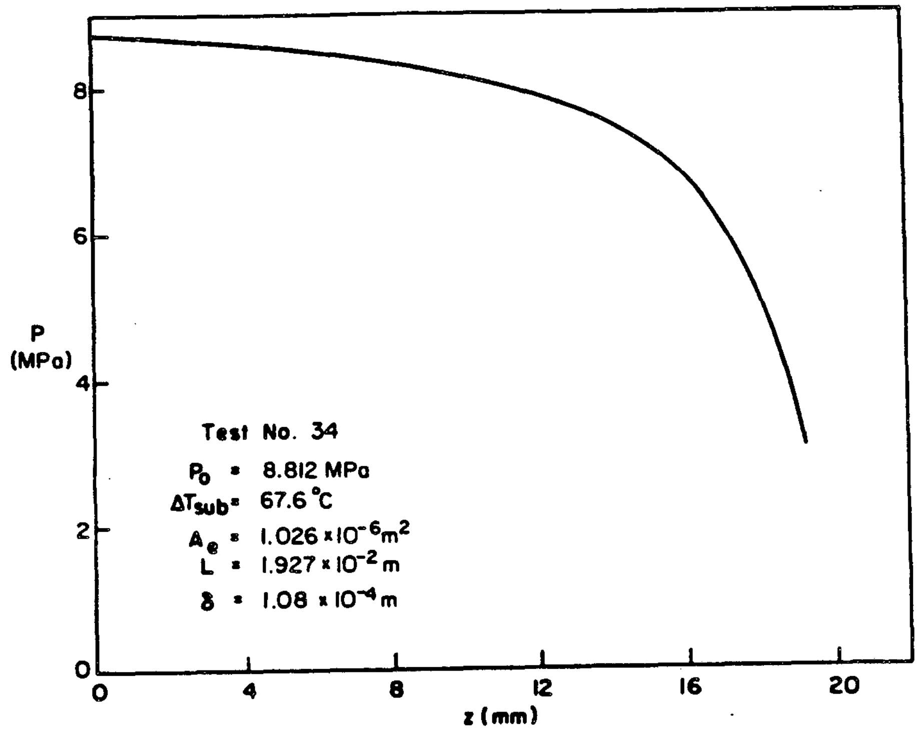
P
(MPa)
8
6
4
2
0
0
4
8
12
16
20
z (mm)
Test No. 34
Po = 8.812 MPa
ΔTsub = 67.6 °C
Ae = 1.026 x 10^-6 m^2
L = 1.927 x 10^-2 m
δ = 1.08 x 10^-4 m

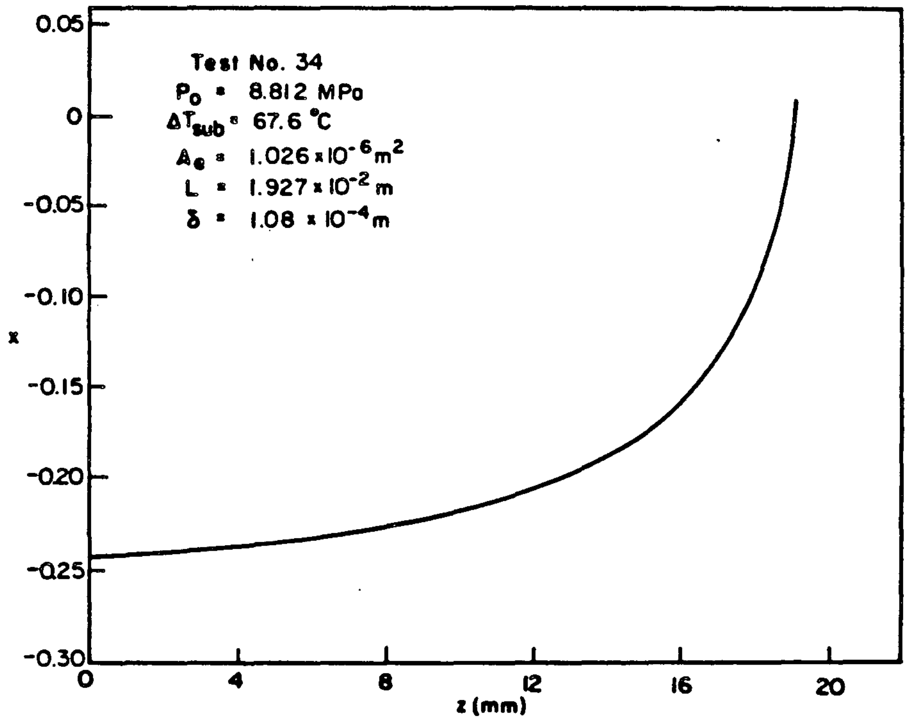
x
0.05
0
-0.05
-0.10
-0.15
-0.20
-0.25
-0.30
0
4
8
12
16
20
z (mm)
Test No. 34
Po = 8.812 MPa
ΔTsub = 67.6 °C
Ae = 1.026 x 10^-6 m^2
L = 1.927 x 10^-2 m
δ = 1.08 x 10^-4 m

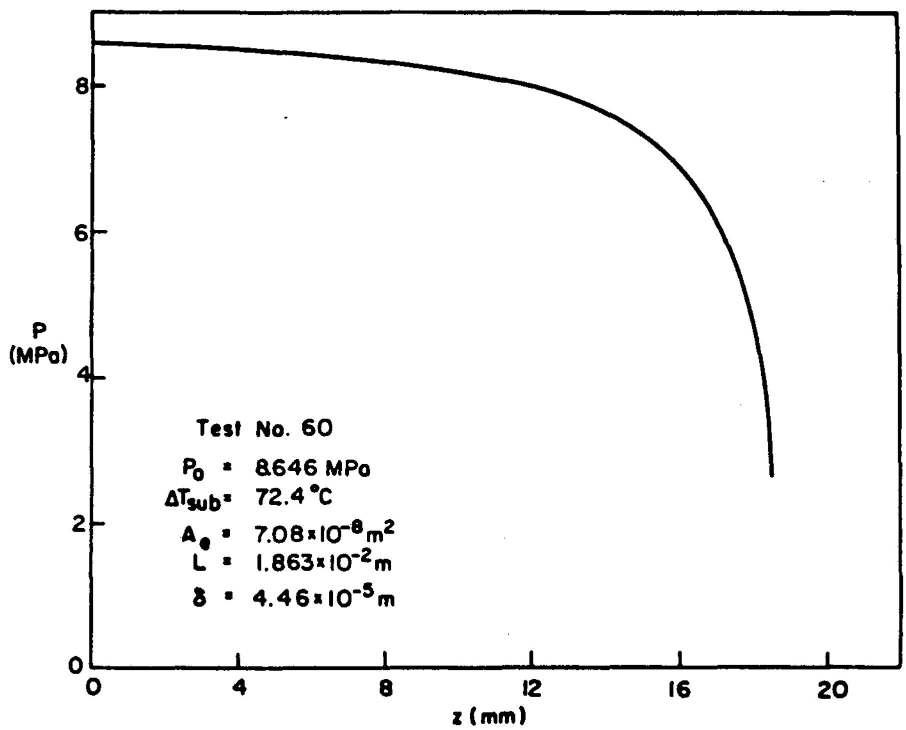
P (MPa)
0
2
4
6
8
0
4
8
12
16
20
z (mm)
Test No. 60
P_0 = 8.646 MPa
ΔT_{sub} = 72.4 °C
A_e = 7.08×10^{-8} m^2
L = 1.863×10^{-2} m
δ = 4.46×10^{-5} m

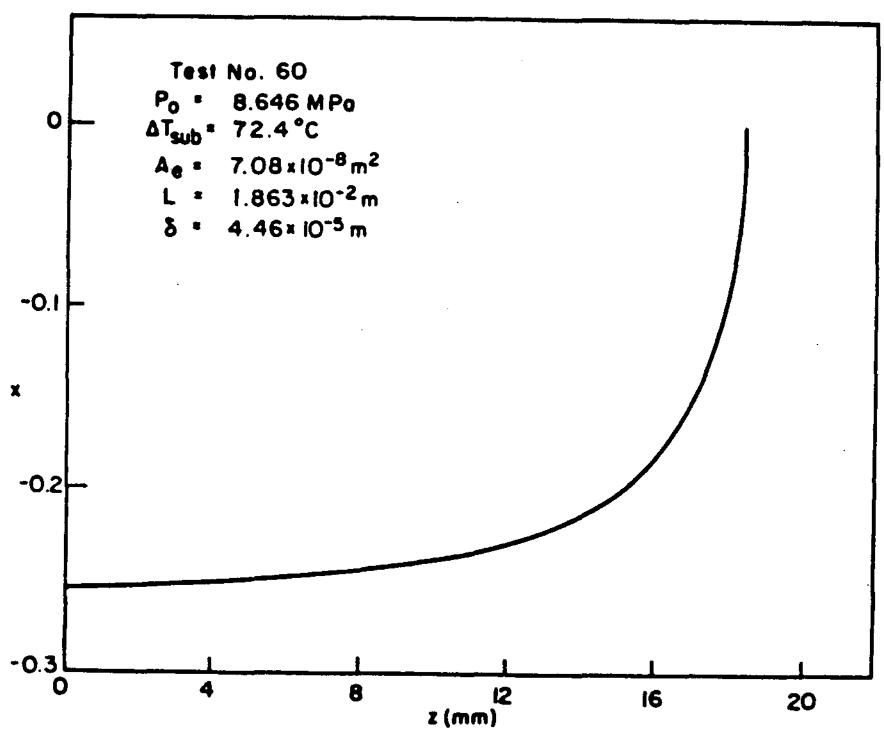
x
0
-0.1
-0.2
-0.3
0
4
8
12
16
20
z (mm)
Test No. 60
P_0 = 8.646 MPa
ΔT_{sub} = 72.4 °C
A_e = 7.08×10^{-8} m^2
L = 1.863×10^{-2} m
δ = 4.46×10^{-5} m

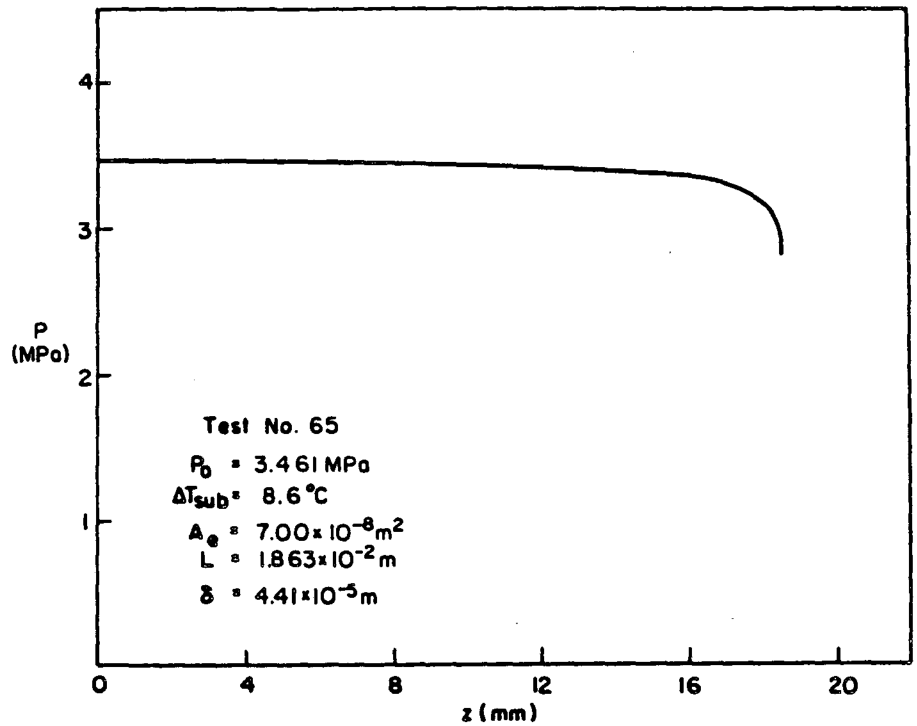

Test No. 65
P_0 = 3.461 MPa
ΔT_{sub} = 8.6°C
A_e = $7.00 \times 10^{-8} m^2$
L = 1.863×10^{-2} m
δ = 4.41×10^{-5} m
P (MPa)
z (mm)

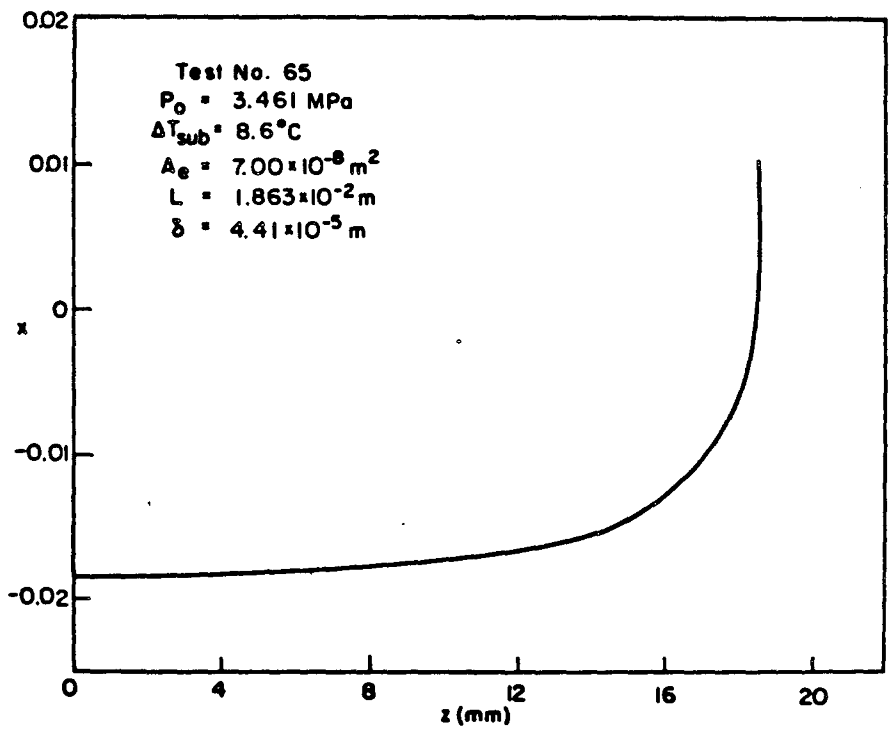

Test No. 65
P_0 = 3.461 MPa
ΔT_{sub} = 8.6°C
A_e = $7.00 \times 10^{-8} m^2$
L = 1.863×10^{-2} m
δ = 4.41×10^{-5} m
x
z (mm)

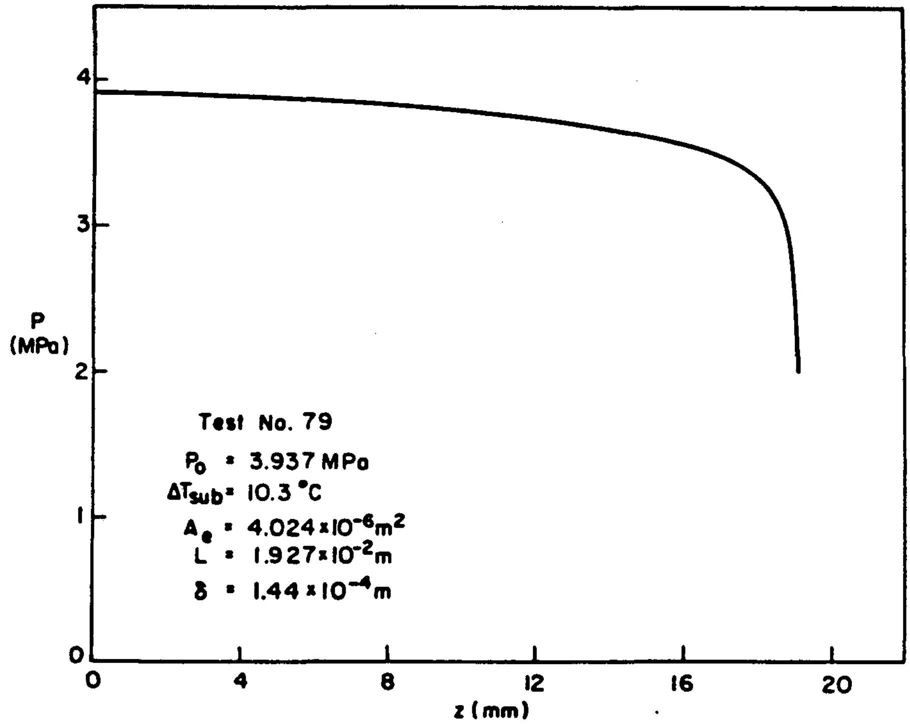
Test No. 79
P_0 = 3.937 MPa
ΔT_{sub} = 10.3 °C
A_e = $4.024 \times 10^{-6} m^2$
L = $1.927 \times 10^{-2} m$
δ = $1.44 \times 10^{-4} m$
P (MPa)
z (mm)
0
1
2
3
4
0
4
8
12
16
20

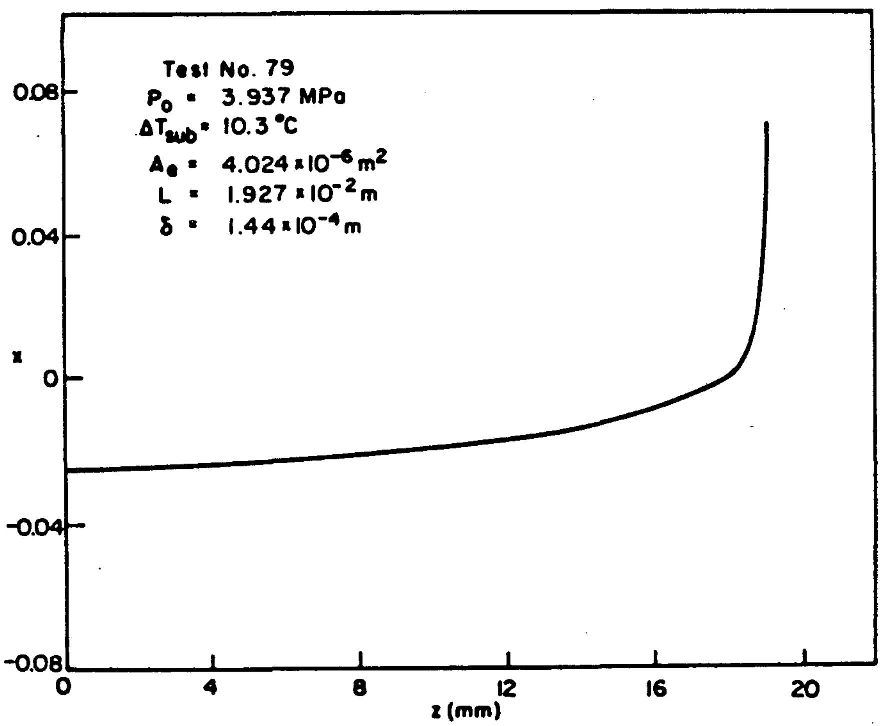
Test No. 79
P_0 = 3.937 MPa
ΔT_{sub} = 10.3 °C
A_e = $4.024 \times 10^{-6} m^2$
L = $1.927 \times 10^{-2} m$
δ = $1.44 \times 10^{-4} m$
x
z (mm)
0.08
0.04
0
-0.04
-0.08
0
4
8
12
16
20

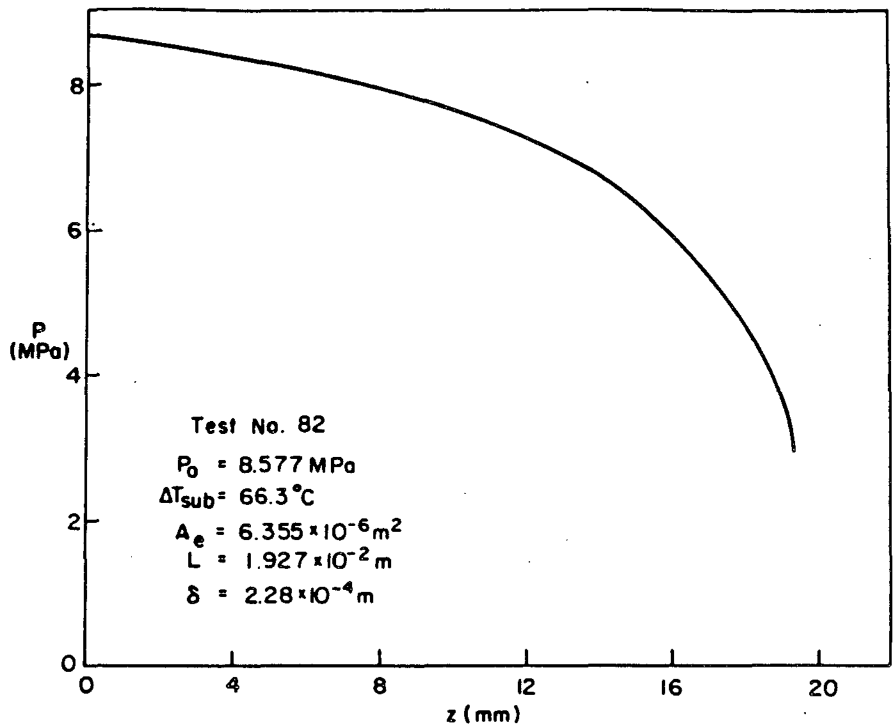
P
(MPa)
8
6
4
2
0
0
4
8
12
16
20
z (mm)
Test No. 82
Po = 8.577 MPa
ΔTsub = 66.3 °C
Ae = 6.355 x 10^-6 m^2
L = 1.927 x 10^-2 m
δ = 2.28 x 10^-4 m

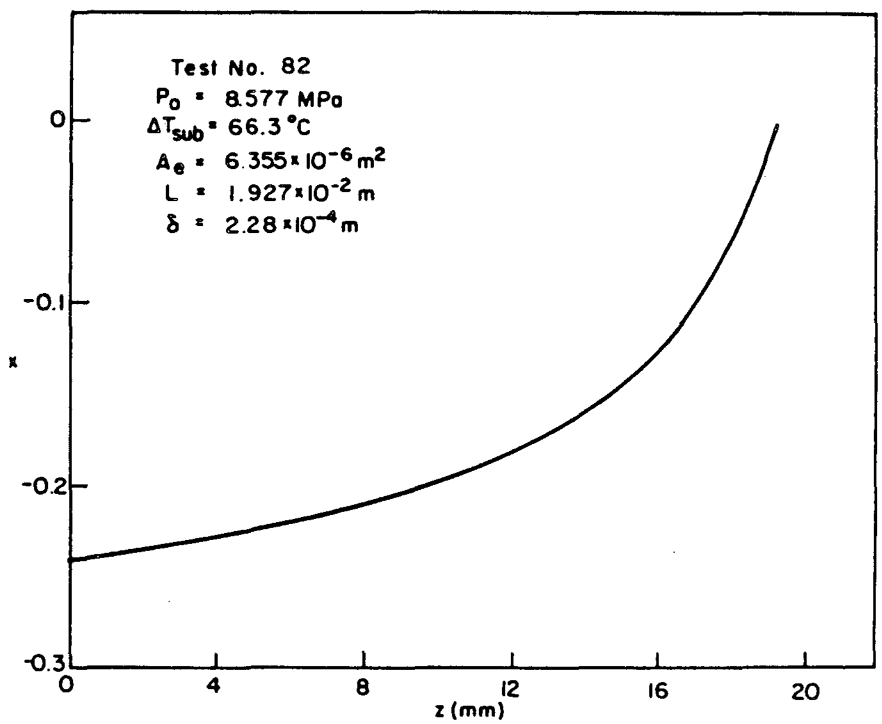
Test No. 82
Po = 8.577 MPa
ΔTsub = 66.3 °C
Ae = 6.355 x 10^-6 m^2
L = 1.927 x 10^-2 m
δ = 2.28 x 10^-4 m
x
0
-0.1
-0.2
-0.3
0
4
8
12
16
20
z (mm)

APPENDIX E

Thermodynamic Properties of Saturated Water and Steam

The code SOURCE uses the subroutine STEAM to calculate the thermodynamic properties of saturated water and steam. The input parameter to STEAM is pressure. For given value of pressure, STEAM first calculates the corresponding saturation temperature, and then uses this value of saturation temperature to calculate the other parameters, h_f, h_g, v_f, v_g, s_f and s_g. STEAM also calculates the derivatives of the saturation properties, enthalpy, specific volume and the entropy, with respect to pressure. For this calculation, the derivatives of each property with respect to the pressure are expressed in the following form, for example, for specific volume of water,

$$dv_f/dp = v_c \cdot \frac{d}{dp}(v_f/v_c)$$

$$= v_c \cdot \frac{d}{dT}(v_f/v_c) \cdot \frac{dT}{dp} .$$

The listing of the subroutine STEAM is included in the main program listing SOURCE. When subroutine STEAM is called upon in SOURCE with a pressure value, it returns the saturated values of specific volume, enthalpy and entropy and their derivation with respect to pressure for the input pressure value.

The thermodynamic properties equations are due to Ishimoto et al. [15] and are presented below.

1. Saturation temperature:

$$\frac{T_c}{T} = \left(1 + \sum_{i=1}^{5} A_i \ X^i\right) \Big/ \left(1 + \sum_{i=6}^{7} A_i \ X^{i-5}\right)$$

2. Specific volume of saturated water:

$$v_f/v_c = \left(1 + \sum_{i=1}^{9} B_i \ Y^i\right) \Big/ \left(1 + \sum_{i-10}^{12} B_i \ Y^{i-9}\right)$$

3. Specific volume of saturated steam:

$$v_c/v_g = \left(\frac{T}{T_c}\right)^6 \left(1 + \sum_{i=1}^{7} C_i \ Y^i\right) \Big/ \left(1 + \sum_{1=8}^{12} C_i \ Y^{i-7}\right)$$

4. Specific enthalpy of saturated water:

$$h_f/h_c = \left(1 + \sum_{i=1}^{6} D_i \ Y^i\right) \Big/ \left(1 + \sum_{i=7}^{10} D_i \ Y^{i-6}\right)$$

5. Specific enthalpy of saturated steam:

$$h_g/h_c = \left(1 + \sum_{i=1}^{6} E_i \; Y^i\right) / \left(1 + \sum_{i=7}^{10} E_i \; Y^{i-6}\right)$$

6. Specific entropy of saturated water:

$$s_f/s_c = \left(1 + \sum_{i=1}^{6} F_i \; Y^i\right) / \left(1 + \sum_{i=7}^{10} F_i \; Y^{i-6}\right)$$

7. Specific entropy of saturated steam:

$$s_g/s_c = \left(1 + \sum_{i=1}^{6} G_i \; Y^i\right) / \left(1 + \sum_{i=7}^{10} G_i \; Y^{i-6}\right)$$

Critical Properties for Water:

$h_c = 2.107209\text{x}10^6$ J/kg

$P_c = 2.2119256\text{x}10^7$ N/m^2

$s_c = 4.4427222\text{x}10^3$ J/kg,K

$T_c = 647.27$ K

$v_c = 3.1698\text{x}10^{-3}$ m^3/kg

Symbols:

β = reduced pressure P/P_c

$X = \ln (1/\beta)$

$Y = 1 - \theta$

Constants:

$A_1 = 0.129\ 542\ 684\ 9\text{x}10^0$

$A_2 = 0.451\ 360\ 243\ 6\text{x}10^0$

$A_3 = 0.212\ 237\ 843\ 6\text{x}10^0$

$A_4 = -0.358\ 143\ 709\ 6\text{x}10^{-2}$

$A_5 = 0.909\ 031\ 628\ 3\text{x}10^{-4}$

$A_6 = 0.333\ 853\ 062\ 2\text{x}10^1$

$A_7 = 0.142\ 655\ 898\ 5\text{x}10^1$

Constants (continued)

$B_1 = 0.103\ 083\ 704\ 2\times10^{5}$

$B_2 = 0.553\ 842\ 656\ 9\times10^{7}$

$B_3 = 0.179\ 977\ 219\ 3\times10^{9}$

$B_4 = -0.474\ 384\ 340\ 7\times10^{9}$

$B_5 = 0.201\ 974\ 977\ 9\times10^{10}$

$B_6 = -0.625\ 856\ 400\ 9\times10^{10}$

$B_7 = 0.123\ 093\ 751\ 0\times10^{10}$

$B_8 = -0.135\ 116\ 048\ 0\times10^{11}$

$B_9 = 0.635\ 376\ 971\ 4\times10^{10}$

$B_{10} = 0.116\ 326\ 898\ 4\times10^{5}$

$B_{11} = 0.768\ 677\ 553\ 4\times10^{7}$

$B_{12} = 0.369\ 408\ 938\ 0\times10^{9}$

$C_1 = 0.411\ 687\ 661\ 4\times10^{4}$

$C_2 = 0.882\ 469\ 159\ 6\times10^{6}$

$C_3 = 0.433\ 265\ 710\ 0\times10^{7}$

$C_4 = -0.283\ 542\ 718\ 9\times10^{8}$

$C_5 = 0.365\ 887\ 547\ 4\times10^{8}$

$C_6 = 0.129\ 983\ 597\ 3\times10^{7}$

$C_7 = -0.172\ 949\ 642\ 3\times10^{8}$

$C_8 = 0.478\ 039\ 111\ 9\times10^{4}$

$C_9 = 0.143\ 626\ 686\ 2\times10^{7}$

$C_{10} = 0.273\ 219\ 597\ 4\times10^{8}$

$C_{11} = -0.861\ 139\ 257\ 8\times10^{8}$

$C_{12} = 0.898\ 119\ 690\ 3\times10^{8}$

$D_1 = 0.503\ 588\ 841\ 8\times10^{4}$

$D_2 = 0.852\ 988\ 031\ 0\times10^{6}$

$D_3 = 0.397\ 566\ 129\ 4\times10^{7}$

$D_4 = -0.132\ 121\ 217\ 4\times10^{8}$

$D_5 = 0.747\ 256\ 735\ 8\times10^{7}$

$D_6 = -0.169\ 003\ 475\ 3\times10^{7}$

$D_7 = 0.528\ 873\ 227\ 7\times10^{4}$

$D_8 = 0.982\ 421\ 289\ 1\times10^{6}$

$D_9 = 0.782\ 590\ 628\ 8\times10^{7}$

$D_{10} = -0.462\ 022\ 817\ 7\times10^{7}$

$E_1 = 0.498\ 130\ 313\ 7\times10^{4}$

$E_2 = 0.155\ 796\ 661\ 1\times10^{7}$

$E_3 = 0.321\ 871\ 068\ 9\times10^{8}$

$E_4 = 0.958\ 496\ 511\ 4\times10^{7}$

$E_5 = -0.439\ 895\ 952\ 3\times10^{8}$

$E_6 = 0.272\ 498\ 390\ 8\times10^{8}$

$E_7 = 0.480\ 296\ 564\ 1\times10^{4}$

$E_8 = 0.138\ 587\ 610\ 4\times10^{7}$

$E_9 = 0.232\ 356\ 620\ 5\times10^{8}$

$E_{10} = 0.813\ 454\ 111\ 0\times10^{6}$

Constants (continued)

$F_1 = 0.500\ 361\ 430\ 5\times10^4$

$F_2 = 0.827\ 385\ 789\ 8\times10^6$

$F_3 = 0.389\ 385\ 240\ 7\times10^7$

$F_4 = -0.115\ 966\ 636\ 4\times10^8$

$F_5 = 0.336\ 964\ 036\ 5\times10^7$

$F_6 = 0.122\ 650\ 602\ 1\times10^7$

$F_7 = 0.518\ 729\ 581\ 3\times10^4$

$F_8 = 0.916\ 803\ 401\ 9\times10^6$

$F_9 = 0.631\ 959\ 188\ 4\times10^7$

$F_{10} = -0.676\ 264\ 517\ 9\times10^7$

$G_1 = 0.592\ 250\ 267\ 9\times10^4$

$G_2 = 0.212\ 150\ 645\ 3\times10^7$

$G_3 = 0.436\ 715\ 991\ 8\times10^8$

$G_4 = -0.175\ 543\ 802\ 6\times10^8$

$G_5 = -0.370\ 624\ 752\ 5\times10^8$

$G_6 = 0.430\ 345\ 978\ 4\times10^8$

$G_7 = 0.578\ 290\ 580\ 1\times10^4$

$G_8 = 0.195\ 084\ 025\ 9\times10^7$

$G_9 = 0.335\ 195\ 702\ 5\times10^8$

$G_{10} = -0.360\ 433\ 023\ 1\times10^8$